N O T I C E

NASA CR-159993

ACTIVE EXPERIMENTS

IN MODIFYING SPACECRAFT POTENTIAL:

RESULTS FROM ATS-5 AND ATS-6

R. C. Olsen and E. C. Whipple

UNIVERSITY OF CALIFORNIA
SAN DIEGO

La Jolla, California

Department of Physics

Space Physics Group

Active Experiments in Modifying Spacecraft Potential:

Results from ATS-5 and ATS-6

R. C. Olsen and E. C. Whipple
Physics Department - B-019
University of California, San Diego
La Jolla, California 92093

March 1979

Prepared for

GODDARD SPACE FLIGHT CENTER
Greenbelt, Maryland 20771

1. Report No. SP-79-01	2. Government Accession No.	3. Recipient's Catalog No.
4. Title and Subtitle Active experiments in modifying spacecraft potential: results from ATS-5 and ATS-6		5. Report Date March 1979
		6. Performing Organization Code 410
7. Author(s) R. C. Olsen and E. C. Whipple, Jr.		8. Performing Organization Report No. UCSD-SP-77-01
9. Performing Organization Name and Address University of California, San Diego La Jolla, California 92093		10. Work Unit No.
		11. Contract or Grant No. NAS5-23481
		13. Type of Report and Period Covered Final, April 1977 to Feb. 1979
12. Sponsoring Agency Name and Address Goddard Space Flight Center Greenbelt, Md. 20771 Attn: Robert Bartlett -408.		
		14. Sponsoring Agency Code

15. Supplementary Notes

16. Abstract

    See page iii.

17. Key Words (Selected by Author(s)) Spacecraft charging Differential charging Ion engine operation Electron emission	18. Distribution Statement		
19. Security Classif. (of this report) Unclassified	20. Security Classif. (of this page) Unclassified	21. No. of Pages 149	22. Price*

Abstract

From 1976 to 1978, instruments on ATS-5 and ATS-6 were operated to study the phenomena of spacecraft charging. The ion engine neutralizers were operated in attempts to modify the spacecraft potentials. The neutralizer on ATS-5 is a hot filament emitting electrons, while the neutralizer on ATS-6 is a low energy plasma bridge. The diagnostics used were the UCSD particle detectors, counting electrons and protons as a function of energy. Operations were conducted in daylight and eclipse.

This report describes the processing of data from these and earlier operations. In preliminary analysis of these data, we obtained the following results: (1) electron emission ($E \leqslant 10$ electron-volts) does not perturb the status of a satellite at low potential ($|\phi| \leqslant 50$ volts) by more than 50 volts (the ATS-5 low energy limit), (2) emission of a low energy plasma ($E \leqslant 10$ volts) does not change low potentials ($|\phi| \leqslant 5$ volts) by more than a few volts (ATS-6 low energy resolution), (3) when ATS-6 enters eclipse in the presence of a high energy plasma (10 keV), the neutralizer suppresses any rise in $|\phi|$ (within a few volts resolution), (4) when the electron emitter on ATS-5 is operated, it serves to discharge negative potentials from thousands to hundreds of volts, and (5) when the neutralizer on ATS-6 is operated, it serves to discharge kilovolt potentials to below 50 volts.

As part of the charging study, a review of earlier experiments was conducted. The study showed that in low altitude (100-300 km) experiments with kilovolt electron beams, emission of unneutralized beams resulted in large return currents. These currents were sufficient to hold payload potentials below 100 volts. Operation of the main thruster on ATS-6 clamped the spacecraft at -5 V, and virtually eliminated differential charging.

A study of differential charging effects on the two satellites showed that insulators ~ 1 meter from our detectors could, when shaded, charge negatively several hundred volts with respect to the spacecraft, and generate barriers of similar potential to electron fluxes.

TABLE OF CONTENTS

LIST OF FIGURES

LIST OF TABLES

LIST OF SPECTROGRAMS

1.0 INTRODUCTION

This report is written to complete contractual requirements on NAS-5-23481. This contract was issued by Goddard Space Flight Center for Lewis Research Center.

It is designed to provide a review of experiments involving the modification of spacecraft potentials, with an emphasis on ATS-5 and ATS-6. We will present the operations performed under this contract, and a users' manual for the study of the data obtained under this contract, and in earlier experiments on ATS-5 and ATS-6.

A considerable amount of evidence has been accumulating over the last few years that anomalous behavior of spacecraft instrumentation is associated with electrostatic charging of spacecraft (Rosen, 1976). Charging effects appear to be particularly severe at synchronous orbit. Because of the importance of the synchronous altitude for a wide variety of spacecraft missions, this phenomenon has become a matter of concern to the aerospace community.

For example, McPherson et al. (1976) have shown that the occurrence of anomalies in synchronous spacecraft behavior correlates with local time and is most likely between local midnight and 0600. Reasoner et al. (1976) have shown that charging events on ATS-6 where the spacecraft potential goes more negative than -50 volts has the same correlation with local time. The failure of an entire Air Force satellite has been attributed to a spacecraft charging event.

As a result of this concern over anomalous behavior of satellites at geosynchronous altitude, a joint technology program between NASA and the Air Force has been initiated to study environmental charging phenomena. A satellite to study these phenomena (Lovell, 1976) (SCATHA) was launched in 1979. Until this data becomes available, the ATS-5 and ATS-6 satellites are the only spacecraft which can provide detailed data on charging effects of synchronous orbit. Both NASA (Lewis Research Center) and the Department of Defense have expressed great interest in studying the data now

available from these satellites and also in performing active experiments on spacecraft charging.

The NASA/Air Force panel which established the program generated a schedule to follow in the investigation, shown in Figure 1. ATS-5 and ATS-6 provided opportunities to acquire environmental data, measure the effect on spacecraft potentials, and to conduct active experiments in altering spacecraft potential.

Large spacecraft potentials have been observed on both ATS-5 and ATS-6. The largest potentials have occurred during eclipse conditions when photoelectrons are no longer emitted by the spacecraft, and during magnetic storms when the cool ambient plasma has disappeared. The largest potential observed so far was -19,000 volts on ATS-6 during an eclipse, but potentials as large as -2,200 volts have been observed in sunlight.

The recent analysis of low energy particle data on ATS-6 has shown that the local potential distribution about the satellite is dominated by the presence of differential charging of the spacecraft (Whipple, 1976a, b). Different portions of the spacecraft surface which are insulated from the main body can charge to very different potentials because of shadowing effects, anisotropic particle distributions, and non-homogeneous surface properties. As a result, large electrostatic fields can exist in the spacecraft vicinity. Possible consequences could be discharges across surfaces with associated material damage and electromagnetic interference. The UCSD experiment on ATS-6 has observed large spikes of accelerated electrons whose origin has been definitely traced to differentially charged portions of the spacecraft.

The packages of experiments on ATS-5 and ATS-6 have the capability not only of studying these effects, but also of performing active experiments by operating the ion engine instruments. These instruments had been operated a few times but not in a coordinated program with the

other experiments or during special conditions. However, preliminary analysis indicates that during at least some of these operations the electrostatic configuration of the spacecraft was changed (Goldstein and DeForest, 1976).

UCSD has been under a contract to study the modification of spacecraft potentials. This report is a description of the objectives and accomplishments under this contract. Part 2 describes the overall charging program, and part 3 consists of a review of previous work in this area. In part 4 the specific objectives and accomplishments under this contract are described. Part 5 gives recommendations for further experiments and data analysis. Appendices are provided with descriptions of the thruster commands, command logs, eclipse times and a guide for the commands for the ATS-6 detector.

2.0 SPACECRAFT CHARGING INVESTIGATION

2.1 OBJECTIVES

The objectives of the ATS-5 and ATS-6 data reduction and experiments were defined by the NASA/Air Force panel which began the program:

"Conduct additional ATS-5 and ATS-6 environmental studies. Additional space environment data will be obtained from the ATS-5 and ATS-6 particle and fields experiments to determine the present environmental conditions for quiet times and for substorms. The main device that will be utilized will be the University of California at San Diego (UCSD) Auroral Particles Experiment. The data obtained in this task will be incorporated into the Climatological Atlas (Task I). As part of this task, a study of active control devices in space will be undertaken. This study will use the neutralizers of the cesium electric thrusters on the ATS-5 and ATS-6 satellites. The objectives of this study are to determine the ability of the electron sources to control the spacecraft ground potential and to investigate the voltage sheath surrounding the spacecraft. This work will be directed by the NASA Lewis Research Center." (Lovell, 1976).

The objective, as shown in Figure 2, is to study the feasibility of actively controlling spacecraft potentials by charged particle emission. The devices to be used are the ATS-5 electron emitter, the ATS-6 plasma emitter, and the UCSD particle detectors on both satellites.

The ATS-5 and ATS-6 spacecraft and complement of instruments are compared in Table 1 and the differences in the operation of the particle-emitting devices on the two spacecraft are shown in Table 2 (Purvis, 1976). Diagrams of both spacecraft showing the relative locations of the detectors and engines are included. ATS-5 is shown in Figure 3, ATS-6 in Figure 4. Descriptions of the detectors and engines follow.

4

2.2 ATS-5 DETECTORS

The ATS-5 satellite was launched into synchronous orbit $(6.6 \ R_e)$ in August 1969 and has been kept near 105 degrees west longitude since early September 1969. The orbital inclination is 2.30 degrees. Since the satellite continues to spin with a period of 0.79 seconds, the booms intended to provide gravity gradient orientation cannot be safely extended. The spinning motion improves the plasma data in that it provides the possibility of measuring important portions of the angular distribution. The spin axis is oriented parallel to the earth's rotational axis.

The four cylindrical plate spectrometers consist of two pairs of electron and proton analyzers directed parallel and perpendicular to the spin axis. The parallel analyzers point north and thus detect particles coming from the northern hemisphere. The particles are detected with Bendix type 4010-3 channel electron multipliers which have narrow angle cones that give a 3 mm diameter sensitive area. Biases of -2700 volts are applied to the front of the multipliers for post-analysis acceleration of protons and +500 volts for electrons. These biases result in a constant high efficiency for the protons at all energies analyzed and for electrons below one keV. The efficiency of channel multipliers decreases at higher electron energies. This decrease has been accurately measured. The potential of a grid immediately in front of the sensors is held at zero in the proton analyzers and at -30 volts in the electron analyzers to suppress secondary electrons. All pulses greater than about 10^{-3} of the typical pulse size are counted so there is little change in efficiency with large changes in the channel multiplication factor.

Three simultaneous accumulations 0.26 seconds long are taken every 0.32 seconds. Two analyzer outputs are selected by ground command to third accumulator. Accumulation is stopped for 4 microseconds after each pulse counted so that the small afterpulses which can occur during the first one or two microseconds after a particle is detected are not counted. Deadtime corrections are applied so that rates up to 10^6/sec are believed to be measured accurately.

The analyzers have an energy resolution of about 13% and a geometric factor such that dividing the counting rate by 4.3×10^{-5} cm^2 sr yields the differential energy flux in units of eV/cm^2 sec sr eV. The angular response to a uniform energy distribution extends over a rectangular solid angle of about 5 by 8 degrees.

The inner and outer plates of the analyzers are connected in parallel to two high voltage supplies which can be stepped through 62 exponentially spaced voltages 12% apart (with less than 0.1% accumulative error' thus varying the energy analyzed from 50 eV to 50,000 eV. Two zero voltage steps are also included to provide background measurements (in practice the background is usually low and is not subtracted).

The normal operational mode during the charging experiments was to cycle through the 64 steps every 20.48 seconds.

2.3   ATS-6 DETECTORS

The five electrostatic charged particle detectors of the UCSD instrument were designed to obtain the temporal, spectral, and angular properties of low to moderate energy magnetospheric particles. One electron-ion pair of detectors was designed to rotate in a north-south (NS) plane, while another pair were designed to rotate in an east-west (EW) plane. A third ion detector points east. A unique double focusing feature of the detectors allows for high count rates while maintaining good angular resolution. A balance between spectral and temporal information is obtained through various programmed sequences consisting of SCANS (full spectra) and DWELLS (fixed energy). The voltage bias on the Bendix channeltron particle detectors can be manipulated (high and low bias) to preserve channeltron health. Table 3 gives numerical specifics concerning the experiment.

2.4   ATS-5 ION ENGINE

The cesium contact ion thruster used on ATS-4 and ATS-5 is displayed in Figure 5. Cesium vapor is fed to a single aperture. Upon reaching the surface of the porous tungsten button, the cesium is ionized. "The accelerating geometry consists of contoured ionizer, beam-forming electrode, accelerating and decelerating electrodes, and neutralizers. The copper accelerator electrode is cut into four segments to permit beam deflection for thrust vectoring. Deflection is produced by symmetric biasing of opposing pairs of quadrants; one quadrant is positive and the other negative with respect to the nominal accelerating potential."

"The decelerator electrode is mounted to thruster common and provides support for the two hot-wire neutralizers. These neutralizers, 0.007 in. diam, are Ta doped with 50 ppm yttrium to retard grain growth. One neutralizer operates and one remains as backup" (Worlock, 1969).

2.5   ATS-6 ION ENGINE

ATS-6 carries two ion thrusters of the type diagrammed in Figure 6. They utilize the magnetoelectrostatic containment (MESC) concept, where the magnetic and electric fields provide boundaries to contain a uniform plasma. These are 8 cm in diameter, producing one millipound (.004 N) thrust. Two parallel grids are used to extract the plasma, with the outer accelerator grid at -560 volts, and the inner screen grid at +560 volts. The grids accelerate about .1 amp of cesium ions to a kinetic energy corresponding to the 1.1 kV potential drop. Inside the hemispherical section is a cesium hollow cathode with a .010 in. orifice. Approximately ten percent of the cesium is fed through the cathode, and is controlled by the discharge current. The remaining ninety percent is provided by a main feed ring biased at the potential of the boundary anodes. A plasma anode is placed in front of the cathode to provide control (Worlock, 1973).

A neutralizer is provided, operating at spacecraft ground, located 5.0 cm from the accelerator electrode and pointing 60 degrees down-stream (James, 1973).

"A plasma bridge neutralizer is incorporated into the system. A tantalum emitter is installed inside the hollow cathode behind a 0.006-in. diameter orifice. Both cathode and vaporizer have external sheathed heaters. An auxiliary electrode is mounted slightly downstream from the cathode. This electrode, referred to as the probe, is initially biased 150 V positive with respect to the neutralizer and acts like an anode, drawing enough emission current to start the neutralizer when the thruster is off." (James, 1970)

"After the neutralizer discharge starts, the probe is operated from a high impedance plus fifteen volt power supply. In this mode, about 50 milliamperes of emission current is extracted from the cathode. The probe serves as a plasma bridge potential sensing element for control purposes." (Bartlett, 1975).

"The emission characteristics of this neutralizer vary with the cesium flow through it and with the cathode temperature. At very low cathode temperatures, operation becomes emission limited, but over a wide range the cathode temperature affects the beam coupling only slightly. Neutralizer control is accomplished by presetting the cathode power and regulating the vaporizer power to maintain a given ion beam potential as approximated by the potential of the probe immersed in the plasma bridge." (James, 1970).

"To operate the neutralizer, the master converter is first com-manded on. Power is then applied to the cathode heater and the plasma probe striker supply. The tantalum emitter comes to its operating tem-peratuer of 700 degrees centigrade in approximately ten minutes. The cesium vaporizer heater operates at about 300 degrees centigrade and is controlled by the "Neutralizer On" command. About fifteen minutes

after this command is executed, the cesium vapor pressure in the hollow cathode is sufficient to strike a discharge. The initial discharge is referred to as the plume mode of operation and is characterized by low electron emission current and high extraction potentials. As the cesium feed increases, the neutralizer operation shifts to what is known as the spot mode which is characterized by high emission current at low extraction potentials. Both of these names are derived from the physical appearance of the neutralizer discharge. In the spot mode, the neutralizer is emission limited at about three amperes." (Bartlett, 1975)

2.6   SPECTROGRAMS

The main method of data presentation used by UCSD in this report is the spectrogram. This provides a visual display of particle count-rate as a function of time and energy, permitting rapid qualitative analysis of the data, and indicating directions for the analysis of the raw data. In the following two sections the formats for these spectrograms are discussed.

2.6.1 Description of ATS-5 Spectrograms

<u>Format</u> (Reference Spectrogram 2, 10-11)

The spectrograms are produced in pairs: one showing the spectra from the perpendicular proton and the perpendicular electron analyzers and one showing the spectra from the parallel proton and electron analyzers. They are labeled by a large ⊥ or ‖ on the middle left side. The proton part is always below the electron part. The day of the year (January 1 equals day 1) and year is given at the bottom. The month, day in month, and year are also given at the left just above the ⊥ or ‖ label. The times at the beginnings and ends of the spectrograms

can be arbitrarily set, and can cover any desired time span. Time scales covering as little as 10 minutes and as great as 4 days have been used. Times are given in Universal Time (UT).

Grey Scale Interpretation

The primary value of spectrograms is their ability to reveal patterns in the energy-time plane. The determination of actual flux levels from them is of secondary importance.

Should one desire to estimate the flux at a given point on a spectrogram, first locate the corresponding level on the grey scale at the lower right and determine the value of "G" on the scale marked 0 to 3. The differential energy flux in eV/cm^3 sec sr eV is then given by

$$(10^G - 1) \, 10^{b + 4.367}$$

where b is given by "EL" for the electron fluxes or "PR" for the proton fluxes. The value of "ST" gives the change in G between each of the 33 discrete grey levels available.

Energy Scales

The computer program which generates the spectrograms can utilize any arbitrary function of energy for the energy scales for exhibiting all or any part of the measured spectra. The entire range from 50 eV to 50 keV is usually plotted with a logarithmic scale with 50 eV at the center for both protons and electrons. This gives an inverted energy scale for the protons.

Subsidiary Data

A number of useful quantities are given along the top of the spectrogram, or in the lower left hand corner in older spectrograms. The analyzers in the "master" and "mate" channels are identified by numbers following "MASTR" and "MATE" according to the scheme:

1. perpendicular electron analyzer

2. perpendicular proton analyzer

3. parallel electron analyzer

4. parallel proton analyzer

TA = averaging time for the spectra in minutes

TS = time between spectral averages in mintes

TM = averaging time for the magnetic data in minutes

The seven bit command word is given immediately below "COMMAND". The first three bits give the channel assignments and are therefore redundant to the master and mate identifications given above. Bits 4 and 5 specify the operating mode according to the scheme:

Bit	4	5	Mode
	0	0	track-scan
	0	1	single step scan only
	1	0	track only
	1	1	double step scan only

Bits 6 and 7 not set to zero correspond to other modes which are rarely used. "TRACK" refers to a mode where the energy is varied to track a peak in the counting rate.

"ST", "EL", and "PR" are described above.

"PSNG" specifies the quantity being plotted in the spectrogram according to the scheme:

1. differential energy flux

2. differential number

3. ratios of the flux averaged over "TS" minutes to the flux averaged over the previous "TA" - "TS" minutes.

4. ratios of adjacent energy steps

Options other than the first are rarely used.

11

<u>Magnetic Field</u> (See Spectrograms 10a and 10b)

Data from the ATS-5 magnetometer have been kindly supplied by
T. Skillman of the Goddard Space Flight Center and are plotted above
the spectral data along with lines at 0, 50, 100 and 150 gammas. The
data are not corrected for the effects of time changes in the spacecraft
current systems. These perturbations can be as large as 15 gammas.
The absolute value of the magnetic field component parallel and per-
pendicular to the spin axis is given by the darker and lighter points
respectively (and usually the upper and lower respectively) with the
spectrograms of the perpendicular analyzers. The perpendicular com-
ponent is obtained using only the coarse (33 gamma step size) data and
is thus uncertain by at least ±10 gammas. Most of the scatter in this
component is due to using only the coarse data.

The magnitude of the field and the angle of the field to the spin
axis are given by the lighter and darker points respectively (and usu-
ally the upper and lower respectively) with the spectrograms of the
parallel analyzers. The angle to the spin axis is given in degrees.
Both the magnitude and angle are subject to the additional uncertain-
ties in the perpendicular component.

2.6.2 Description of ATS-6 Spectrograms

<u>Format</u> (See Spectrogram 1)

These spectrograms are produced in a format similar to that of
ATS-5. One spectrogram is produced for each detector pair, and
they are labeled N/S or E/W on the left hand side, where the electron
and ion labels are printed. The day of the year and the year are given
on the bottom, with the month/day/year printed at the top left corner.
The time of day is printed on the bottom. The electron spectrum is
always placed above the ion spectrum.

The count rate is modified slightly before plotting. The major
modification is the background to be subtracted from channels 0-15
of the electron detectors.

Axes

The energy axes on the sides is a combination of linear (0-10 eV) and logarithmic (10 to 80 eV). The electron scale is on top, the ion scale, usually inverted, is on the bottom. The time axis on the bottom is in universal time, and normally specifies hours and minutes.

Intensity

The intensity scale runs from 1 to 16. The program converts the count rate to this scale according to the following formula.

$$I_n = 0.4 * \lceil \langle \log_{10}(1 + CR * 10^{-x}) \rangle / DBS + 4 * c \rceil$$

where:

I_n = intensity

CR = count rate

x = DBE or DBP, an offset factor that determines the minimum count rate which gives a non-zero intensity

DBS = contrast, smaller DBS gives higher contrast

c = weighting factor, about 1.0, 1.25, 1.5, 1.75; needed for plotting purposes.

For maximum contrast, it is desirable to work on the straight line portion of the intensity curve. This implies setting 10^x approximately equal to the minimum count rate of interest. For normal DBS (about 0.06 or 0.07) 2 orders of magnitude in count rate will raise I_n to 16. There is an overflow mode where the scale cycles. In this mode, the intensity reaches a maximum lightness, then recycles to black, and starts over again.

The most useful parameters printed at the top of the spectrogram are the longitude (LNG) and the command. Appendix 5 is provided to help interpret the command, which gives the detector status at the beginning of the spectrogram. A black triangle just above the electron spectra indicates a command change.

13

The magnetic field data is plotted across the top of the page. The different plots should be distinguishable by their different behaviors, and their intensity (thickness). The north/south and east/west spectrograms are treated differently. On the north/south spectrogram, we find the pitch angle (α) of particles seen by that detector, B_x, B_t, and I, the inclination of the magnetic field. On the east-west spectrogram, the north/south pitch angle is replaced by the angle of the detector with respect to the EME package, since α is almost always $\approx 90°$. The magnetometer suffered a failure on day 251/75: the y axis was lost at this time. Also, the z axis misbehaves if the outward field is greater than 20 γ. After this date, B_t and I are replaced by $-B_z$. The relative intensities are as follows:

Pitch and detector angle	15
B_x	8
B_t	8
I	10
B_{-z}	10

If the detectors are rotating, the angle plot is immediately noticeable as such, except in spectrograms covering 6 hours or more. In this case, the minimum angle is plotted whenever it occurs. This usually shows up as a series of small dots near the bottom of the scale. The scales for the magnitude of B and B_x are on the left hand side, in gammas. The scale for angles on the right side is more complicated. The scale for the north/south pitch angle is at the bottom of the plot area, with only 0° and 45° labeled. The +90, 0, -90 above these marks are the scale for the inclination of the magnetic field. The east/west spectrogram is similar, but replaces pitch angle with spacecraft angle.

3.0 REVIEW OF PREVIOUS WORK

3.1 INTRODUCTION

Active control of spacecraft charging is possible by emitting charged particles. Variation of spacecraft potential in this way has not been the primary purpose of any known experiments. However, it has been a by-product of a number of experiments.

In particular, those experiments involving ion thrusters have been our main source of data on ion emission. Electron emission has been done with the hot filament of the ATS-5 neutralizer, and with a variety of electron guns in ionosphere and magnetosphere studies. Ion emission has primarily been from satellites, electron emission from rockets.

A review of earlier experiments follows. Gendrin (1974) gives a good review of electron gun experiments and mentions several unpublished shots as well as discussing the physics of beam propagation.

3.2 AEROBEE 17.03 (JANUARY 26, 1969)

This was Wilmot Hess's experiment to test the feasibility of emitting an electron beam from a rocket. The rocket was launched from Wallops Island, reaching an apogee of about 270 km. It carried 10 guns working off a common accelerator at 10 keV and .5 amp. The stated purpose of the experiment was to generate an aurora artificially, and the experiment was successful.

To enhance vehicle neutralization, the rocket carried an aluminized mylar screen. Unfortunately, it did not fully deploy so the collection area was unknown. (Full diameter was 26 m.) The current from the screen to the rocket was measured.

The payload included two retarding potential analyzers covering 0-90 eV and 100-2000 eV. There was no clear break in the particle spectrum. On this evidence, it is believed that the potential remained below 2000 volts. The low energy RPA saturated when $I_{beam} \geq 50$ ma. Other results are as follows:

1) "The spectrum of returning electrons showed an average of 4-20 eV with no obvious break points."

2) "The ambient electrons were strongly heated by the beam."

3) The return current did not initially equal the beam current on pulses with $I_{beam} \geq 50$ ma, but rose slowly to match the beam current over a period on the order of 100 msec.

4) "Enhanced fluxes of hot electrons persisted after the pulses." These decayed in times on the order of 100 msec (Hess, 1969, 1971; Trichel, 1971).

This group was involved in another experiment in 1972. On October 15, an electron accelerator was launched from Hawaii. They succeeded in generating at least one artificial aurora in the Southern Hemisphere, using a 1-sec burst at 24 keV and ≈ 200 ma (Davis, 1973).

3.3 ECHO: INTRODUCTION

This is a series of rocket flights (four so far) designed to study the ionosphere and magnetosphere. The basic premise is that electrons may be injected along field lines and bounced back from the southern hemisphere to the sending rocket. (ARAKS is based on the same idea.) The project is headed by Dr. John Winckler of the University of Minnesota. They have succeeded in the basic idea, and are now moving toward analyzing the interaction of the beam with the magnetosphere, atmosphere, and aurora.

There are some indications of positive potential during gun firing, but none of the potential measurements seem definite as yet (Winckler, 1976).

16

3.3.1 Echo I (August 13, 1970)

This was the prototype for the project, and proved the feasibility of the echo idea. A number of one and two bounce echoes were seen. This rocket also carried extensive neutralization apparatus and diagnostics.

The electron gun swept from 34-43 keV, with 70 ma output for 16 msec. The bounce period was about .65 sec at the McIlwain L parameter $L \approx 2.56$. (Apogee ≈ 350 km.) Quick echoes were seen from below the rocket in times 0-30 milliseconds.

The first additional neutralization device used was an argon plasma source. Ground tests showed it to emit approximately 100 ma of 25 eV argon ions and 10 eV electrons. The current was neutral.

Before the argon source was switched off, an aluminized mylar shield was deployed. It was predicted that it would intercept a thermal current of about 700 ma, about 10 times the beam current.

The main diagnostic was a Faraday cup. It showed that the bare rocket body, a conductor, drew a sufficient return current to approximately neutralize the effect of the beam with $\phi \leqslant 75$ always, and $\phi \sim 1$ volt usually (Hendrickson, 1972).

3.3.2 Echo II (September 25, 1972)

This experiment represented an attempt to repeat the results of Echo I at a new launch site, with $L = 8.5$, apogee = 264 km. Based on results from Echo I, no neutralization equipment was carried. Langmuir probe measurements showed that the bare rocket body was sufficient to maintain $\phi \leqslant 100$ volts. There were no confirmed echo observations (Winckler, 1975a).

3.3.3 Echo III (April 17, 1974)

Echo III and IV were launched from Poker Flats, Alaska, at
L $\simeq$ 5.4, apogee $\simeq$ 275 km. Echo III was designed to begin investigation
of the near-rocket interactions, including the quick-bounce below the
rocket and the strong electron flux to the rocket during beam emission.
Therefore, thi rocket carried a photometer (3914 Å) and a back-
scattered electron detector to observe the beam atmosphere interaction.
It also carried the standard scintillation/photometer with a low energy
cutoff at about 25 keV, a low energy ion spectrometer (0-5 eV), and a
new feature, a variety of metal tabs to measure the return current in
various directions.

The gun was activated between 30 and 40 kV, at about 80 ma.

The results of this flight are being debated in the literature
(Israelson, 1974, 1975, 1976; Hanser, 1976).

The ion detector has resolution in the milliseconds regime, and
seems to have shown $\phi \leqslant 10$ V immediately after the gun firing. The
"DESA" analyzer for backscattered electrons also had msec resolution,
and covered 0-50 keV. Analysis of the 8 msec gun pulses shows a great
deal of time-energy structure. The indication is that there is a heating
effect of the plasma near the rocket, enhancing the return current. The
result as indicated by the ion spectrometer, is that the rocket goes from
positive during firing to tens of volts negative immediately afterwards,
gradually returning to $\phi \approx -1$ volt.

This experiment seems to offer a great deal of promise in providing
information on the spacecraft and beam interactions with the atmosphere
(Winckler, 1976).

3.3.4 Echo IV (January 31, 1976)

Echo IV was a refinement of Echo III, spinning at a slower rate ($T \approx 1$ sec), and carrying an attitude control system that allowed alignment of the rocket axis almost parallel to $\vec{B}$. New capabilities were the ability to release N_2 from the attitude control system to enhance neutralization, a Langmuir probe for potential measurements, photometers for 5777 Å , electric field booms, and several current and particle detectors.

Echoes were detected by both particle and photon detectors. In addition, ground television monitors observed a number of downward injections (Hallinan et al., 1978).

Langmuir probe measurements showed the rocket to be about +20 volts with respect to the probe during the 30 kV gun pulse. It is not clear how this relates to the potential with respect to the distant plasma (Winckler, 1976). Israelson and Winckler (1978) give the fascinating results of the N_2 dump. Whereas normally the return current measurements generally showed $I_{return} < I_{beam}$, during the N_2 dump, the detectors saturated, indicating $I_{beam} < I_{return}$. This indicates that the return currents are localized on the rocket surface, and that a neutral gas around the rocket will enhance the return current. A current oscillation of about 22 Hz was set up after a 1 second, 40 kV, 80 ma gun pulse. A similar oscillation was seen by onboard photometers at the same time.

3.4   ZARNITZA (MAY 29, 1973)

A preliminary experiment in the ARAKS series occurred in 1973.
Launched at L ≈ 2 from the Volgograd region, it reached an apogee of
161.5 km.

Zarnitza carried an electron gun, and its beam was seen to travel at
least 40 km by ground observers.

No potential measurements were made.   The beam was .5 A at 10 keV.

A glow discharge was seen around the rocket, and is believed to be
connected to the return current to the rocket.   As of publication (Cambou,
1975), the relationship has not been established.

3.5   ARAKS

This is a joint French-Russian operation to study electron beams in
the ionosphere.

Two flights with an Eridan rocket have been reported.   Both were
launched from the Kerguelen Islands; the first northward on January 26,
1975, the second eastward on February 15, 1975.   Each was equipped
with electron guns operating between .5 and 1.0 amp at 15 and 27 keV.
They carried active neutralization devices, cesium plasma sources, and
various particle detectors (Cambou, 1976), (Cambou et al., 1978).

The charging data in a report by Winckler (1976) shows ϕ to be less
than 300 volts for one flight.

3.6   PRECEDE (OCTOBER 17, 1974)
EXCEDE II (APRIL 13, 1975)

These two rockets are part of a DNA/Air Force Geophysical
Research Lab project to study auroral phenomena.

PRECEDE was launched from White Sands to an apogee of 120 km.
A retarding potential analyzer was carried.   A 25 kV, .8 amp electron

beam was emitted. At 120 km, the spacecraft potential was less than 120 volts. At 90 km, it was less than 17 volts (O'Neil et al., 1978a).

EXCEDE II was launched from Poker Flats to an apogee of 137 km. The retarding potential analyzer suffered a partial failure but the spacecraft potential was less than 200 volts for the 3 kV, 10 amp beam (O'Neil et al., 1978b).

An interesting theoretical result showed that ϕ should oscillate at about 10^5 Hz. Unfortunately, this is beyond the instrumental time resolution (Bien, 1974, 1975).

3.7 JAPAN

K-9M-41 (January 17, 1973)

A wave oriented experiment was conducted in 1973 by Matsumoto (1975). An electron emitting cathode was mounted on the rocket. This provided an electron beam at about 3 eV, due to the potential of the rocket. This potential was caused by a d.c. bias on the receiving antennas.

No potential measurements were made.

A large variety of wave phenomena were seen, suggesting that the emitted electrons were escaping and exciting waves.

A similar experiment was done by Miyatake (1974) on K-9M-35.

K-9M-46 (September 15, 1974)

A carefully reported (Kawashima et al., 1978) mother-daughter rocket shot was made with a plasma gun and Langmuir probe diagnostics. No potential measurements were made.

K-10-11 (September 24, 1975)
K-10-12 (January 18, 1976)

These two successful electron beam rockets were reported on briefly by Kawashima (1976).

Both carried Langmuir probes and electrostatic analyzers. They both were fired to an apogee of 200 km, and showed potentials of only a few volts. The electron guns operated at 200-300 volts, from .3 ma to 3 amps.

There was a neutral gas release.

The following data are from a University of Tokyo book: Sounding Rocket Data in Japan, Vol. 3, (1976-1977), March 1, 1979.

K-9M-57 (Aug. 31, 1976)

This was another plasma wave/electron gun experiment.

K-9M-58 (January 16, 1977)

This was an electron beam experiment in artificial aurora production. Electron beams from 0-5 keV and 0-350 mA were used. Auroral lines were created. A potential rise was measured by a floating probe and the heating of the ambient plasma by a Langmuir probe.

K-9M-61 (January 27, 1978)

A similar operation, using a 0-2 keV, 0-35 mA beam. The vehicle potential rose to more than 60 V at 300 km and more than 400 V at 200 km when the 2 keV, 35 ma setting was used. Artificial aurora were created, indicating escape of the beam. The spatial distribution of the potential around the rocket was measured. Low frequency ($\sim$ 100 Hz) oscillations in potential and return current were seen at I_{beam} = 10 ma.

SEPAC

A proposed shuttle experiment is described by Obayashi et al. (1975).

3.8   SERT II (LAUNCHED FEBRUARY 3, 1970)

Ion thruster operations are principally represented by SERT. This spacecraft carries a mercury thruster with a hollow cathode neutralizer in a 1000 km circular polar orbit. In its first year SERT II was continually in sunlight. The thruster provides .25 amp of Hg^+ at 3 kV. The neutralizer is a low energy plasma emitter. It may nominally be biased to 0, ±25, ±50 volts with respect to the main frame. The neutralizer may be operated independently of the thruster at zero or negative bias (driving the spacecraft in the positive direction). Potentials were determined with hot wire emissive probes.

The large solar arrays had exposed conductors at an unknown (presumably positive) voltage. They could have caused some of the effects seen by serving as particle sinks, but were not generally cited (J. M. Sellen, private communication, 1977).

Passive spacecraft potentials varied from -5 to -12 volts, depending on geomagnetic latitude and whether the spacecraft was on the sunrise or sunset side of earth.

During active operations with the neutralizer at zero bias, about 1/4 amp (Hg^+) was emitted. The potential varied between -15 and -30 volts.

With the neutralizer biased, the potential could be effectively controlled, and driven to zero. Positive voltages were not obtained. The neutralizer power supply became current limited when this was attempted. A variety of loop currents could explain this, including a current to the positive spacecraft (solar array). Spacecraft potential was driven as far as 77 volts negative.

Tests using only the neutralizer were made in 1974. Potential was successfully held between 0 and -5 volts in this manner. Negative bias on the neutralizer did drive the spacecraft positive.

3.9 ATS-4 (LAUNCHED AUGUST 10, 1968)

This satellite carried a cesium ion engine identical to ATS-5's. Failure of the launch vehicle forced the satellite into a low altitude orbit (218 km perigee, 760 km apogee), but several tests were conducted.

The satellite remained attached to the launch vehicle, which provided a large surface area for return current collection.

Neutralizer current varied with altitude (density), sunlight, and beam current. Low altitude and darkness seemed to be the environment favoring a higher neutralizer current. Currents up to 346 μamps were seen, at a beam current of 387 μamp.

In the last test, spacecraft potential was measured. At a beam current of 756 μamps, there were maxima in potential and neutralizer current. These were -132 volts and 330 μamp, respectively, in daylight. It is believed that the neutralizer was emission limited, but it is not known why.

The spacecraft reentered the atmosphere shortly thereafter, and no further data was obtained (Hunter, 1969).

3.10 ATS-5 (LAUNCHED AUGUST 1969)

This satellite carries a cesium ion thruster with a hot filament electron emitter to serve as a neutralizer. The primary diagnostic is the UCSD Auroral Particles Detector. It measures ions and electrons from 50 eV to 50 keV in 64 steps. The satellite remained at 105° West longitude from launch until late 1976. It is at geosynchronous altitude spinning with a period of .8 seconds.

The thruster was designed to accelerate ions through a 5 kilovolt potential, supplying a current between .2 and 1.0 milliamp. Due to the

accidental spinup of the satellite, ordinary operation of the thruster never occurred. In spite of the difficulties the thruster was operated once in 1972 and once in 1973. Results are limited by the sparseness of the data. However, it was possible to conclude that, at geosynchronous altitude, normal use of the thruster did not alter the potential of the spacecraft, which was less than 50 volts. In a brief non-neutralized operation, the spacecraft charged to the accelerating potential (DeForest, 1973).

A much greater body of data is available from the operations with the hot filament. Preliminary reports have been given by Goldstein (1976), and Purvis (1976). The filament is a 7 mil wire, made of yttrium doped tantalum, and operates at 1750° centigrade ($\approx$. 2 eV). The filament is operated at 3.5 volts a.c. It was operated regularly in each eclipse period from fall, 1974, to fall, 1976. Particle data shows the potential dropping rapidly from thousands of volts negative to a few hundred volts negative when the neutralizer is switched on. The transition time is less than the instrumental response time. The potential rapidly returns to a value between the pre-neutralizer and initial operation values while the neutralizer is on, then resumes its pre-operation value at neutralizer off.

3.11 ATS-6 (LAUNCHED MAY 1974)

Applied Technology Satellite-6 is a large multi-purpose satellite which resembles ATS-5 in that it carries particle detectors and a cesium thruster at geosynchronous altitude.

The particle detectors cover the 0-80 keV region in 64 steps, and combine high angular resolution with the ability to rotate in two planes. The ion thruster carries a hollow cathode neutralizer which is the major difference between the thrusters on ATS-5 and ATS-6 for purposes of

this study. As with SERT II, this neutralizer is a low energy plasma source, which may be operated independently of the thruster.

On July 18, 1974, the first ion engine was operated for one hour. Attempts were made to restart the engine on July 20, 1974. Due to excessive high voltage arcing, it was impossible to restart the engine. A number of attempts were made to restart the engine over the following month, but thruster operation was never obtained.

Following the fall eclipse season, a 100 hour test was made. From October 19 to 23, 1974, the second engine was operated. Once turned off, it too proved impossible to restart.

The reasons for the failures involve problems with the cesium flow and engine contamination. The neutralizers are still usable, subject mainly to power constraints.

A neutralizer test was performed on February 26, 1976 in daylight. The effect was small, but it did show that the neutralizer was operating.

Operations during the latter part of 1976 will be discussed in a later section.

Proper analysis of the ion engine operations has not yet been done. Goldstein (1976) has done some work on these operations. Preliminary indications are that when the engine is operated, the spacecraft potential shifts to -5 volts and stays there, independent of environment. Any potential barrier is breached or destroyed. It is possible, but unproven, that ions from the thruster make their way to the detector. In the 100 hour test, an injection of high energy particles failed to cause the spacecraft to charge to a high negative potential, which is the space-craft's normal response.

One peculiar effect is the observation of electrons from the -550 volt ion accelerator electrode during the July firing (Barlett, 1975).

4.0 EFFORTS UNDER THIS CONTRACT

The objectives of this contract are listed in Figure 2. A major portion of this contract involved the reduction of data acquired in previous years to spectrograms. Spectrograms are the main method of presenting the data in this report. The format for these spectrograms is discussed in section 2.6. The approach implemented to achieve the objectives listed in Figure 2 is detailed in section 4.1.

Experiment plans were prepared to implement these objectives. These plans were prepared by UCSD personnel in consultation with both NASA/Goddard and NASA/Lewis. The plans called for special operation of both the ATS-5 and ATS-6 particle emitters and the UCSD particle detectors. They are given in section 4.2. One of the aims of the active experiments was to obtain data on the effects of particle emission on spacecraft potential during an eclipse. Because of the fact that spacecraft power is a critical item during an eclipse, only limited operations could be performed. Early operations were performed successfully and good data was obtained. As a result, additional operations were scheduled with similar success. A summary of all the active and eclipse data which has been obtained with the two spacecraft is shown in Table 4.

4.1 APPROACH OF THIS INVESTIGATION

The ion thrusters on ATS-5 and ATS-6 are not available for operation. Hence active experiments were restricted to use of the neutralizers. With this restriction, the following activities were feasible in reaching our objectives:

1. The comparison of the ATS-5 and ATS-6 spacecraft potentials, both in and out of eclipse conditions, and both with and without the operation of the neutralizers.

2. The investigation of the effects of the neutralizers as a function of local time for both spacecraft.

3. The investigation of the effects of the neutralizers during geo-
magnetic storms, for both spacecraft.

4. Operation of the low E bridge on ATS-6 to determine quantita-
tively the effect of the emitter on the potential barrier.

4.2 EXPERIMENT

August, 1976:

Operate the emitters on both ATS-5 and ATS-6 throughout a 24-hour
period. On ATS-5 the emitter should be operated for 10 minutes out of
every hour. On ATS-6 the emitter should be operated for one-half hour
every two hours.

September, 1976:

A. Select the first three days in September when ATS-5 is scheduled
for operation. During those days, operate the emitter on ATS-5 for
10 minutes during eclipse if the eclipse is less than 30 minutes in length.
If the eclipse is longer than 30 minutes, operate the ATS-5 emitter for
two 10-minute periods during the eclipse. During these same three days,
turn on the ATS-6 emitter before the ATS-6 enters eclipse, and turn the
emitter off approximately half-way through eclipse.

B. After the data from these operations have been evaluated, a plan
will be formulated for operating the emitter on ATS-6 in at least three
more eclipse days, based on the results that have been obtained.

Spring 1977

ATS-5

Based on a desire to study the time decay of the neutralizer current, two long operations were planned. Authorization was obtained to drain batteries to the danger point during neutralizer operation.

ATS-6

Based on desire to see the leading edge of the neutralizer on transition, operations were scheduled so that neutralizer ignition occurred during eclipse. Three operations were scheduled at the beginning, and four at the end of eclipse period.

Summer 1977

ATS-6

Operation of the neutralizer was scheduled in attempts to transmit cesium ions along magnetic field lines to GEOS, with the GEOS mass spectrometer as the diagnostic. This would give information on the escape of the neutralizer plasma from the spacecraft.

Operations were conducted from 164 to 178/77. (GEOS did not report seeing any cesium)

Fall 1977

Spring 1978

ATS-5

The attempts at longer operations ($\approx$ 10 minutes) are to be continued. The following plan was also developed:

ATS-5 Ion Engine Experiment Plan

To date, all ATS-5 eclipse ion engine tests have used engine number two only. The purpose of this series is to verify that the other ion engine has the same effect on spacecraft charging and to measure the effect of two ion engines operating simultaneously.

Test 1. In eclipse, operate ion engine number one in the same fashion as the previous ion engine tests as allowed by the spacecraft power budget.

1. Turn EME ON

2. Turn Ion Engine Regulation No. 1 ON

3. Turn Ion Engine No. 1 Ionizer ON

4. Turn Ion Engine No. 1 Ionizer OFF

5. Turn Ion Engine No. 1 Regulator OFF

6. Turn EME OFF

Note: Ion Engine No. 1 is on Telemetry Encoder No. 1 only.

Test 2. Operate both ion engines simultaneously in eclipse as allowed by the spacecraft power budget.

1. Turn EME ON

2. Turn Ion Engine Regulators 1 & 2 ON

3. Turn Ion Engine No. 1 Ionizer ON

4. After a 3 to 5 minute delay, turn Ion Engine No. 2 Ionizer ON

5. After a 3 to 5 minute delay, turn Ion Engine No. 1 Ionizer OFF

6. After a 3 to 5 minute delay, turn Ion Engine No. 2 Ionizer OFF

7. Turn Ion Engine Regulators 1 & 2 OFF

8. Turn EME OFF

If the power budget would allow a longer operation with both engines it would add useful information. However, if pressed for power, the test would still be useful if both engines were commanded on without delay.

ATS-6

The UCSD detectors failed in May 1977. Therefore, operations were scheduled in Fall 1977 (Days 281-285) using the University of New Hampshire experiment as the diagnostic. The Spring 1977 pattern was followed. The UNH experiment does not have the energy resolution of the UCSD instrument, but does have the possibility of finer time resolution. Operations in Fall 1977 determined that the energy range was not sufficient for our purposes, and no further analysis was done.

4.3 RESULTS

4.3.1 Data Obtained

Table 4 lists all the data collected and processed under this contract.

4.3.1.1 Passive data: eclipses

ATS-5

From 1976-8, most of the eclipses involved operations of the neutralizer. For pure eclipse data, it is necessary to go back to 1969-70.

ATS-6

This spacecraft has taken data continuously in each eclipse period from launch until fall, 1976. During portions of the fall, 1976, and spring, 1977, eclipse seasons, the detectors were in low bias, in order to extend the detector lifetimes.

4.3.1.2 Active operations

Pre-Contract

Ion engine operations occurred in 1974 on ATS-6, and one daylight neutralizer operation occurred in February, 1976. On ATS-5, neutralizer operations have been conducted in eclipse since fall, 1974.

Daylight

Under this contract, operations began with a series of daylight neutralizer tests on both satellites on August 20 and 21 of 1976. A similar series of operations was conducted on November 14 and 15, 1976. These consisted of 10 minute operations of the neutralizers. On the November dates, the two spacecraft were passing each other, providng the opportunity to obtain data in nearly identical environments.

Eclipse

Fall, 1976 experiments with the ATS-5 neutralizer followed the pattern established in previous years: enter eclipse, neutralizer on, neutralizer off, exit eclipse. Two exceptions to this schedule were on September 1 and 2, when the neutralizer was turned on before entering eclipse, in order to facilitate comparison to ATS-6 data. These operations were on the order of ten minutes long, approximately double the time of previous operations. In the spring of 1977, two operations were run. Based on a request made by UCSD, longer tests were made, for approximately fifteen and eighteen minutes.

In Fall, 1977, several changes were made. Previously, engine No. 2 had been used. It is possible that operation of the main thruster had changed the filament in some way. To check for possible differences, the neutralizer from engine No. 1 was operated. Also, the two neutralizers were operated in tandem, giving a new, unique, data set.

The first operation of the ATS-6 neutralizer in eclipse occurred in September, 1976. In these first tests, the neutralizer was turned on before entering eclipse, and then turned off in eclipse. This pattern was considered safer for the satellite. In spring, 1977, ATS-6 operations were again conducted in eclipse. The neutralizer was turned on and off in eclipse in these tests, duplicating the ATS-5 pattern.

ATS-6 operations after this time did not produce any useful data.

4.3.2 Data Reduction

ATS-5

All available data tapes have been received for the 1974 to 1978 eclipse seasons, reduced, run as spectrograms, duplicated, and delivered under this contract.

ATS-6

All of the data tapes for ATS-6 operations have been received, processed into spectrograms, duplicated, and delivered.

4.3.3 Analysis

4.3.3.1 Passive data: eclipses

A large data bank exists for eclipses of ATS-5 and ATS-6. A qualitative summary follows.

Spacecraft charging is in general at maximum in the midnight to dawn region. Effects are even more dramatic during eclipse. The photoelectric current, one of the major factors in the current balance at this altitude, disappears. The particle flux now determines the charge balance, and when the ambient plasma is highly energetic, potentials from 5 to 10 kilovolts can be observed. At the opposite end of the spectrum, the ambient plasma may be relatively cool, resulting in small potentials on the spacecraft. In this case, the spacecraft seems to ride at a slight positive potential before eclipse. Then, with the photoelectric current vanishing, the spacecraft shifts to a slightly negative potential. This reveals the previously hidden low energy ions. The low energy electron band disappears, which is largely explained by the disappearance of photoelectrons, but may also be due to the absence of secondaries trapped by a potential barrier around the spacecraft. Note that information on low energy data ($E < 50$ eV) and low potentials ($|\phi| < 50$ V) is from ATS-6 only, because of the different instrument ranges.

It is necessary to understand these effects to cope with the thruster data. Particularly, the behavior of spacecraft potential during thruster operation mimics the low energy shift seen in some eclipses.

The major quantitative result to date involves comparison of data between the two satellites (see Figure 7). In fall, 1974, ATS-5 and ATS-6 were 10° apart in longitude. The two completely dissimilar spacecraft charged to roughly the same potential when both were in eclipse. This encourages us to believe results from these satellites may be generalized to other flights (Purvis, 1976).

Reduction of ATS-6 data to spectrograms for recent eclipse seasons reveals data that falls into three main categories. The first is the no change category. A satellite riding between plus 5 and minus 5 volts undergoes no change as it enters eclipse beyond the disappearance of the low energy electrons attributed to photoelectrons. (The resolution limit is 3-5 volts in this region.) Second is the small negative shift category. Here, the potential seems to drop from a few volts positive to a few volts negative, revealing a low energy band of positive ions. Lastly is the dramatic change category, where the spacecraft charges to kilovolt potentials. Spectrogram 1, from October 2, 1975, displays categories 2 and 3 very well.

The first distinguishing feature is the bright band of low energy protons beginning with the eclipse at 20:57. Note also the disappearance of the low energy band of electrons. Then, at 21:22, an injection of high energy particles occurs, as seen by the wide bands of electrons and ions reaching above 10 kilovolts. These particles cause the spacecraft to charge to about -3000 volts. This is shown by the absence of ambient ions below this energy, with an abrupt transition from no particles to an extremely high count rate. (The thin black line along this boundary is caused by the overflow of the gray scale to the next level.) When the eclipse terminates at 22:00, the spacecraft immediately drops to about -50 volts, with most of the ambient particles now visible.

Category 2 mimics the behavior of the particle data in operations of the neutralizer and the thruster on ATS-6 when it is at low potentials. (The energy range that permits differentiation between categories 1 and 2 is not available on ATS-5.)

It is possible that cases 1 and 2 are differentiated by the presence (or lack) of low energy ions.

4.3.3.2 Active operations

ATS-5 Thruster Operations

A large quantity of old data was reduced under this contract. Part of this data has been reported on by Purvis (1976).

A data printout for September 20, 1974, was reduced to graphical form in Figure 8. Spectrogram 2 displays the same data. The transitions at 6:31:30 and 6:36 correspond to neutralizer on and off commands. There is an immediate drop in the magnitude of the potential when the neutralizer is switched on. The speed of the transition is beyond the time resolution of ATS-5. It is not known how close to zero volts (or the detectors 50 volt lower limit) the spacecraft is driven. The magnitude of the potential then begins to rise to an equilibrium with an apparent exponential behavior.

In the great bulk of ATS-5 spectrograms, it is apparent that switching on the neutralizer (the electron emitting filament) does drive a negatively charged satellite back towards zero potential. (See Figure 9.) The potential for neutralizer on is from the end of the operation. The success of the neutralizer is not always clear, partly because of the lack of data in the 0-50 volt region.

During some operations, an overshoot in potential is seen at the neutralizer off command. Typically, the magnitude of the potential rises to 10 or 20% more than its pre-operation value, and then returns to that value within 20-40 seconds. This is seen in Figure 11 at 04:30.

Operations of the neutralizer caused no visible change in the data when the initial potential was less than 50 volts in magnitude.

Operations in the second year of this contract provided some surprises. Until this time, only the neutralizer from I. E. #2 was used. Operated singly, the I. E. #1 neutralizer appears to have given similar results to those obtained previously. Operations of the two together gave an unusual result, illustrated in Figures 10 and 11, for days 50 and 59 of 1978.

The switching on of a second neutralizer had a small effect on the spacecraft potential. More startling is the drop in potential when the first neutralizer is turned off! This result is tentatively ascribed to a buildup of differential charging, but no calculations have been done to explain the result.

ATS-6 Thruster Operations

The initial operation of the ion thruster occurred on July 18, 1974. The results are displayed in Spectrogram 3. In a brief operation, the spacecraft was apparently taken to a slightly negative potential, with any differential charging of the spacecraft greatly reduced. This can be seen in the great reduction in intensity of the broad band of secondary electrons (0-100 volts) at 3:10 when the neutralizer goes into full operation for 5 minutes, and again from 3:31 to 4:03 and from 4:10 to 4:35. The thruster was on in the latter two time periods, which may be the reason for the greater number of low energy ions. This could either be due to a different potential on the spacecraft or to the abundance of cesium ions. Electrons can be seen at 550 volts during the engine operations. These have been attributed to secondary electrons from the accelerator grid of the engine.

The second test ran for 92 hours. It is displayed in Spectrogram 4, which covers day 292, hour 0, to day 296, hour 12. The engine ignited at 8:01 UT on day 292. A low energy band of ions immediately appears. This band continues with small variations throughout the test. (The white indentations occurring between hours 12 and 24 of the first three days are instrumental temperature effects and may be ignored.) This low energy band of ions may be attributed to cesium ions from the engine or ambient ions brought in by a shift in the potential. A negative drop of a few volts in the potential is consistent with both of these explanations.

There are two large injections of energetic particles, the first beginning at approximately 3:00 UT on day 293, the second at about 6:00 UT on day 295. Two injections of slightly lower energy particles occur on days 294 and 296. Charged particle injections have caused ATS-6 to fall to potentials of several hundred volts below ground in daylight. The engine may therefore be compensating for the change in

37

the particle flux. It does hold the satellite within a few volts of ground throughout the test.

The low energy band of electrons associated with differential charging disappears when the engine is switched on. More detailed analysis (Olsen and Whipple, 1978) showed that before 08:00 UT on day 292, a barrier of about -100 volts existed. The spacecraft potential dropped from -50V to near zero at 07:40 UT, when the neutralizer ignited. The differential potential, as seen in the trapped electrons, persisted until 08:07, when the main thruster ignited.

ATS-6 Neutralizer Operations

Daylight Operations

The first daylight operation of a neutralizer occurred at the beginning of the ion engine operation on July 18, 1974. The ability of the neutralizer to push a positive spacecraft negative was demonstrated. By this the neutralizer showed its ability to emit ions when in spot mode.

Some of the highest quality data was obtained during the restart attempts of engine No. 2 on July 20 and July 21, 1974. Only preliminary analysis was done, but the neutralizer demonstrated its ability to shift the spacecraft potential, with only a mild effect on differential charging. These tests showed that electrons could be emitted when in plume mode.

There was a neutralizer operation at the beginning of the October 1974 test as well. It showed the ability of the neutralizer to supply electrons in plume mode. Differential charging was reduced but not eliminated.

There were neutralizer operations during restart attempts after this test, but they have not been analyzed yet.

A neutralizer test was performed on February 26, 1976, in daylight. The effect was small, but it did show that the neutralizer for ion

38

engine 1 was operating and successfully altering the spacecraft potential, while engine no. 2 was completely lost.

During the contract period, two sequences of daylight operations occurred. Spectrogram 5 shows two of the neutralizer operations from August 20, 1976. The effects of particle emission can be seen at hours 8 and 10 in the low energy bands of ions appearing at these times. In the 24 hour spectrogram (not shown) a slight diurnal variation in the potential is seen. This shift, on the order of a volt in magnitude, is not seen on spectrogram 6 for November 14, 1976. This shift may be due to an instrumental temperature dependence.

If these low energy bands are ambient ions, we are seeing a slight negative shift in the potential, bringing into view previously unseen particles. If so, we are seeing the same behavior as in a category 2 eclipse. Another possibility is that we are detecting particles from the neutralizer.

On November 14, 1976, the operations at 11:35 and 13:35 took the spacecraft from -100 volts to within a few volts of ground. The reduction in secondary electrons implies the differential charge on the satellite has been reduced. At 11:35, the barrier seems to drop from 40 volts to 15 volts, while at 13:35 it drops to approximately 0 volts.

Operations in Eclipse

Neutralizer operations during eclipse seasons have been difficult to examine because of degradation in the low energy channels.

Fall 1976

The neutralizer was ignited before the spacecraft entered eclipse. This ignition was difficult to observe in the spectrograms. Generally, ignition came at low potentials and the change in particle data was small. The main effect was the disappearance of the normal low energy band of electrons. It is believed that this corresponds to a shift in potential combined with the breaching of a potential barrier (Whipple, 1976b).

Movement of the spacecraft into eclipse brought small changes in the particle data. Normally, this transition is marked by the disappearance of the low energy electron band attributed to photoelectrons, but these had already disappeared. There were small shifts in potential at this time. Several of the low potential phenomena occurred on October 14, 1976. (See Spectrogram 7.) The pertinent times are:

Neutralizer ignition	03:50
Spot mode	03:57
Full eclipse	04:13
Neutralizer off	04:21
Exit eclipse	04:29

The normal daylight behavior is seen when the neutralizer enters spot mode. Low energy electrons (photoelectrons) disappear, while a low energy band of ions appears. This signals a shift from a few volts positive to a few volts negative. Upon entering eclipse, the spacecraft potential drops a few volts more negative. When the neutralizer is switched off, the spacecraft moves back up a few volts, and then goes positive again upon exiting eclipse.

On a few days, operating the neutralizer caused a dramatic change in the particle data. One such event occurred on September 3, 1976. It is displayed in Spectrogram 8. Significant times here are:

Neutralizer ignition	00:03:00
Begin entering eclipse	00:17:55
Full eclipse	00:20:50
Neutralizer off	00:30:35
Begin exiting eclipse	00:52:00
Full sunlight	00:54:55

A low energy band of electrons (0-10 volts) appears at 00:09 and persists until the neutralizer is turned off. This is directly contrary to

expected behavior, or at least the behavior seen on previous occasions. An equally peculiar feature is the low energy band of ions (0-10 volts) running from 00:19 to 00:27. The beginning may correspond to entering eclipse, but the end does not correspond to any known event. As with the previously seen ions, these may either be from the neutralizer or the ambient plasma.

Once the neutralizer is turned off, it seems to take the satellite approximately two minutes to charge to -4000 volts. This is a typical potential for ATS-6 in eclipse, and is probably the potential it would have charged to without the neutralizer operation. This implies that the neutralizer was succeeding in keeping the satellite from reaching its normal potential in such an environment. Upon leaving eclipse, the potential rises to about -100 volts, again with about a two minute time constant.

Spring 1977

The early eclipse season operations came during a quiet period for magnetic activity, and little new information was obtained. However, at the end of the season, on days 97 and 98 of 1977, we obtained our most impressive data. On these days the neutralizer ignition and turn-off both occurred in eclipse.

Data from day 98 is displayed in Spectrogram 9, with analysis results in Figure 12. The spacecraft is fully eclipsed by 9:07, and exits eclipse at 9:36. The potential swings negative upon entering eclipse, then back toward zero upon exiting. This is the normal behavior of the satellite in an energetic environment. The 0-500 volt error bars reflected the lack of low energy particle data (a detector sensitivity problem). The data shows that at 9:12 the neutralizer ignites, promptly discharging the satellite. Entering spot mode at 9:22 has no visible effect on the spacecraft. Switching the neutralizer off allows the spacecraft to charge back up to its previous equilibrium potential.

41

4.3.3.3 Differential Charging

A portion of our support went toward the analysis of differential charging on ATS-5 and ATS-6.

Two types of differential charging behavior have been noted on ATS-5 and reported by DeForest (1973). The first is the establishment of a barrier to low energy electrons the second is the return of the spacecraft generated ions to our detector.

Spectrogram 10a shows the first effect occurring on Nov. 30, 1969, between 0500 and 1100 UT. During this time, there is an absence of electrons below 500 eV. At the same time, there is a modulation in the low energy ion data. The pattern is caused by the beating of the energy scan frequency and the spin of the spacecraft. No such effects are seen in the perpendicular detector (Spectrogram 10b).

The same phenomena are seen on October 16, 1969, with an additional factor. The data from this day are seen in Spectrogram 11. Here, the spacecraft was in eclipse between hours 6 and 7. The differential charging effect goes to zero about 20 minutes after entering eclipse. During this period enhanced electron fluxes are seen below 100 eV. These could be electrons coming from the differentially charged surface as it discharges. The differential charging takes about 20 minutes to build up after the spacecraft exits eclipse.

These effects have been attributed to the thermal louvers adjacent to the parallel detector inside the spacecraft. The surface of the louver is insulating. When the sunlit spacecraft is tilted perpendicular to the sun, the louver is eclipsed, and charges negatively with respect to the spacecraft. This effect does not occur in the summer months, when the louver is illuminated.

Spacecraft generated ions are identifiable during charging events. During the eclipse on Sept. 20, 1969, the spacecraft charged to several

kilovolts. The perpendicular detector saw ions below the spacecraft potential. The most likely source for these particles is ions sputtered from a surface at a different potential than the main-frame.

On ATS-6, differential charging takes a different form. We commonly see a barrier of about a hundred volts returning secondary electrons and photoelectrons to our detector (Whipple (1976b)). In a companion paper, Whipple (1976a) showed that sheath effects could not produce the observed results, and that differential charging is the culprit.

The effect is seen in Spectrogram 12, on September 5, 1974. Between hours 9 and 10, the spacecraft is charged to about -200 volts, and there is a barrier of about the same magnitude. The barrier is marked by light spots near 100 eV in the electron data. Since these spots always come at the maximum energy of the differential charging barrier, they must come from the source of the barrier, or another surface at a similar potential. For this reason, the spots were studied to determine their source and its characteristics. Our hope is to use these results to model the fields causing the phenomena.

The spots are also given the name 'spike.' The latter name is given because of the shape of the line plots for these high fluxes. Such data can be seen in Figure 13, a line plot for Sept. 5, 1974.

These spikes have very little structure so most of the particle distribution is fitting inside one channel. The channel width ΔE is 0.20 times the channel energy, so the temperature of the particle flux must be several times lower than the energy at which the flux is measured. This fits nicely with the model of secondary fluxes coming from a differentially charged surface to our detector. On rare occasions, magnetically returned electrons have been seen, but the spikes usually occur independently of the magnetic field orientation. Electrostatic forces must be the cause.

Whipple studied the data from day 248/74, and found a strong energy and angle dependence for the charging spikes. He identified two different sources for the fluxes (see Figures 14 - 16). The higher energy spike

43

came at low detector angles (≈ 40°), while a lower energy spike comes in at ≈100°. The 140 eV spike was attributed to particles coming from the solar arrays or dish antennae, while the 100 eV, 100° spike can probably be assigned to a more local (EME package) source. The major point of this data is that there are two distinct sources of electrons that are returning to our detector. It is possible that one of the sources is creating the dominant field, and resulting barrier.

Thirteen days with charging spike data were studied and reported on by Johnson (1978). The data set studied was:

Day	Year	Time (UT)
186	1974	03:30 - 07:00
188	1974	03:00 - 07:30
195	1974	03:00 - 15:00
197	1974	03:30 - 10:00
201	1974	05:30 - 08:00
203	1974	08:00 - 10:00
206	1974	04:00 - 06:45
236	1974	04:30 - 08:30
266	1974	07:00 - 08:15
297	1974	06:30 - 08:00
299	1974	06:00 - 10:30
33	1975	09:30 - 10:30
66	1976	20:30 - 23:00

The first result to notice is that differential charging events have the same local time distribution as spacecraft charging (i.e. ≈ local midnight). (See Figure 17.) This is not a surprising result, since the high energy electron fluxes which cause large negative spacecraft potentials come in these same regions.

Further statistical results are that such spikes are seen at all detector angles in the North/South head. (See Figure 18.). The two

peaks in Figure 18 may again represent two different sources. Data from day 236/74, for example, showed the spike at ~100° over several hours of time. The spikes occurred over the complete range of pitch angles, further reducing the likelihood of magnetic causes.

Since the spikes are considered to come in at an energy equal to (or greater than) the differential potential of their source, a study of their energy should show how the source potential varies. Figure 19 shows the spike energy versus the spacecraft potential. The spike energy rarely exceeded 280 eV, and over 80% stayed below 150 eV. The same charging processes are occurring on insulator and spacecraft, but the insulator charges more negatively. Leakage currents may limit the differential potential that is developed. The difference in potentials would be due to a difference in photoelectric yield, illumination, or secondary yields.

A study of day 33, 1975, sheds some light on the question. Spectrogram 13 and Figure 20 show that between 10:06 and 10:15 UT as the detector potential increases, so does the spike energy. The solid line is from a least square fit of the logarithms of the spike energy and potential. The temperatures of the distributions in the spikes also increases from 30 eV to 50 eV. This is reasonable for secondary or backscattered electrons, but not for photoelectrons (Knott, 1972).

Candidates for the source of the spike have included the solar arrays and the dish antenna, but evidence was found to bring us back to our neighbor, the University of Minnesota Electron-Proton Spectrometer.

The local midnight condition corresponds to the time when the "top" of the EME package is shaded. Without a photoelectric current, it is easy for an insulator to go negative with respect to the main spacecraft. Most of the EME package is covered with a conducting gold foil, and a thermal blanket (also conducting). The U.M. experiment is coated with an insulating white paint, and sticks out of the EME box (see Figure 21). One of the heads rotates, stepping 15° every 8 seconds. It is essentially a cube, but the detector face makes it non-symmetric.

45

Our most convincing evidence came on August 24, 1974. The spacecraft potential was $\approx$ -55 V while the spots were reaching our detector at $\approx$ 60 eV. The north/south detector was set to dwell at 61 eV, looking only at the electron flux. In Figure 22, we see what happened when the U.M. experiment head rotated from 345° to 360° (north). There was a dramatic increase in the flux of secondary electrons in the differential spike at 04:34:46. The change in the flux occurred within milliseconds of the University of Minnesota command to rotate. (In terms of counts, the jump was from 8,000 to 21,000.) The gradual change in flux during this period is due to the rotation of the UCSD detector. Eight seconds later, the UCSD detector scans through this energy and the flux has dropped back to 4,000 counts. This evidence supports the idea that the University of Minnesota rotating detector is a source of accelerated electrons, and possibly for the barrier around the EME package.

4.3.4 Summary

A large data bank has been acquired and reduced to spectrogram form. For ATS-5, we have several years of data involving electron emission to study. It appears that the electron emitter on ATS-5 effectively modifies the potential of the negatively charged satellite, but that it does not ground the spacecraft to the ambient plasma.

Reduction of several years of ATS-6 eclipse data has revealed a rich variety of phenomena both at high and low potentials. The low potential data has been interesting because of the similarity to some of the data from engine operations. Data taken at high potential provides us with an opportunity to determine which particle spectra cause such charging.

Eight experiments were conducted with the ion engine neutralizer on ATS-6 in 1976, and seven were made in the first 100 days of 1977.

This and earlier data have been reduced and given preliminary analysis. As with eclipses, the effect on the spacecraft depends on the particle environment. The ion engine seems to completely dominate all other particle sources, bringing the spacecraft within a few volts of ground and holding it there. Experiments with the smaller plasma bridge (the neutralizer) are not as overwhelming to the spacecraft but seem to hold it near ground before, during, and after the transition into eclipse. When the spacecraft was in sunlight, operation of the neutralizer reduced the differential charge on the satellite, but did not eliminate it.

5.0 RECOMMENDATIONS

This contract supported a preliminary analysis of a rich data set. Analysis of the collected data is continuing. Potentials on the spacecraft surfaces need to be determined, particularly on ATS-6, where the structure is extremely complicated. Coincident with this work should be analysis of the particle fluxes to and from the spacecraft. Special attention should be paid to the time dependence of the particle distribution originating from the thrusters and neutralizers.

Experiments should be conducted on the SCATHA satellite to confirm our results on steady state behavior. New experiments should pay special attention to variations in the spacecraft potential as a function of time.

Acknowledgments
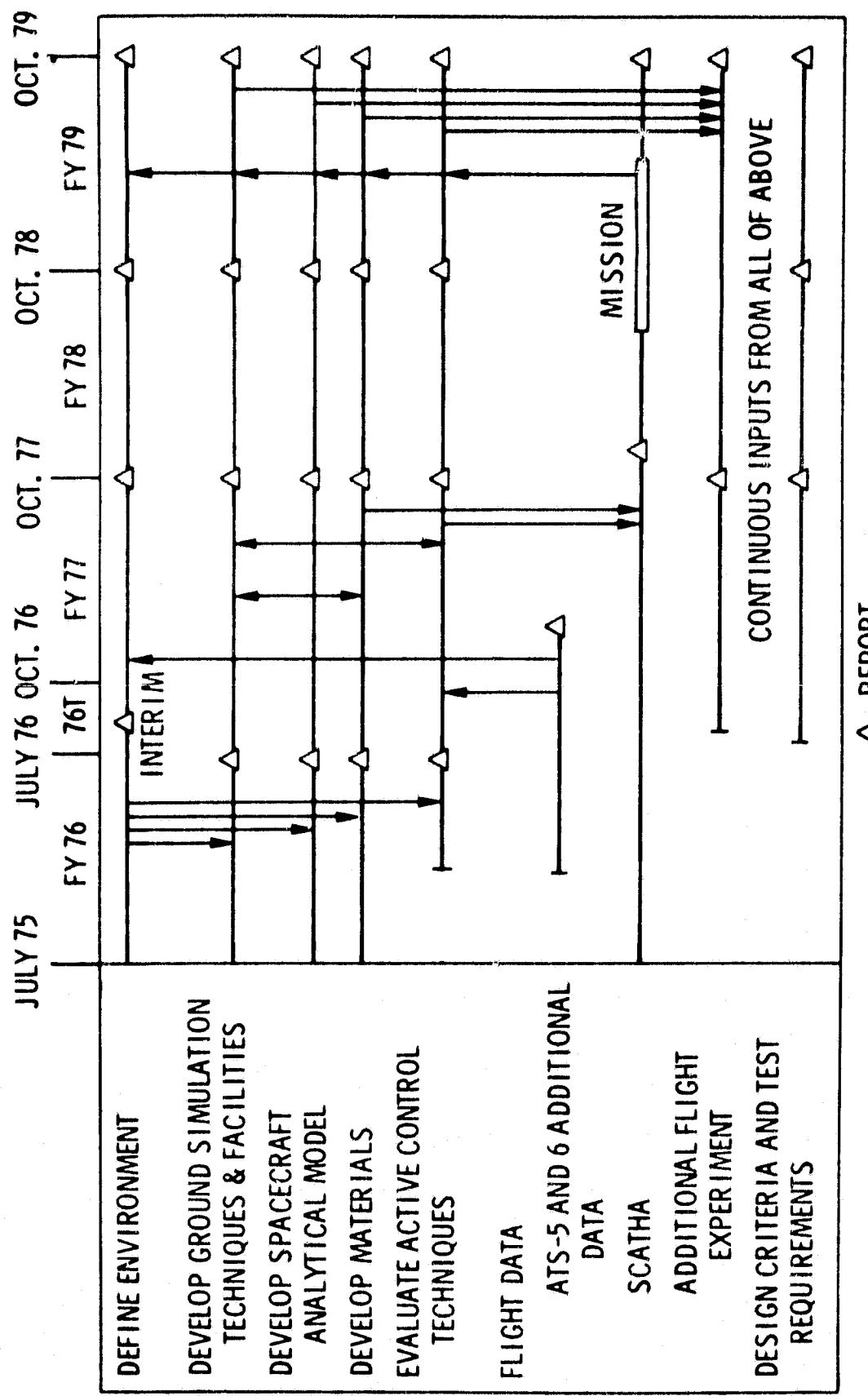
Figure 1. Schedule for Spacecraft Charging Investigation

△ REPORT

Objective

Study feasibility of actively controlling spacecraft
potential by charged particle emission

Approach

Conduct experiments using:

        -- ATS-5 electron emitter

        -- ATS-6 plasma emitter

        -- UCSD particle instruments

Analyze particle data to obtain:

        -- Spacecraft potentials with and without
          particle emission in various environments

        -- Differences in the effectiveness of electron
          and plasma emission

Figure 2. Objective of investigation

THERMAL LOUVERS

UCSD ‖ DETECTOR

ION ENGINE NO. 2

UCSD ⊥ DETECTOR

ION ENGINE NO. 1

ATS-5 SPACECRAFT

79C0·6·004
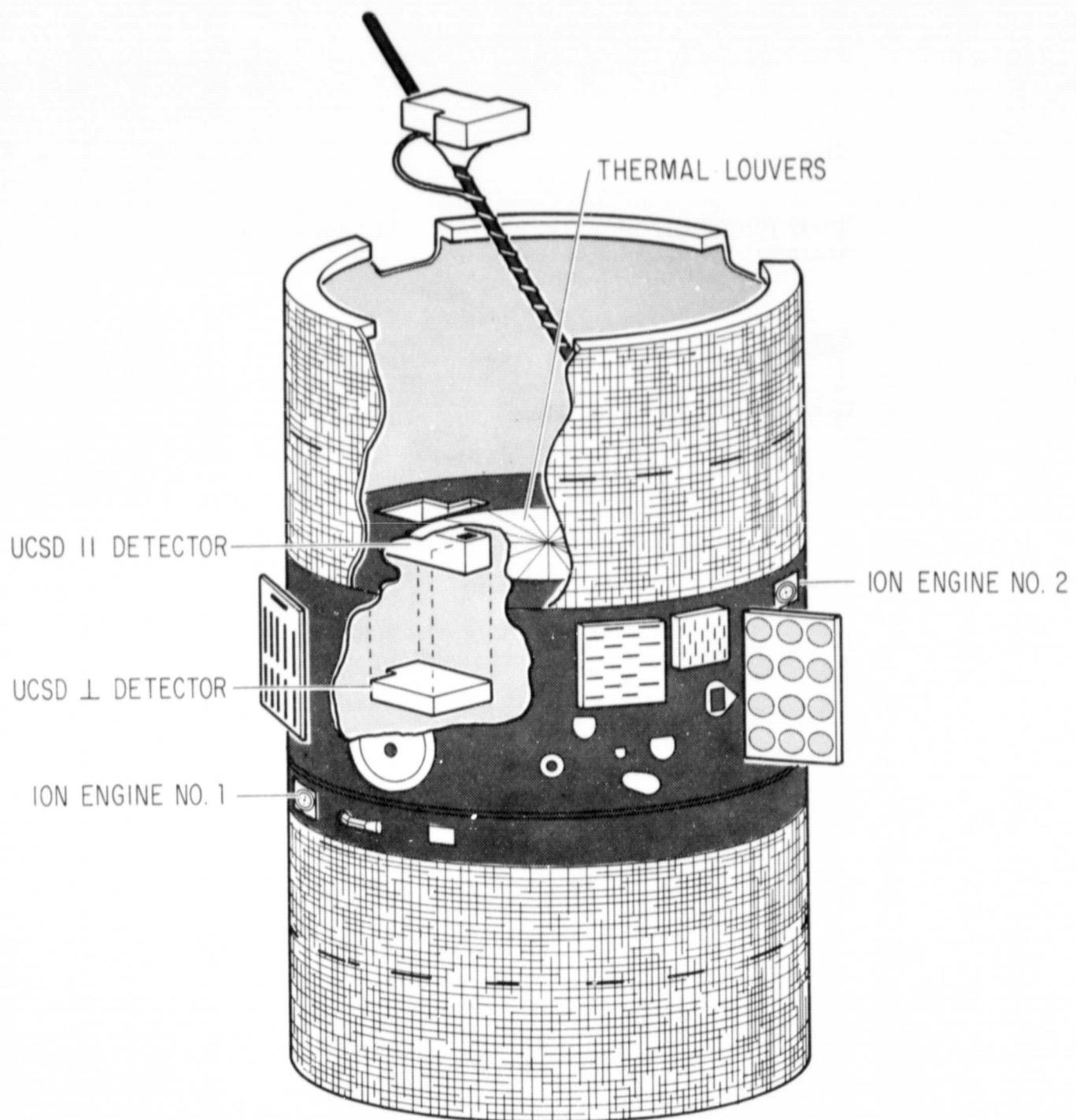
FIGURE 3   ATS-5 DETECTORS AND ION ENGINES

NS Sensor Head

UCSD Auroral Particles Experiment

EW Sensor Head

Solar Panel

Ion Engine 1 (North Face)

30' Dia. Parabolic Reflector

Ion Engine 2 (South Face, Hidden)

+Y
+X
+Z
(EARTH)

+Z(EARTH)
E
+X
N-Y
13°
+Y S
-X
-Z(OUT)
W

N,E,Z = EWE AXES
X,Y,Z = ATS S/C AXES
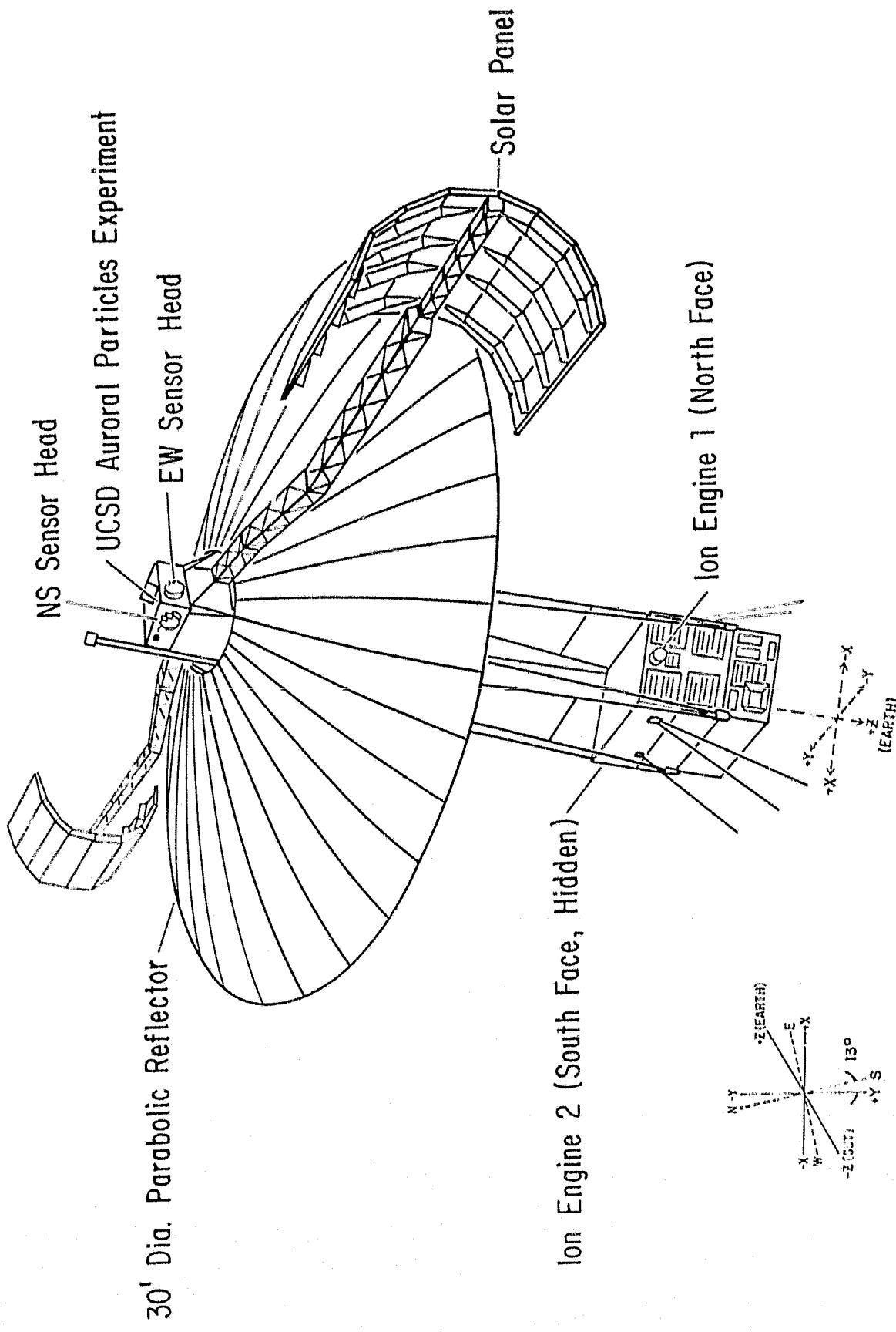
Figure 4. ATS-6: Detectors and Ion Engines

Figure 5. ATS-5: Thruster

SPLIT SEGMENTED
ELECTRODES
ACCELERATE & VECTOR
CESIUM ION BEAM

- 2000 VOLTS POTENTIAL

ELECTRONS INJECTED
INTO CESIUM
ION BEAM

NEUTRALIZER
HEATER
(1750° C)

HIGH
VELOCITY
NEUTRAL
CESIUM
PLASMA

DECELERATING
ELECTRODE

GROUND POTENTIAL

Cs⁺

POROUS TUNGSTEN
BUTTON
(CESIUM IONS ARE
GENERATED AT SURFACE)

+ 3000 VOLTS POTENTIAL

IONIZER
HEATER
(1100° C)

CESIUM VAPOR
FEED TUBE

VAPORIZER
HEATER
(350° C)

POROUS NICKEL WICK
(FEEDS LIQUID CESIUM)

ZERO-G
CESIUM FEED
SYSTEM & RESERVOIR

BI METAL
THERMAL VALVE

FIGURE 6: ATS-6 THRUSTER

Figure 7. ATS·5 and ATS·6: Comparison of Passive Spacecraft Potentials
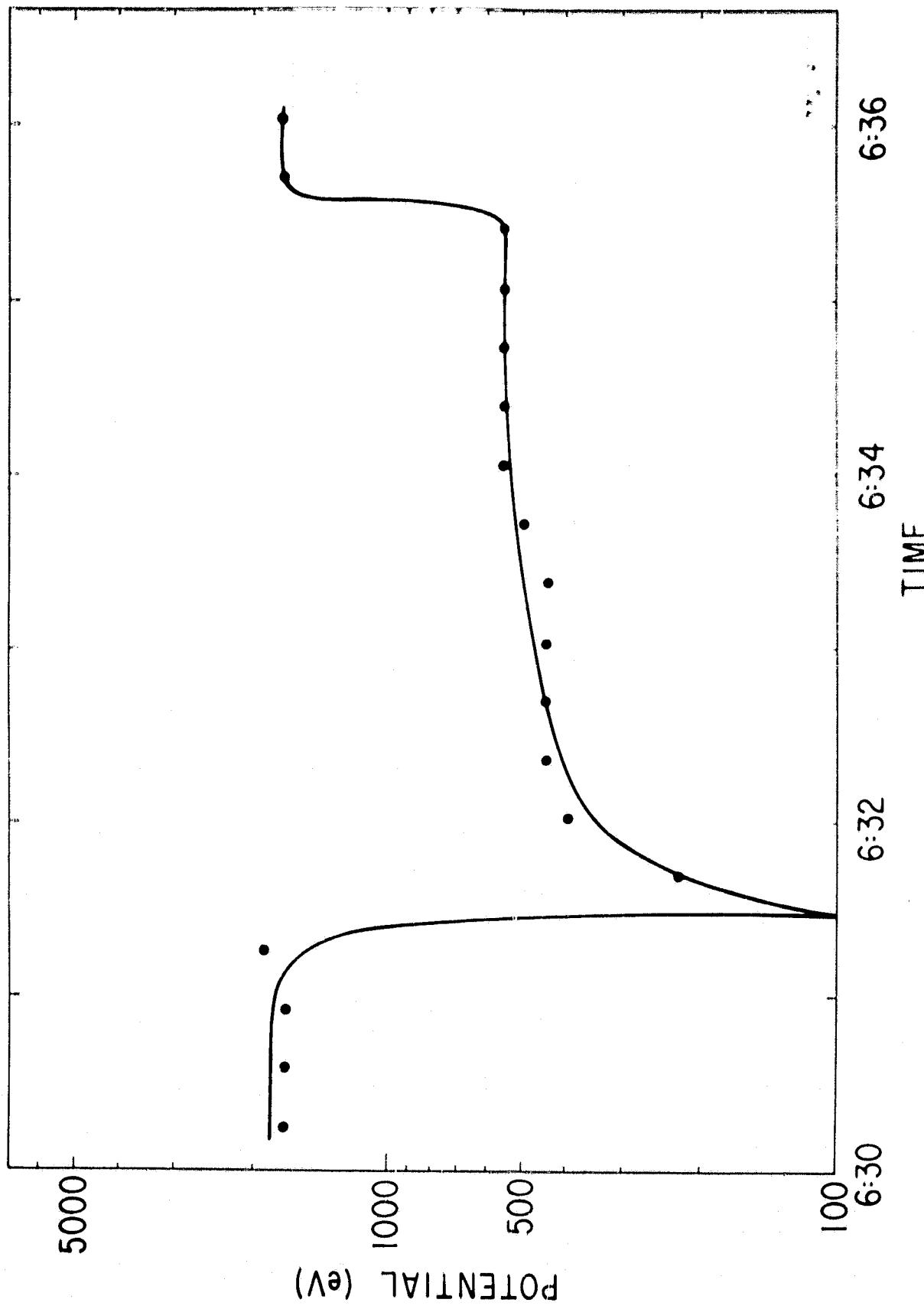
Figure 8. ATS-5: Potential During Eclipse/Neutralizer Operation 9/20/74
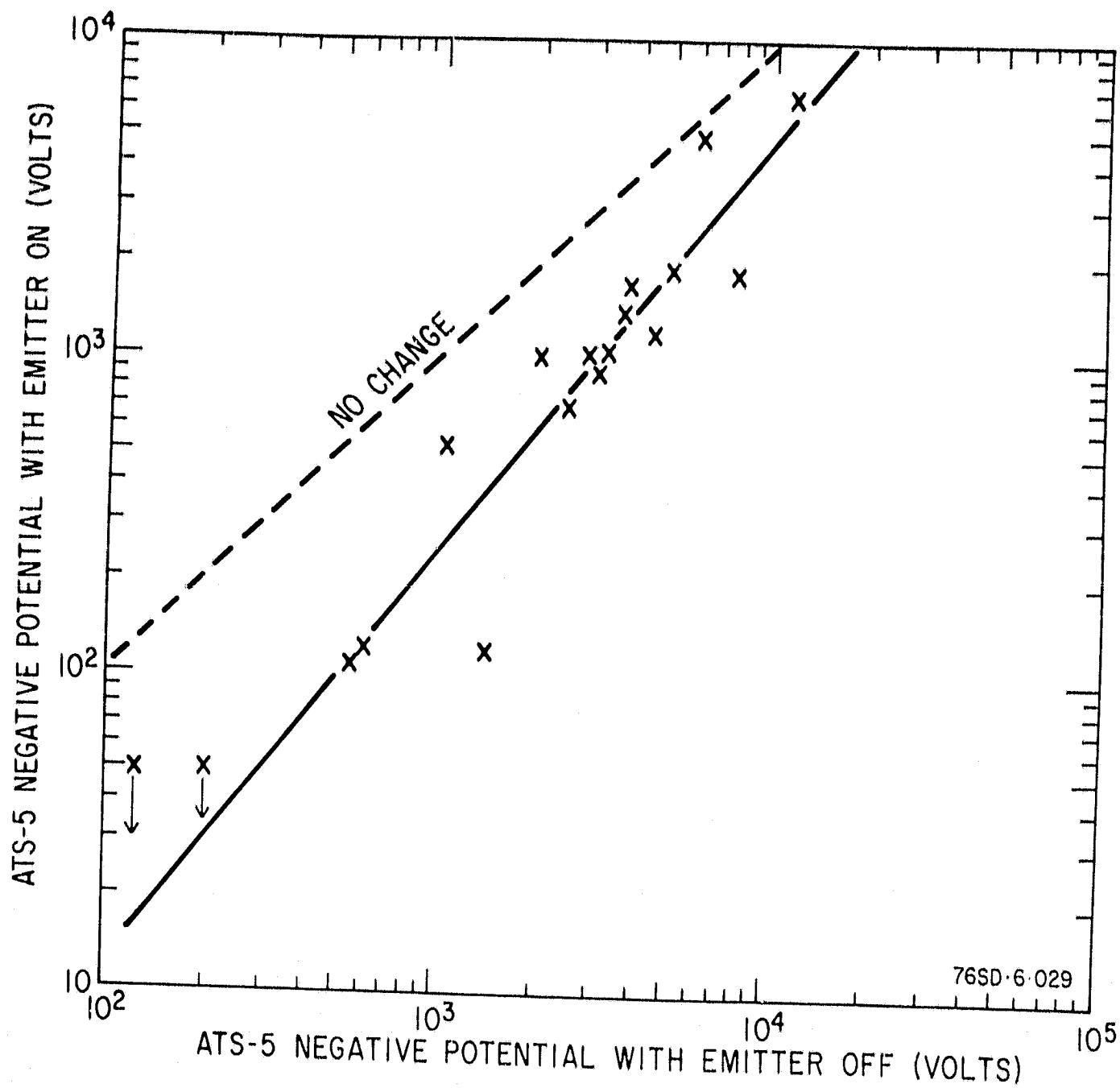
Figure 9. ATS·5: Effect of Electron Emitter on Spacecraft Potentials
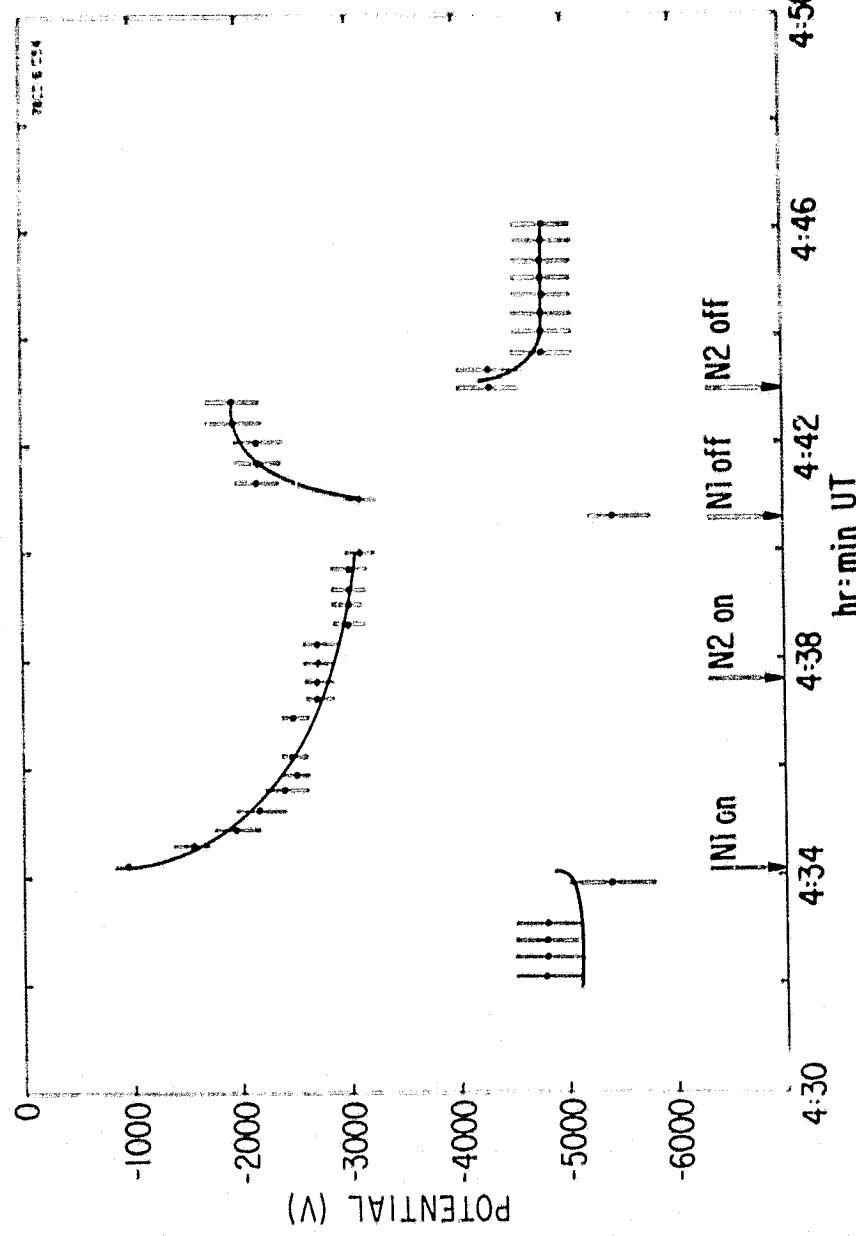
FIGURE 10: ATS-5 NEUTRALIZER / ECLIPSE OPERATION 2/20/78

57
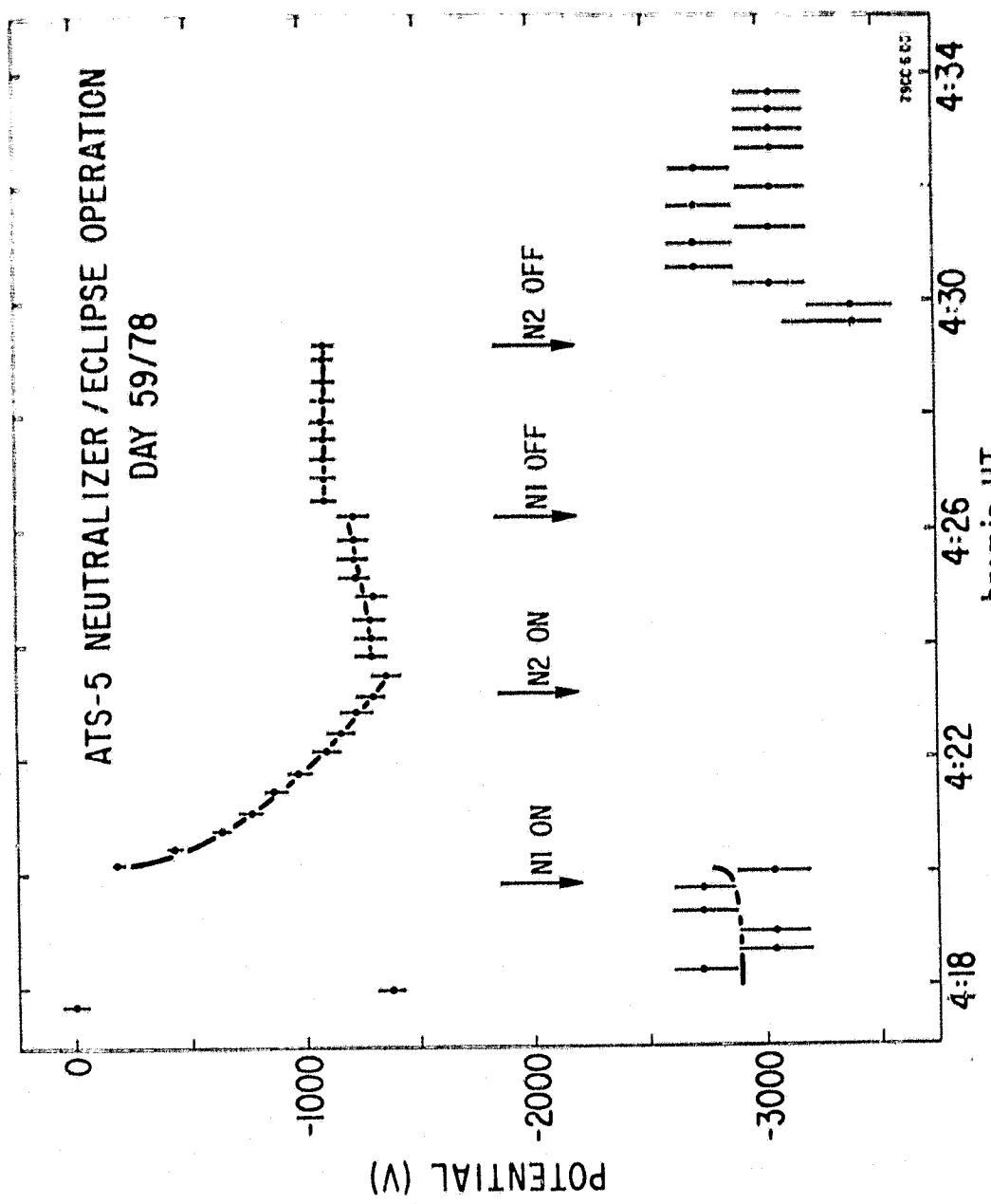
FIGURE II: ATS-5 NEUTRALIZER/ECLIPSE OPERATION 2/28/78
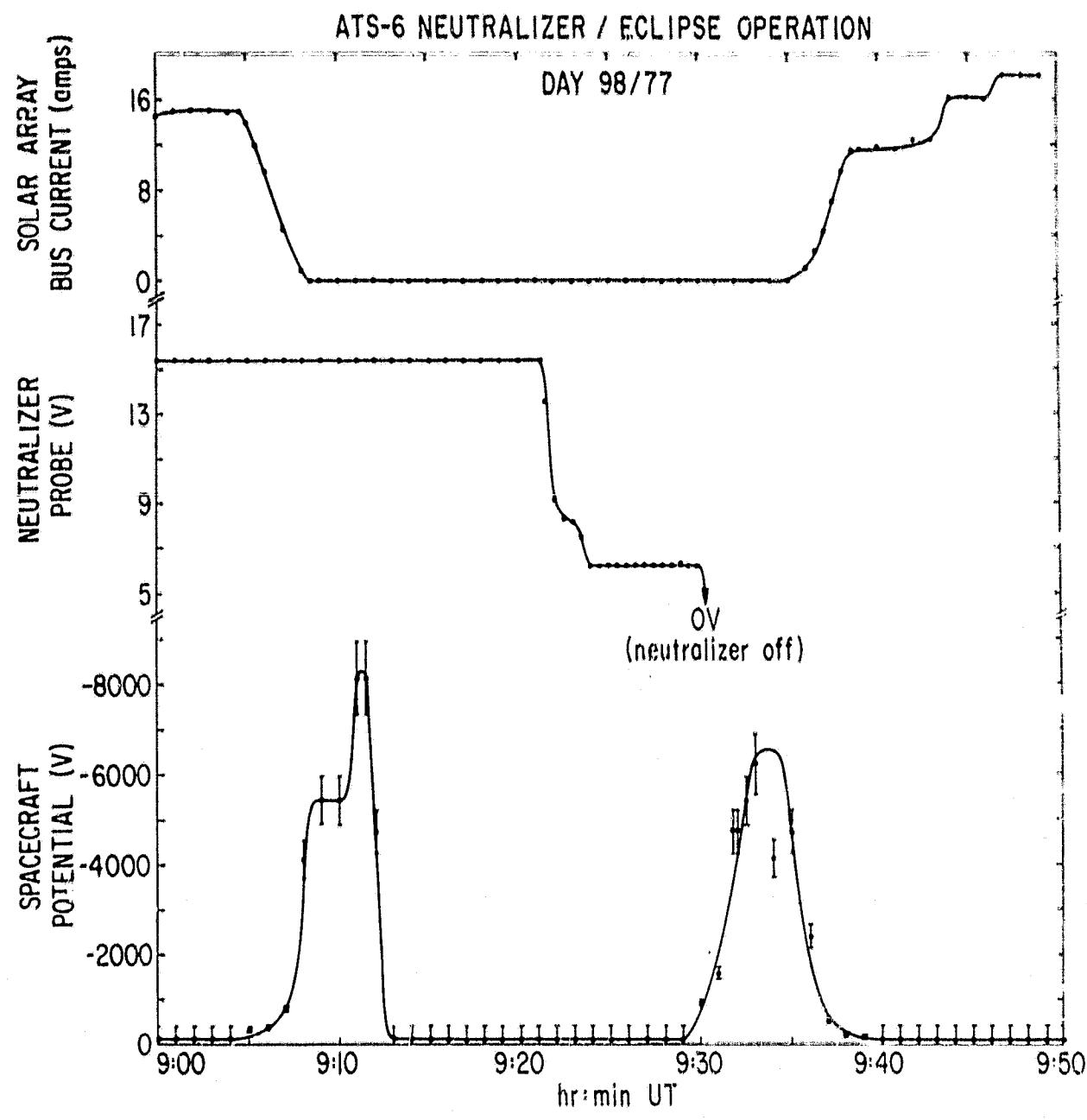
FIGURE 12: ATS-6 NEUTRALIZER / ECLIPSE OPERATION 4/8/77
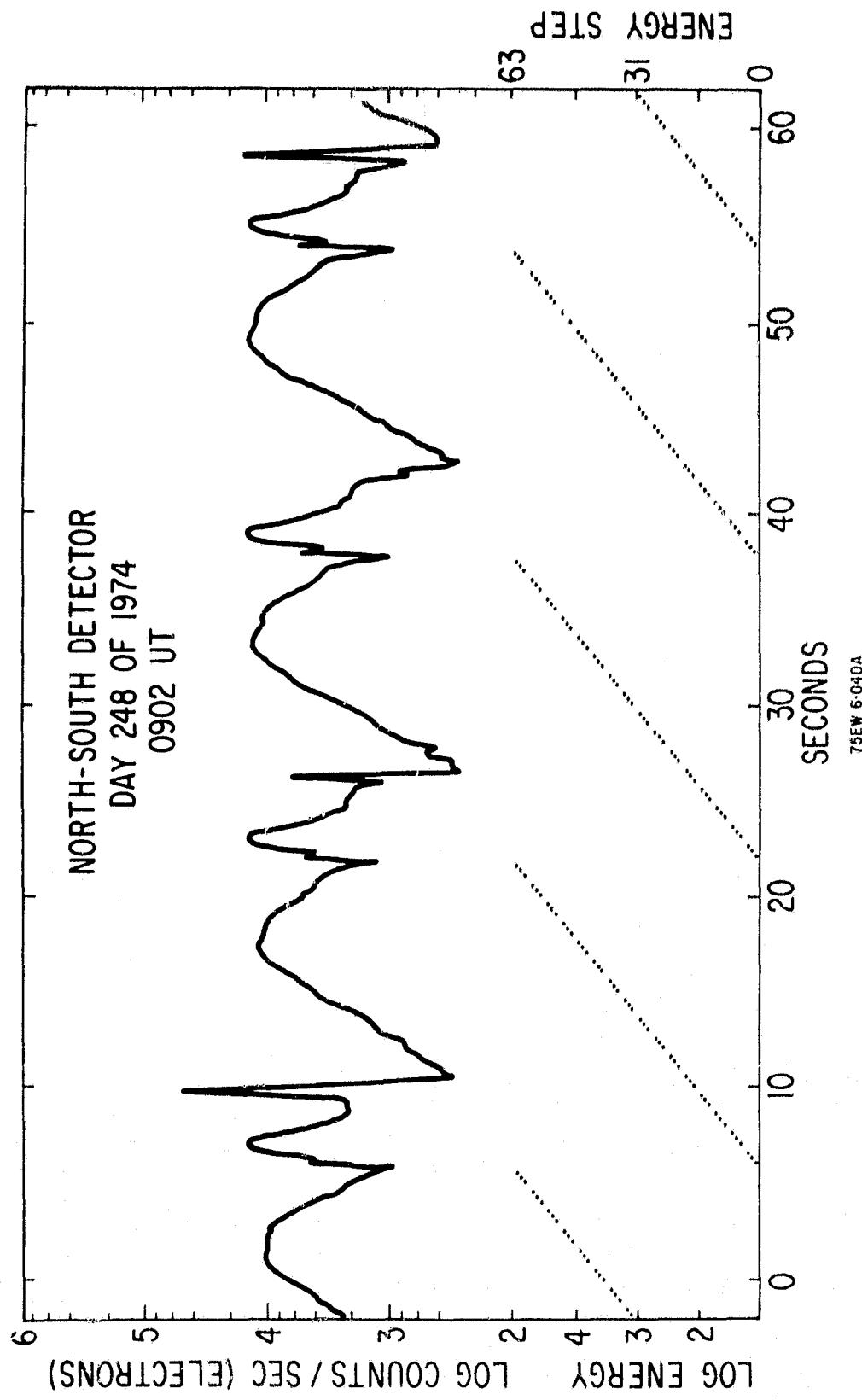
FIGURE 13: ATS-6 LINE PLOT, N/S DETECTOR, 9/5/74

NORTH - SOUTH DETECTOR
DAY 248 OF 1974
0853 - 0856 UT

198°
175°
154°
132°
108°
86°
65°
42°
19°
-2°
-16°

LOG f

75EW·6·041
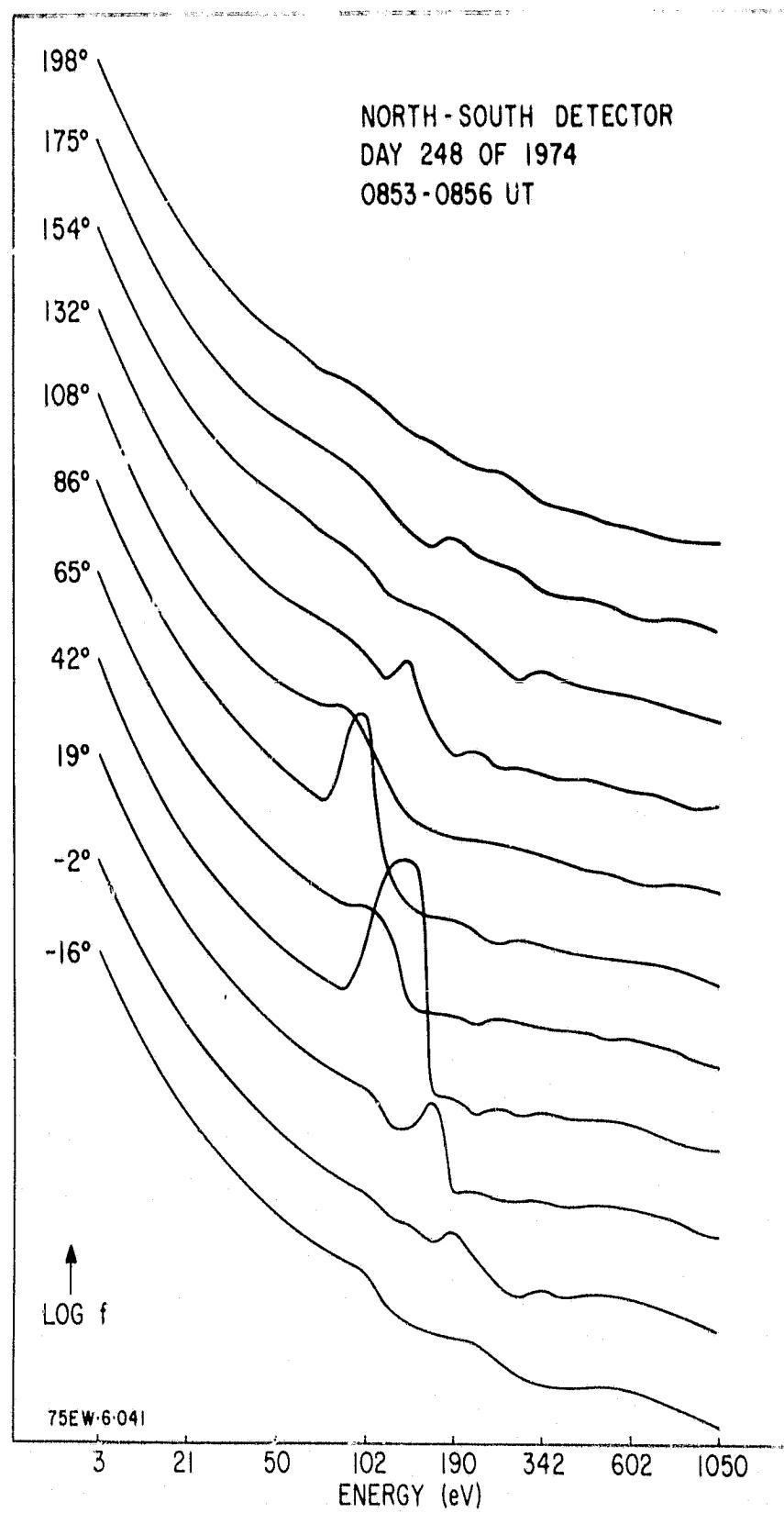
ENERGY (eV)

FIGURE 14: ATS-6 ENERGY PLOT, 9/5/74

61
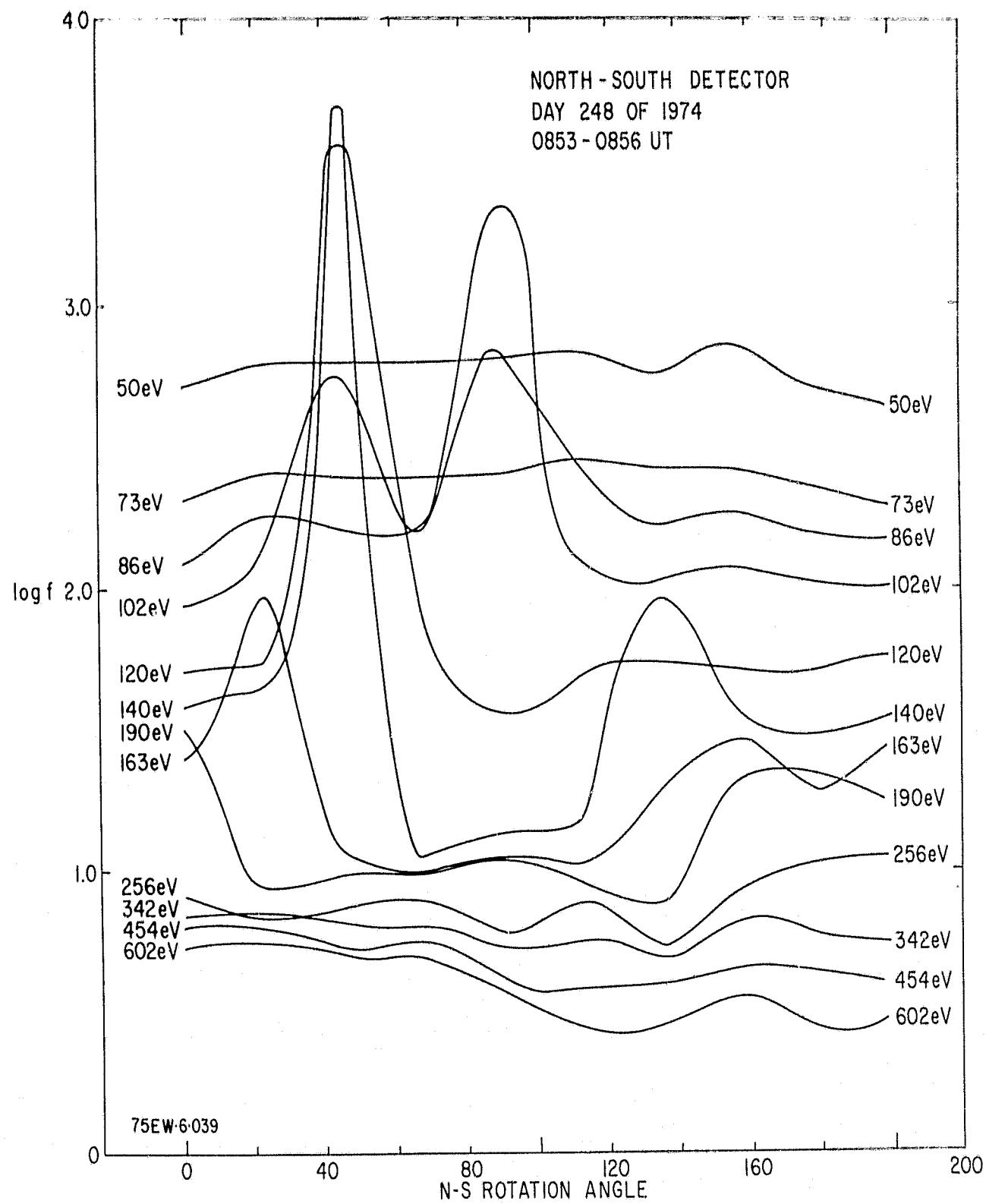
FIGURE 15: ATS-6 ANGLE PLOT 9/5/74

NORTH - SOUTH DETECTOR
DAY 248 OF 1974
0853 - 0856 UT

75EW·6·039
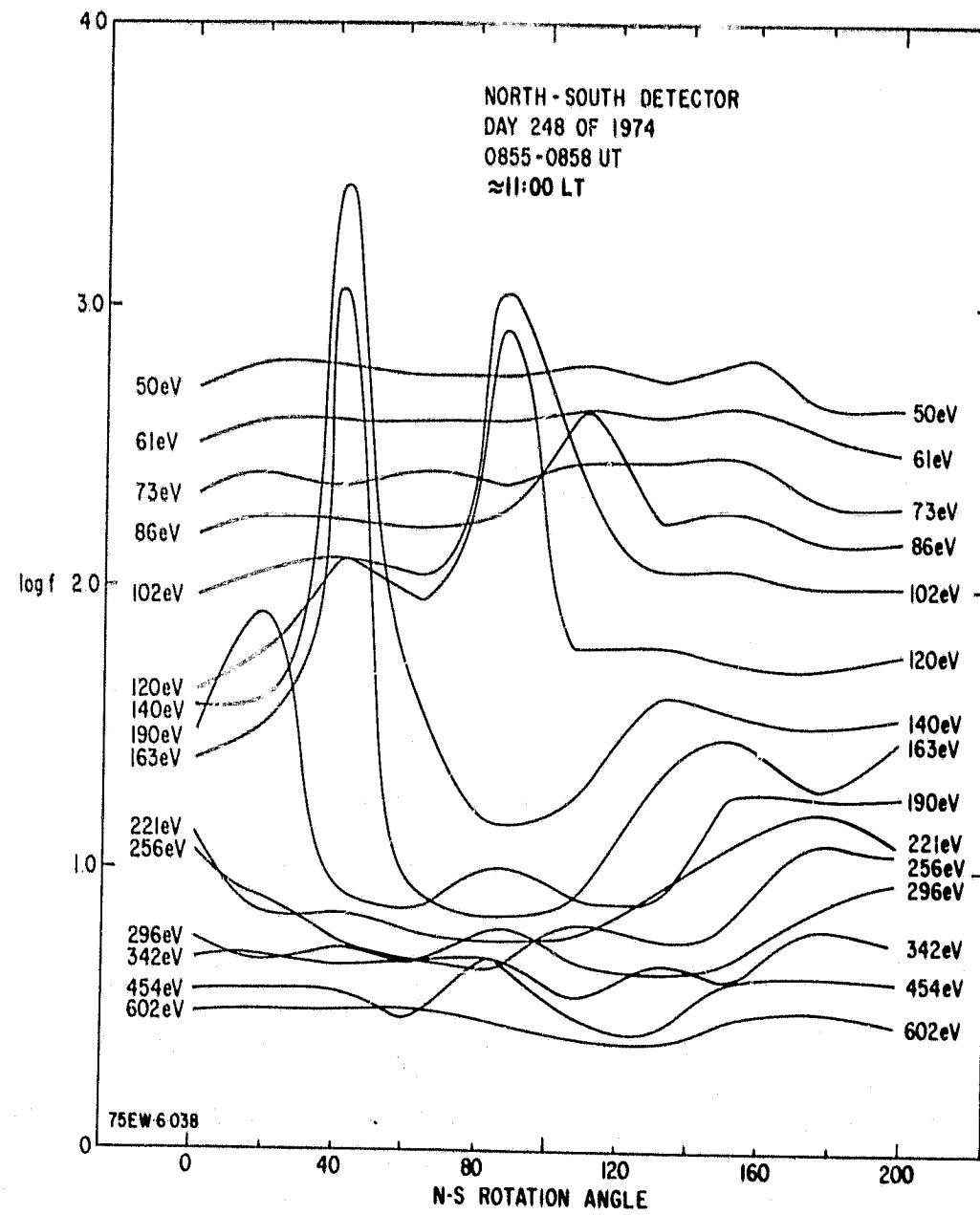
FIGURE 16: ATS-6 ANGLE PLOT 9/5/74

63
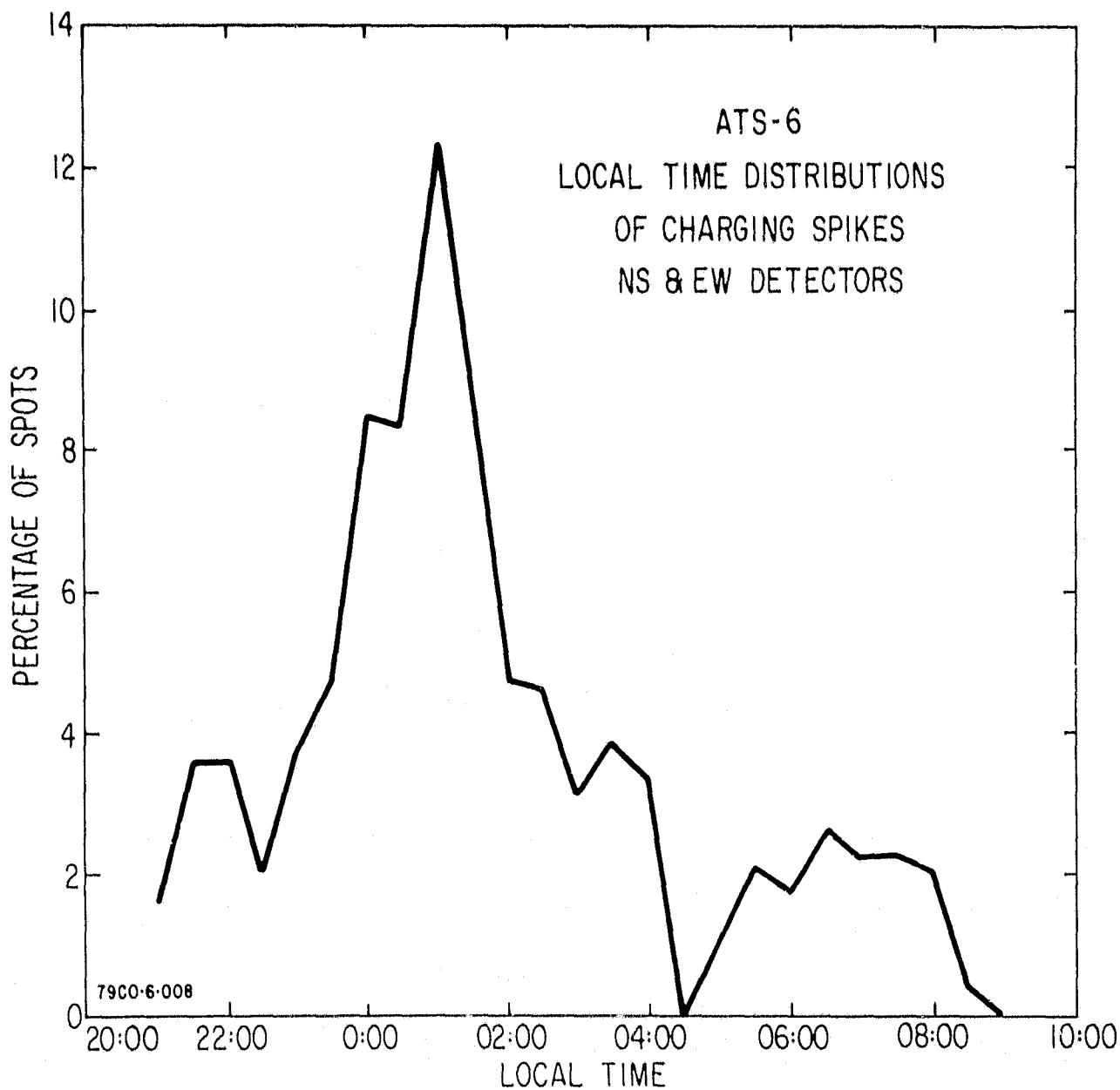
Figure 17. ATS·6: Charging Spike Time Distribution
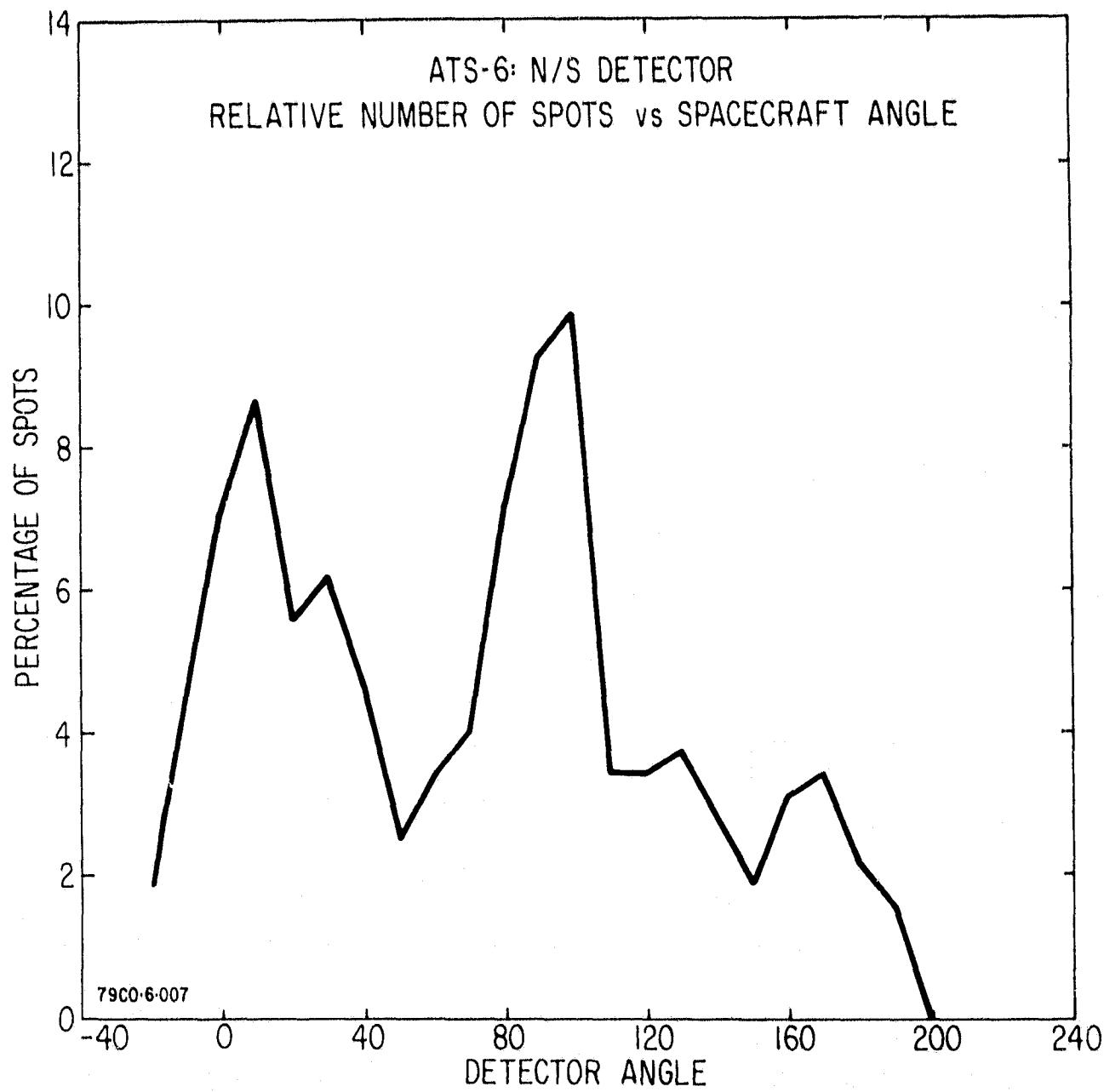
Figure 18. ATS·6: Charging Spike Angle Distribution
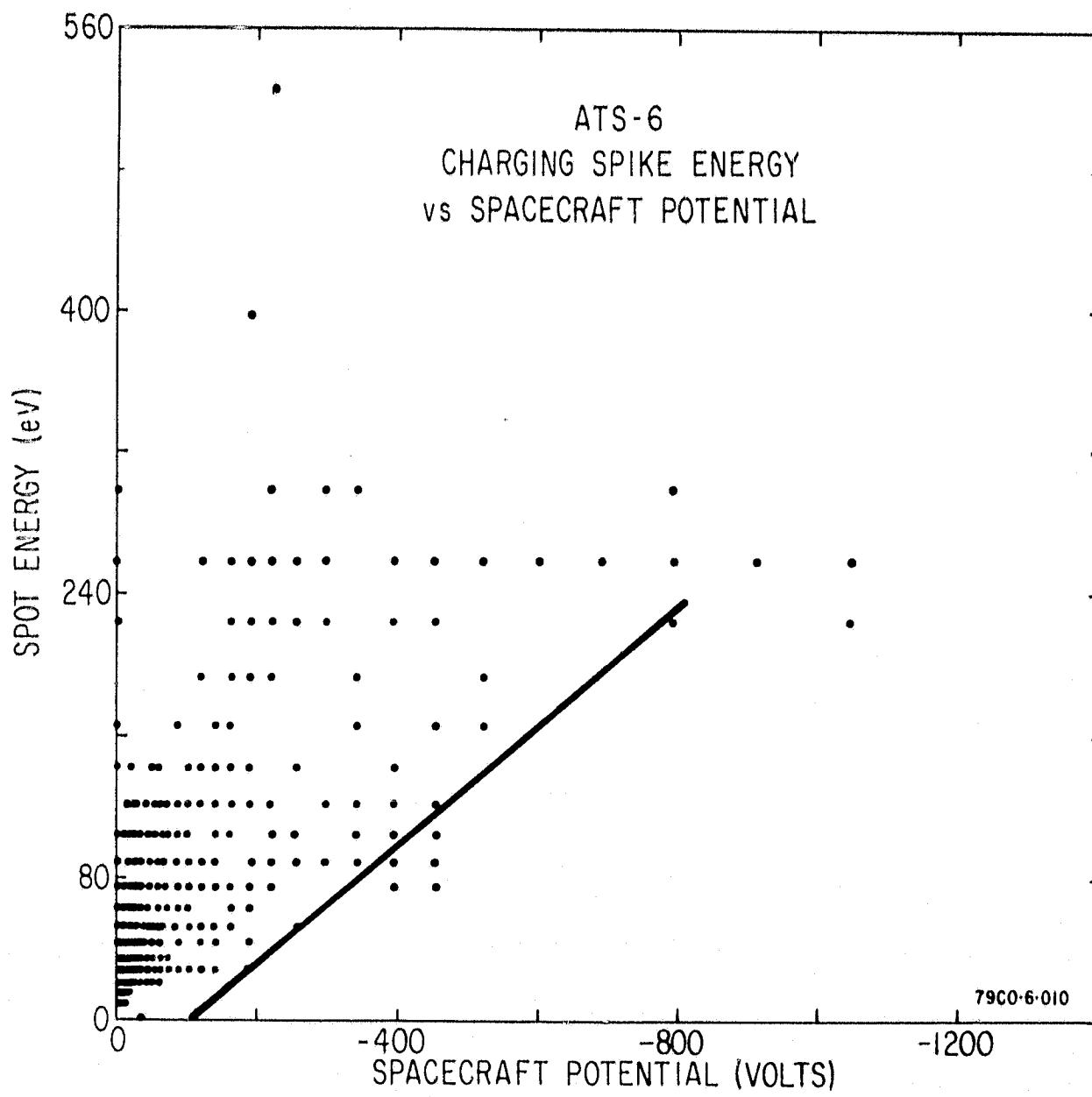
Figure 19. ATS·6: Charging Spike Energy Distribution
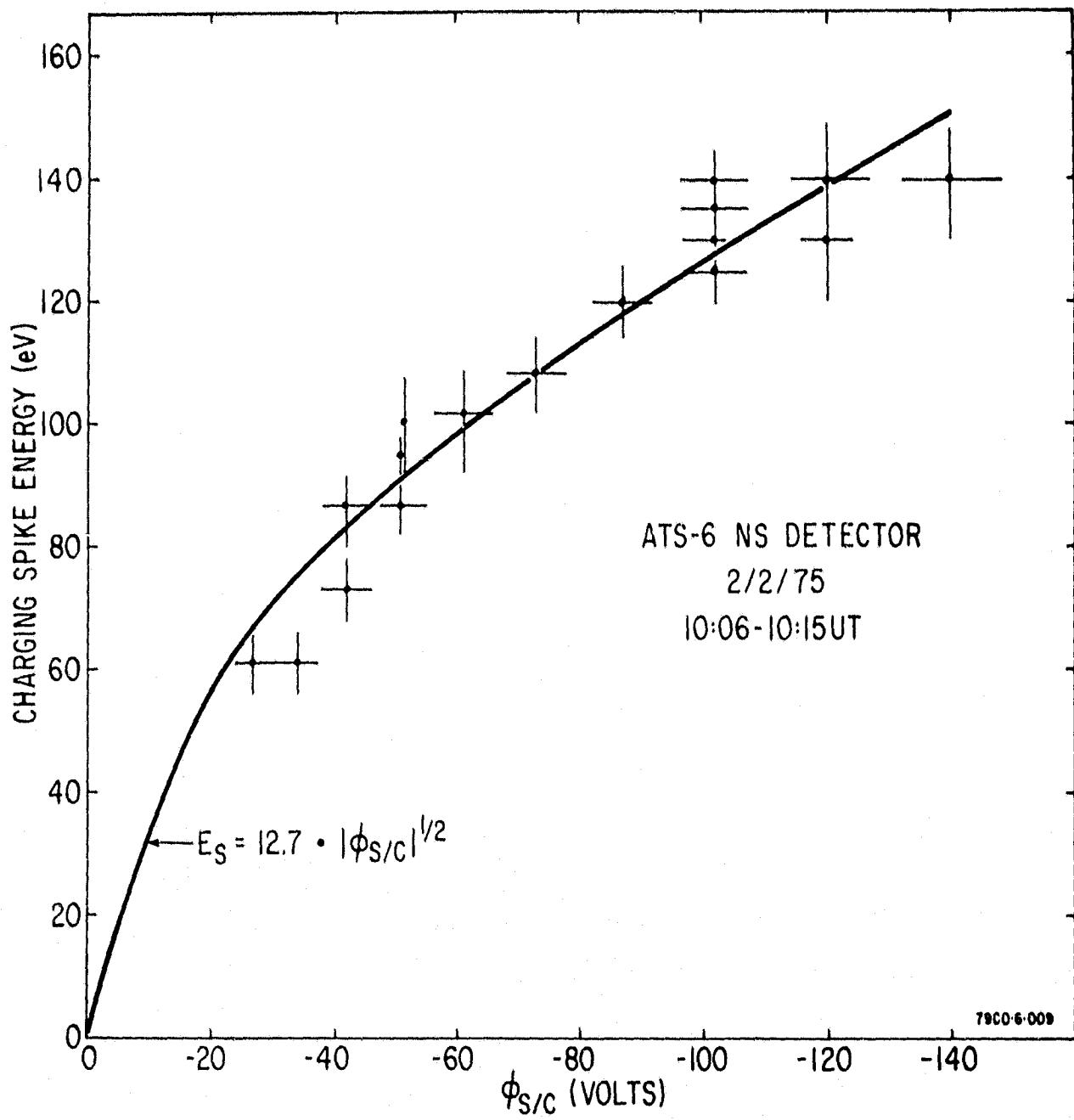
Figure 20. ATS·6: Charging Spike Energy, Day 2/2/75
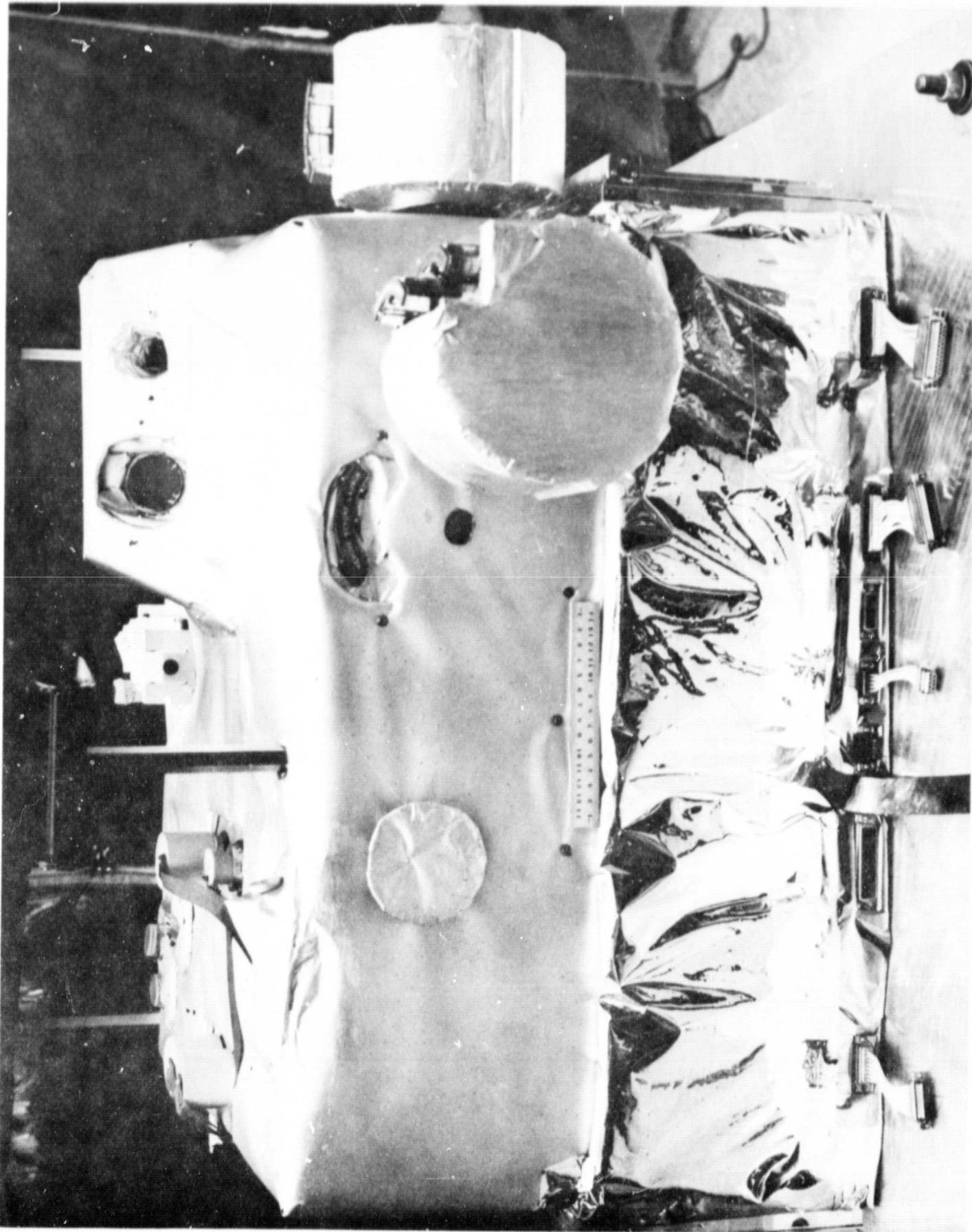
FIGURE 21: EME PACKAGE SHOWING U. OF MINNESOTA
AND UCSD INSTRUMENTS

68
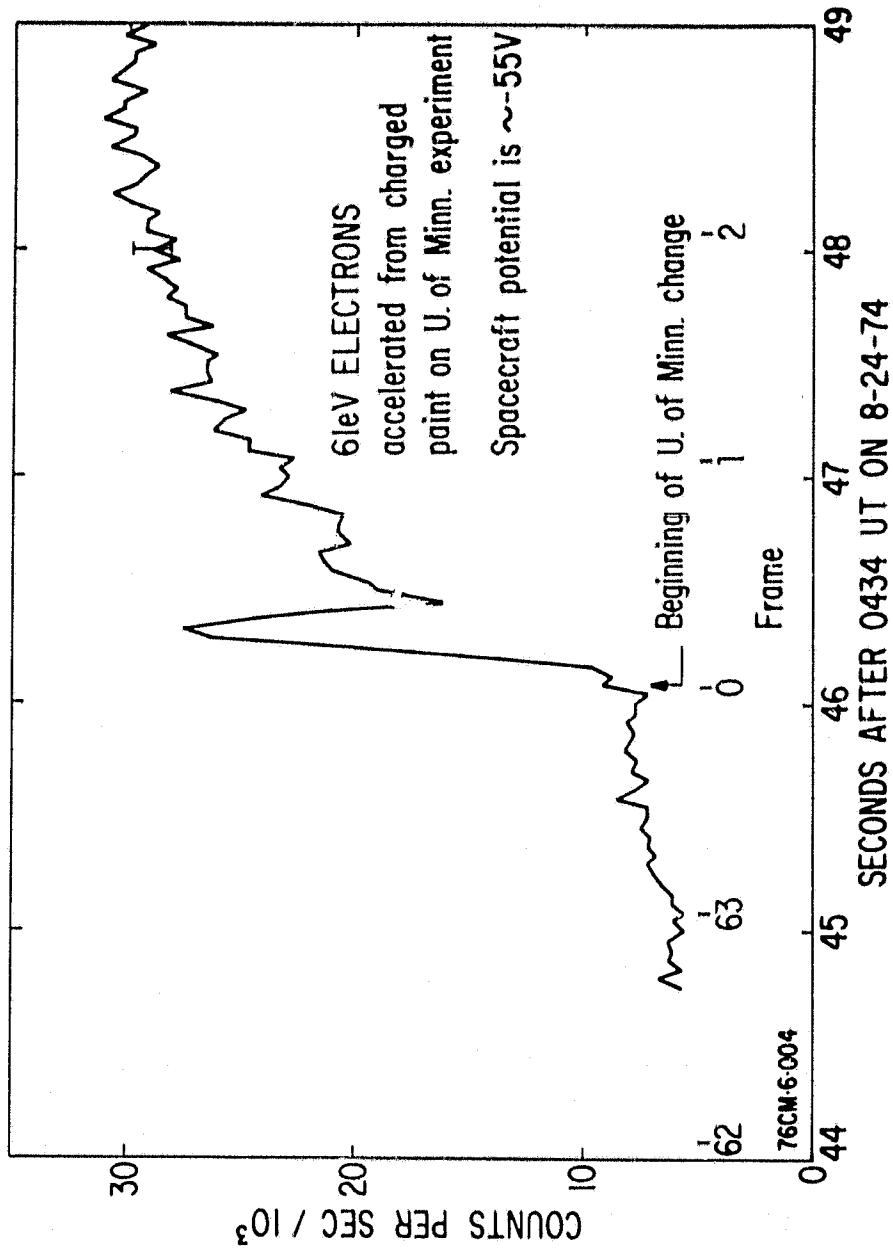
FIGURE 22: ATS-6 MINNESOTA SPOTS

61eV ELECTRONS
accelerated from charged
paint on U. of Minn. experiment

Spacecraft potential is ~-55V

Beginning of U. of Minn. change

SECONDS AFTER 0434 UT ON 8-24-74

COUNTS PER SEC / 10³

Table 1. Comparison of spacecraft and systems

	ATS-5	ATS-6
Characteristic size	2 m	10 m
Stabilization	Spin (axis parallel to earth's)	3-Axis
Outer surface	Mostly quartz (good insulator)	Quartz, kapton, paint, aluminum (mixed insulator and conductor)
Ion engine neutralizer	Thermal emission (electrons only)	Discharge plasma
Neutralizer placement	Recessed: 2.5 cm	Outboard: 17 cm
UCSD detectors	Body mounted (50 eV - 50 keV)	Rotating (1 eV - 80 keV)

Table 2. Comparison of neutralizers

	ATS-5	ATS-6
Turn-On Time:	< 1 min	35 min
Turn-Off Time	< 1 min	~ 2 min
Full-On Operation Time:	5 min	10 min
Emission Limited Current:	< 6 μA	< 1 mA
Energy of Emitted Particles:	~ 2V	~ 7 V

Table 3. ATS-6: UCSD auroral particles experiment

Species	electrons, ions	Energy/charge detectors
Energy ranges	NS 1 eV - 81 keV EW 50 eV - 40 keV	64 log spaced steps $\approx$ 30 log spaced steps
$\Delta E/E$	.18 + 2(eV)/E(eV)	
H	electrons $1.6 \times 10^{-4} cm^2$-ster ions $2.4 \times 10^{-4} cm^2$-ster	Energy Flux $\sim \dfrac{count\ rate}{H}$
Angular Resolution	mono-energetic $2.5^o \times 2.6^o$ full-spectrum $2.5^o \times 7^o$	
Time Lengths	SCAN 16 sec DWELL 1 sec - 128 sec	Full spectra Fixed energy-ground selected
Sampling	4 sample/sec - 24/sec	ground selected
Rotation	NS period 314 sec NS range 220° EW - no longer rotates	centered on radial, anti-earth direction now points west
Power	7. - 12. watts plus 5.4 watts	mode dependent (~average) when rotating (~average)

72

Table 4. Data collected - 1974 to 1978

Year	Day(s)	ATS-5	Day(s)	ATS-6
1974		At 105°W	166	Launch 94°W
	238-285 (246-283)	Fall eclipse (neutralizer op) IE No. 2	199-202 215, 226, 234-5 }	Thruster #2 operation
			247-290	Fall eclipse
			292-296	Thruster #1 operation
1975	51-97 (56-96)	Spring eclipse (neutralizer op)	60-105	Spring eclipse
			~140-174	Moved to ~35°E
	235-283 (263-281)	Fall eclipse (neutralizer op)	244-290	Fall eclipse
1976	49-95 (51-75)	Spring eclipse (neutralizer op)	57	Neutralizer operation
			58-103	Spring eclipse
	233-282	Fall eclipse	215-337	Move to 140° W
	(233-234, 245-246)	(Neutralizer op)	233	Neutralizer operation
	319	Neutralizer op	244-270	Fall eclipse
			(245-247, 285-288)	(Neutralizer operation)
			317	Drifts past ATS-5
			319-320	Neutralizer operation
			338	140° (~110°W) W

Table 4   (Continued)

Year	Day(s)	ATS-5	Day(s)	ATS-6
1977			58-60	Neutralizer operations-eclipse
	90-91	I.E.No. 1 Neut. ops.-eclipse-long	96-99	Neutralizer operations-eclipse
	242-245	Neutralizer No. 1 operations-eclipse		
	275-278	Double neutralizer operations-eclipse	281-285	UNH/Neutralizer operations
1978	49-56 59,60	Double neutralizer operations-eclipse		
	63-91	I.E.No. 2 Neutralizer operations-eclipse		

200-DBE=2.3 DBP=1.4 DBS= .070 SIPE= 3 PSN= 2 NS= 1.0 PR(-360, 360) COM= 24764715 SP= -6 LNG= 35
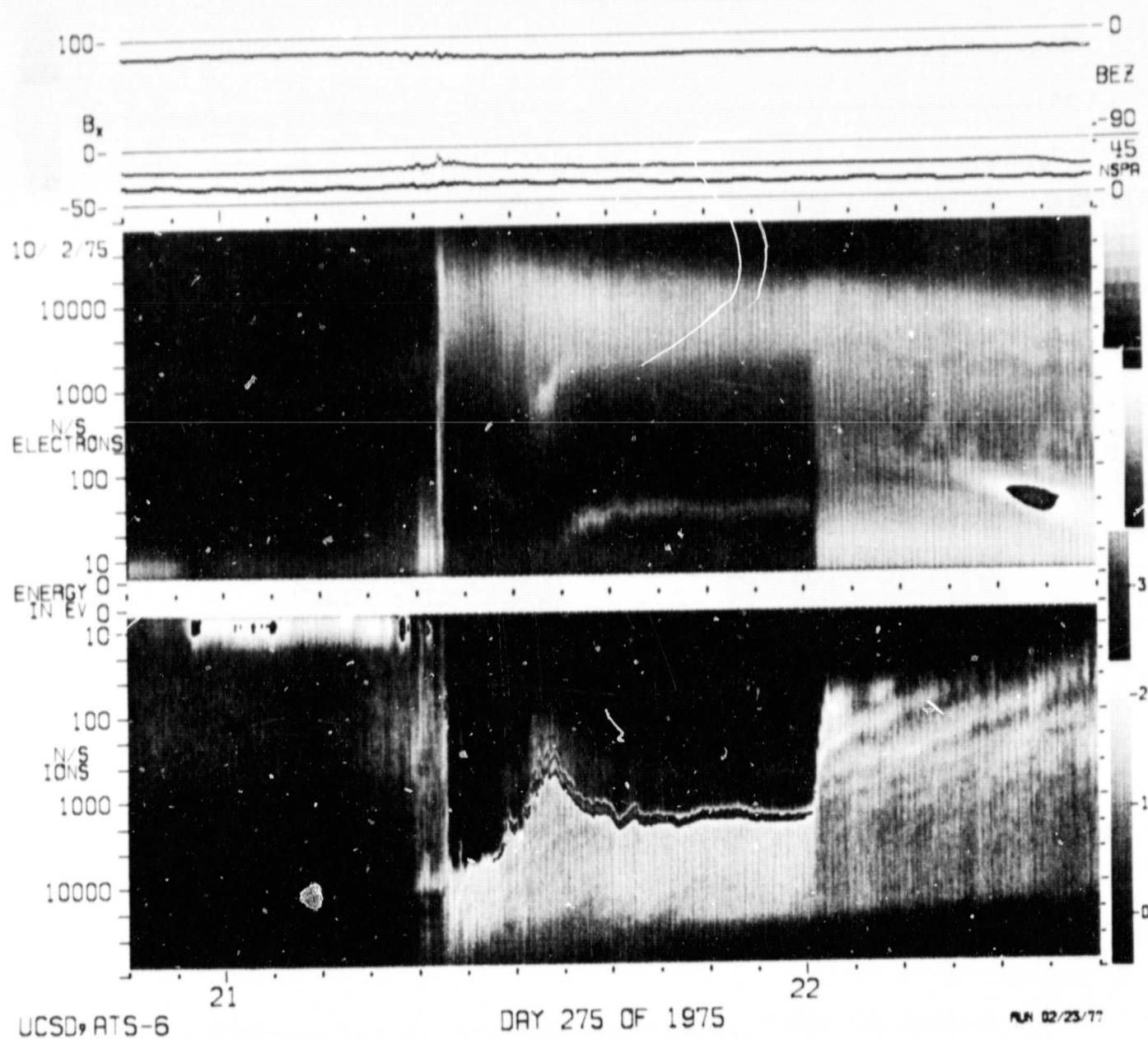
Spectrogram 1.   ATS-6: Eclipse with Injection of Hot Plasma; 10/2/75
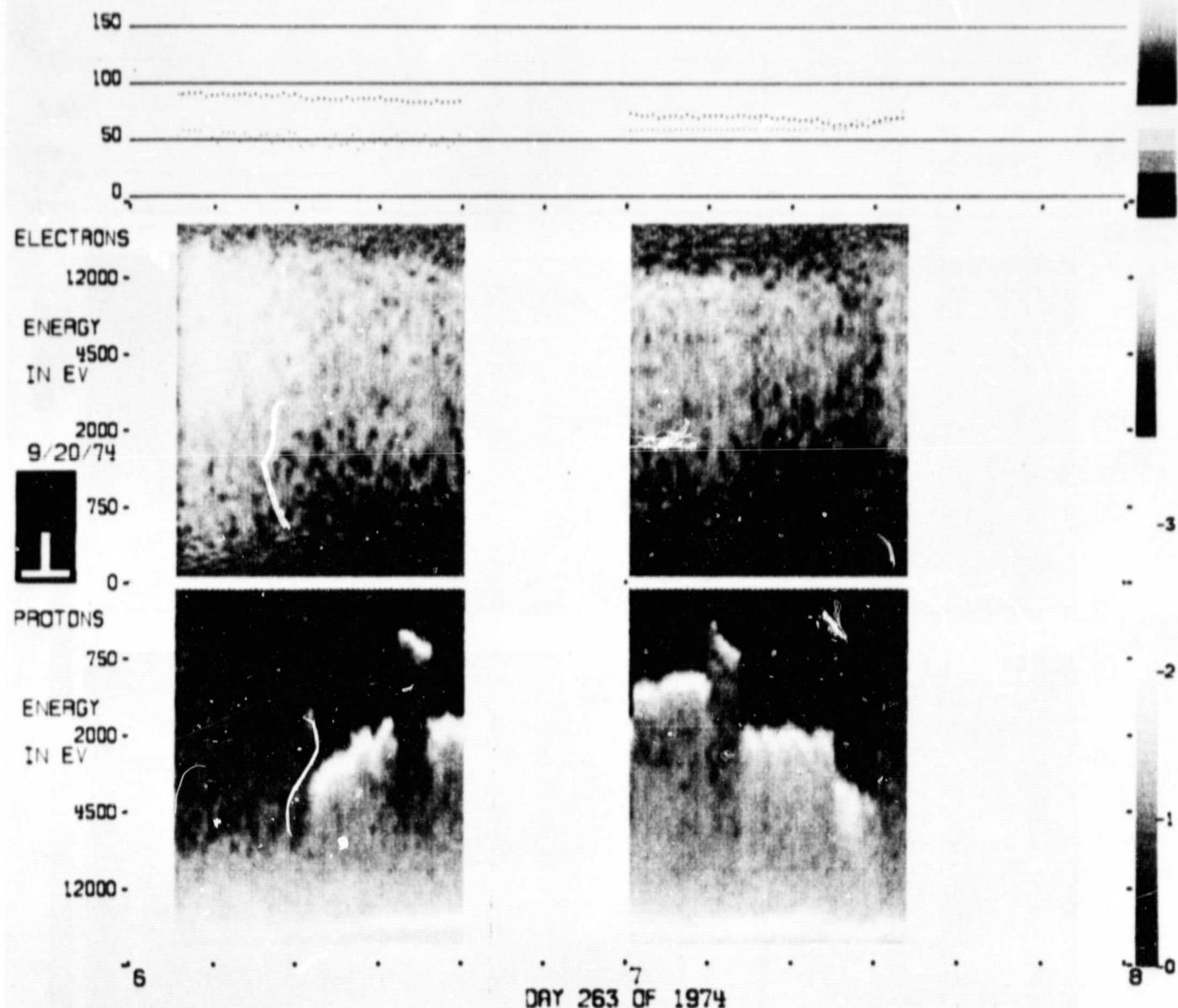
Spectrogram 2. ATS-5: Neutralized Operation in Eclipse; 9/20/74
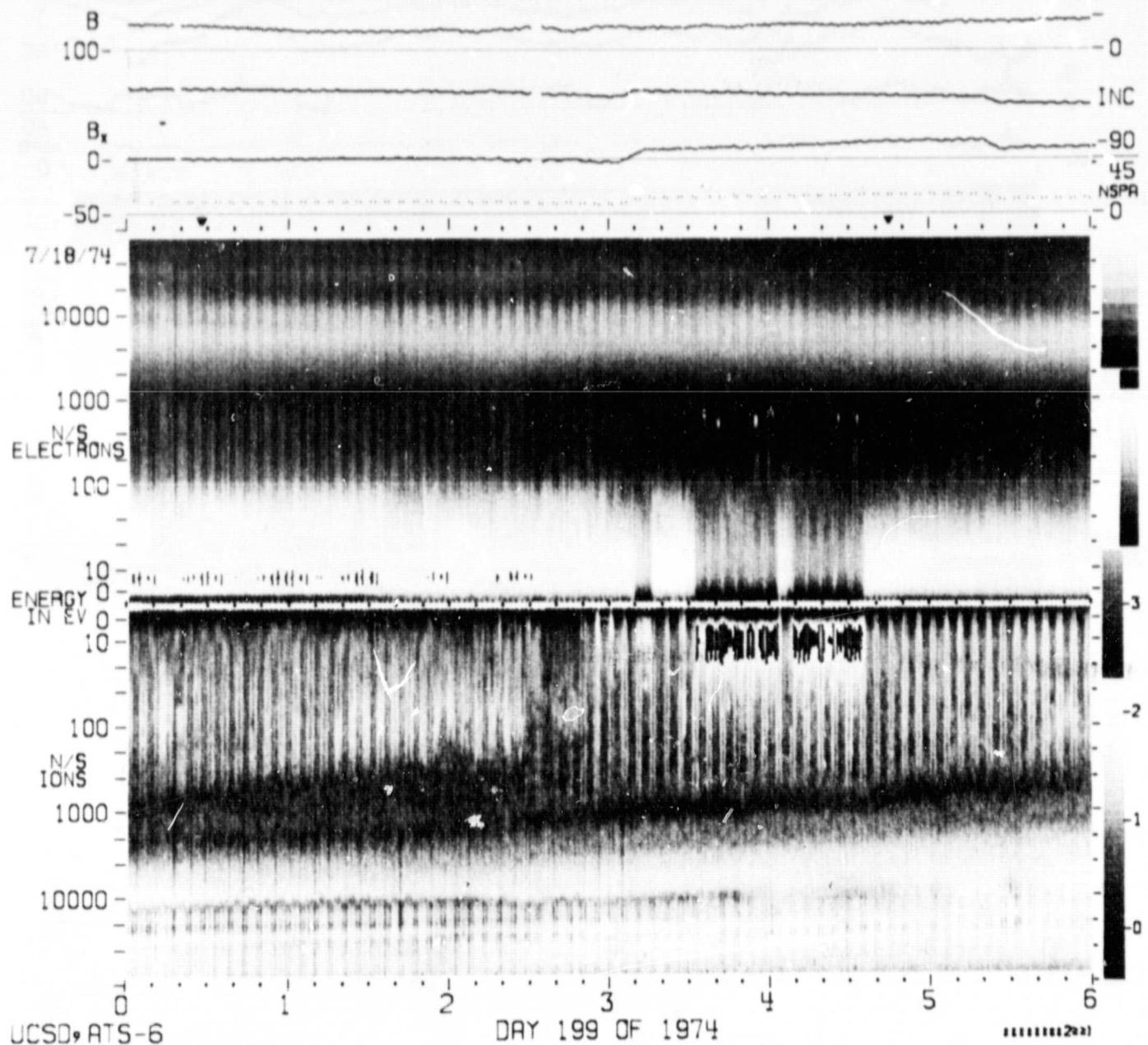
Spectrogram 3. ATS-6: Ion Engine Operation; 7/18/74
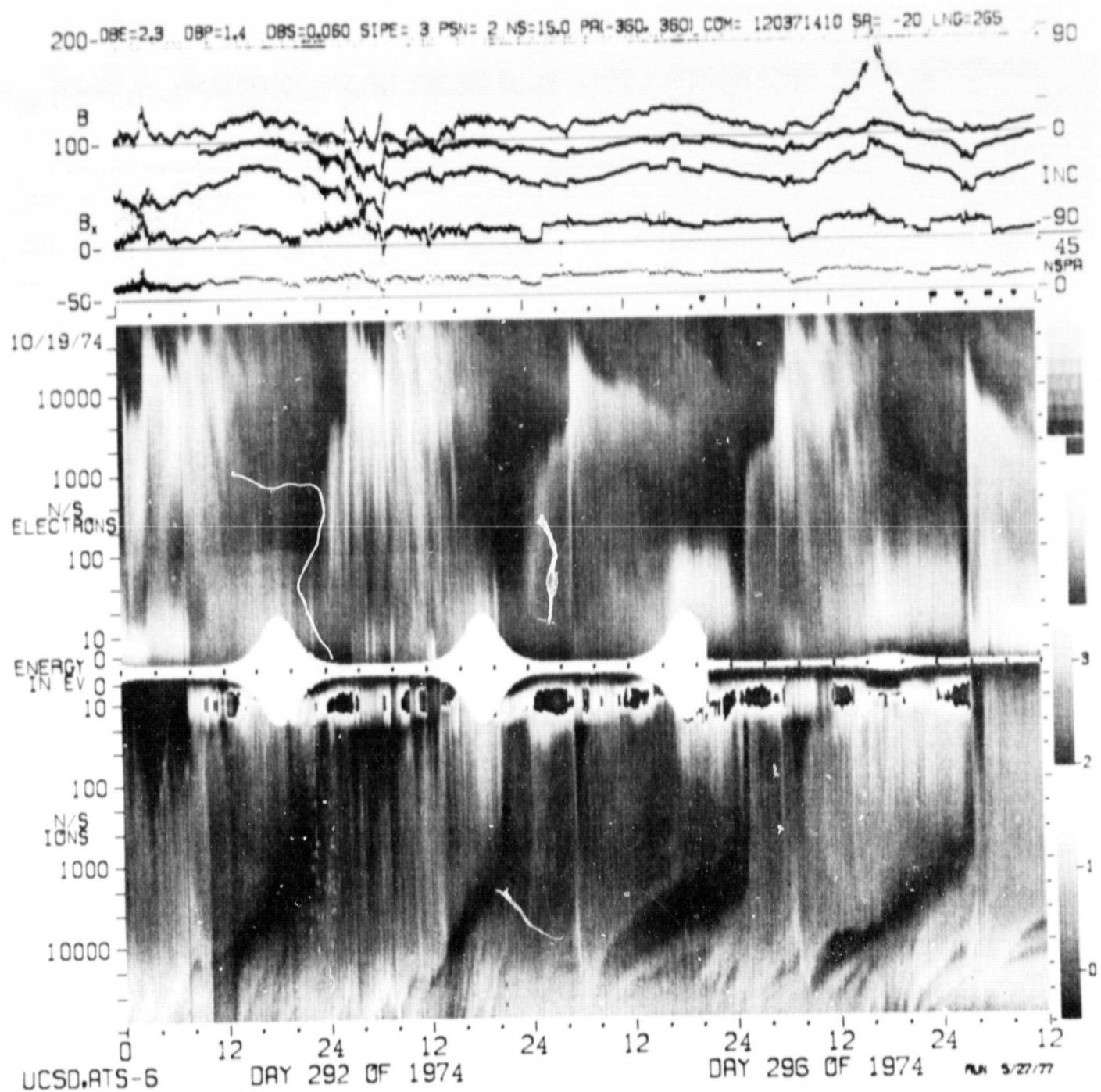
Spectrogram 4. ATS-6: Ion Engine Operation; 100 Hours; 10/19/74

Spectrogram 5. ATS-6 Neutralizer Operation in Daylight; 8/20/76

200–DBE=2.0 DBP=1.2 DBS=0.060 SIPE= 3 PSN= 2 NS= 1.0 PA(-360, 360) COM: 20573414 SA= -6 LNG=244   -90
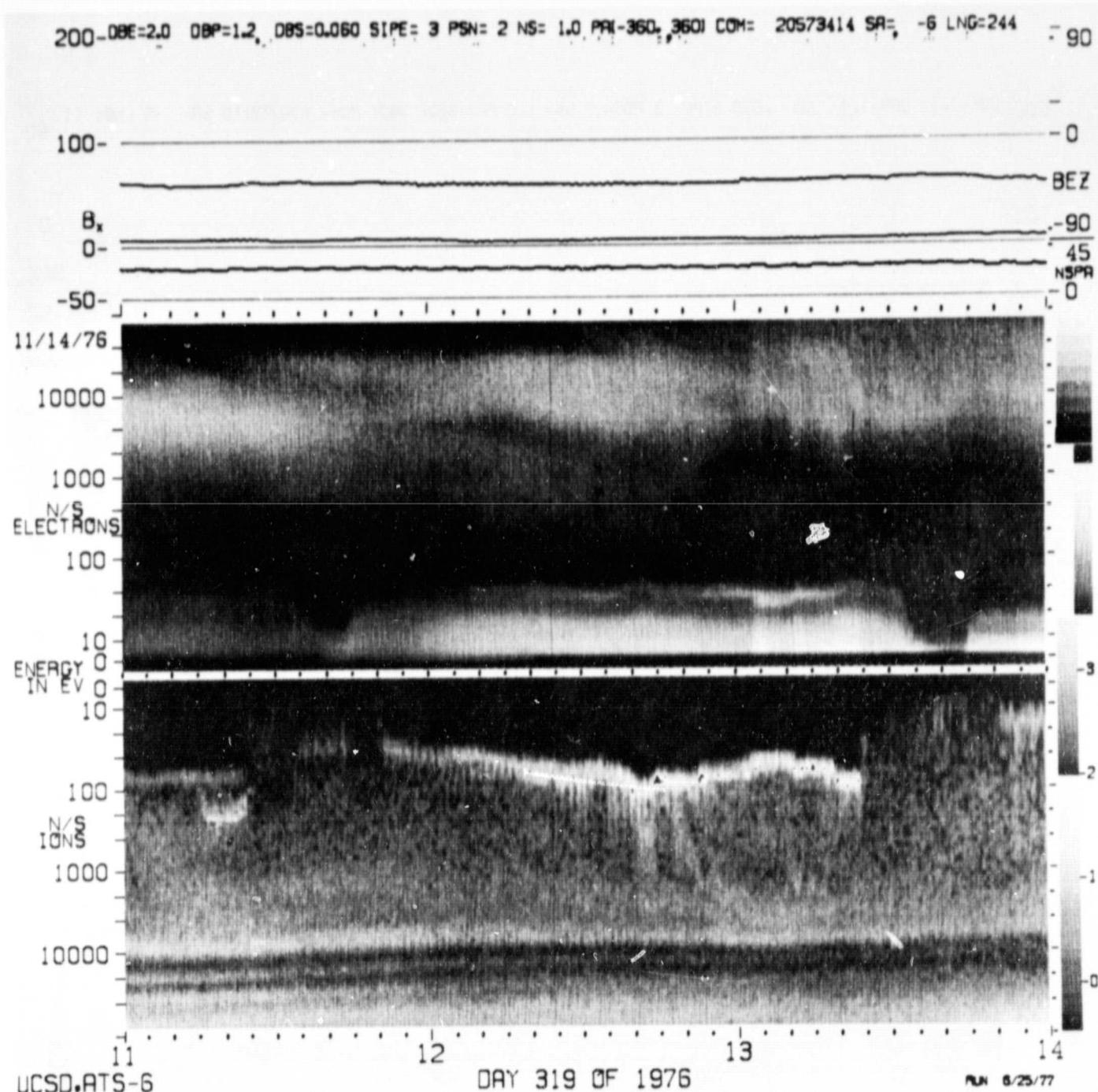
Spectrogram 6. ATS-6: Neutralizer Operation in Daylight; 11/14/76

200-DBE=1.8 DBP=1.4 DBS=0.070 SIPE= 3 PSN= 2 NS= 1.0 PRI-360, 360 COM= 20572404 SA= -6 LNG=291 . -90
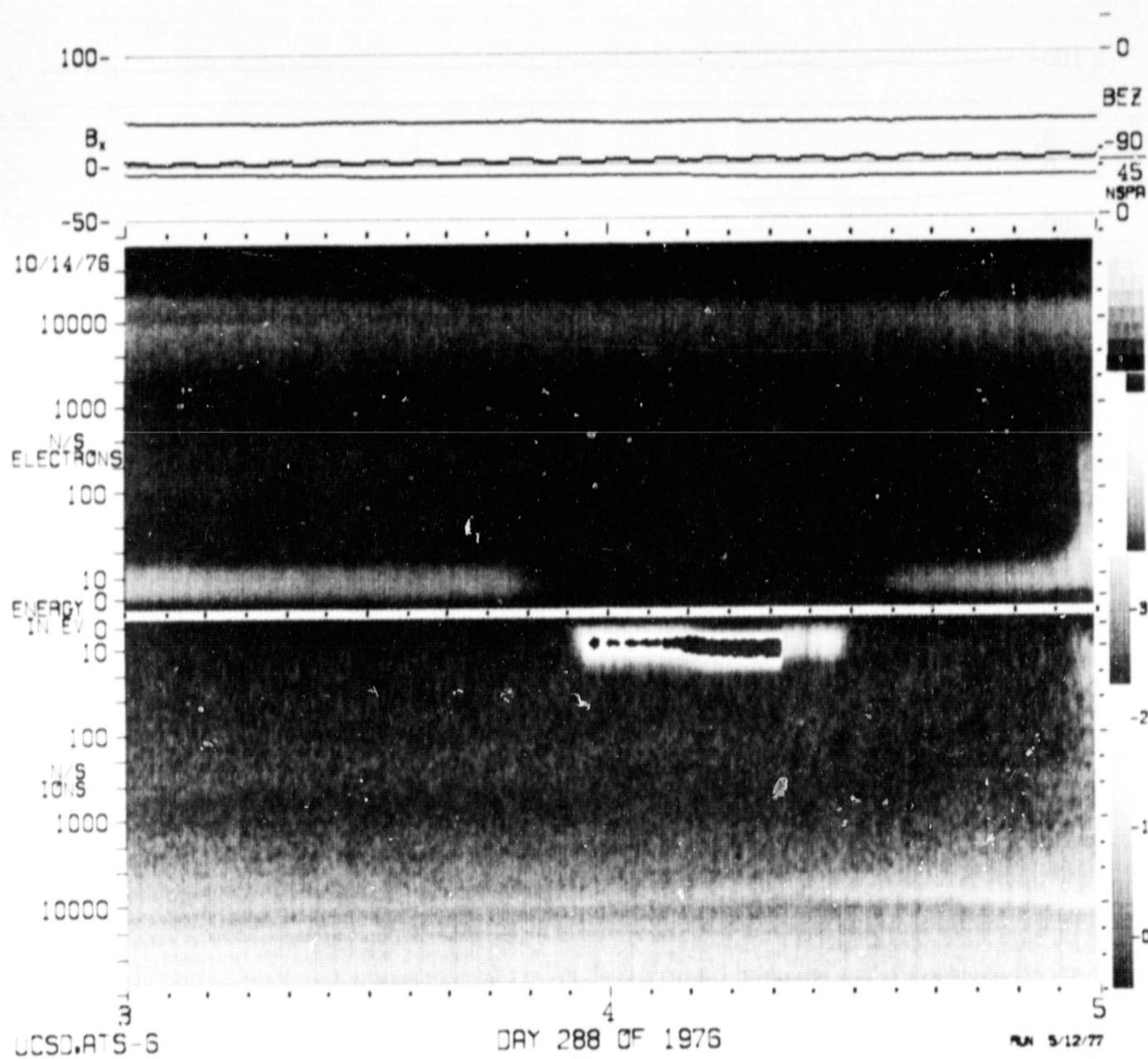
Spectrogram 7. ATS-6: Neutralizer Operation in Eclipse; 10/14/76
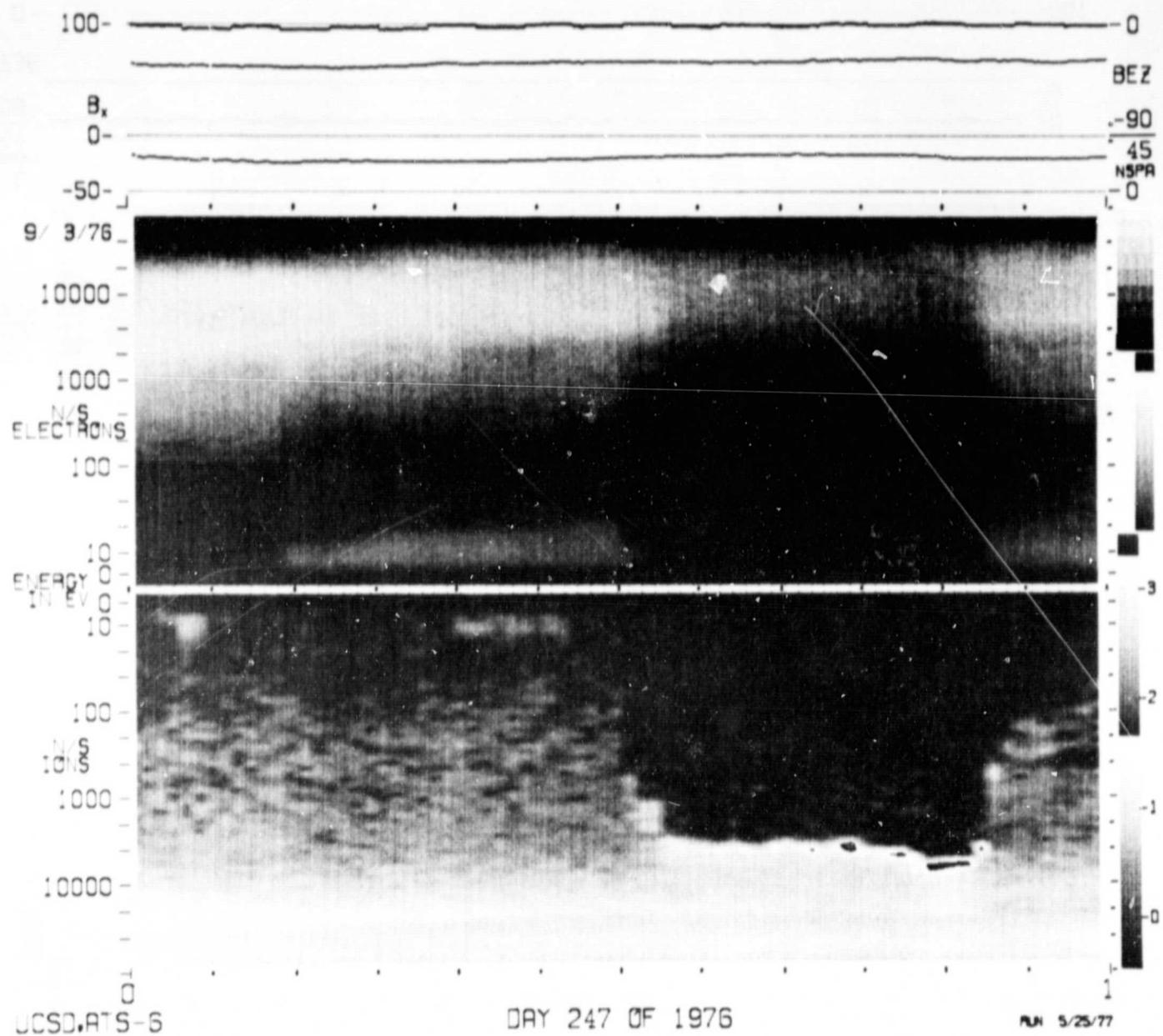
Spectrogram 8. ATS-6: Neutralizer Operation in Eclipse; 9/3/76
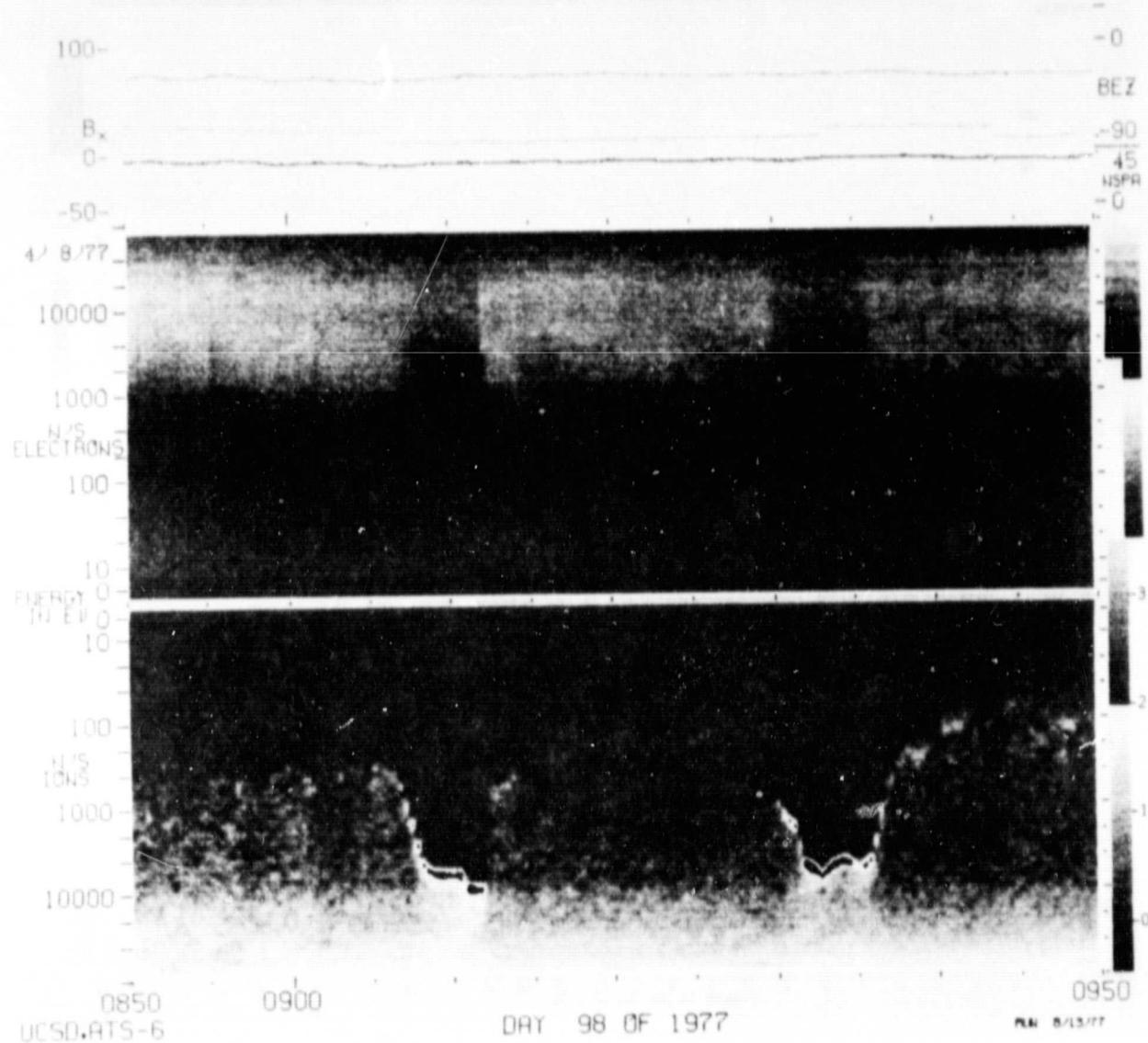
Spectrogram 9. ATS-6: Neutralizer Operation in Eclipse: 4/8/77
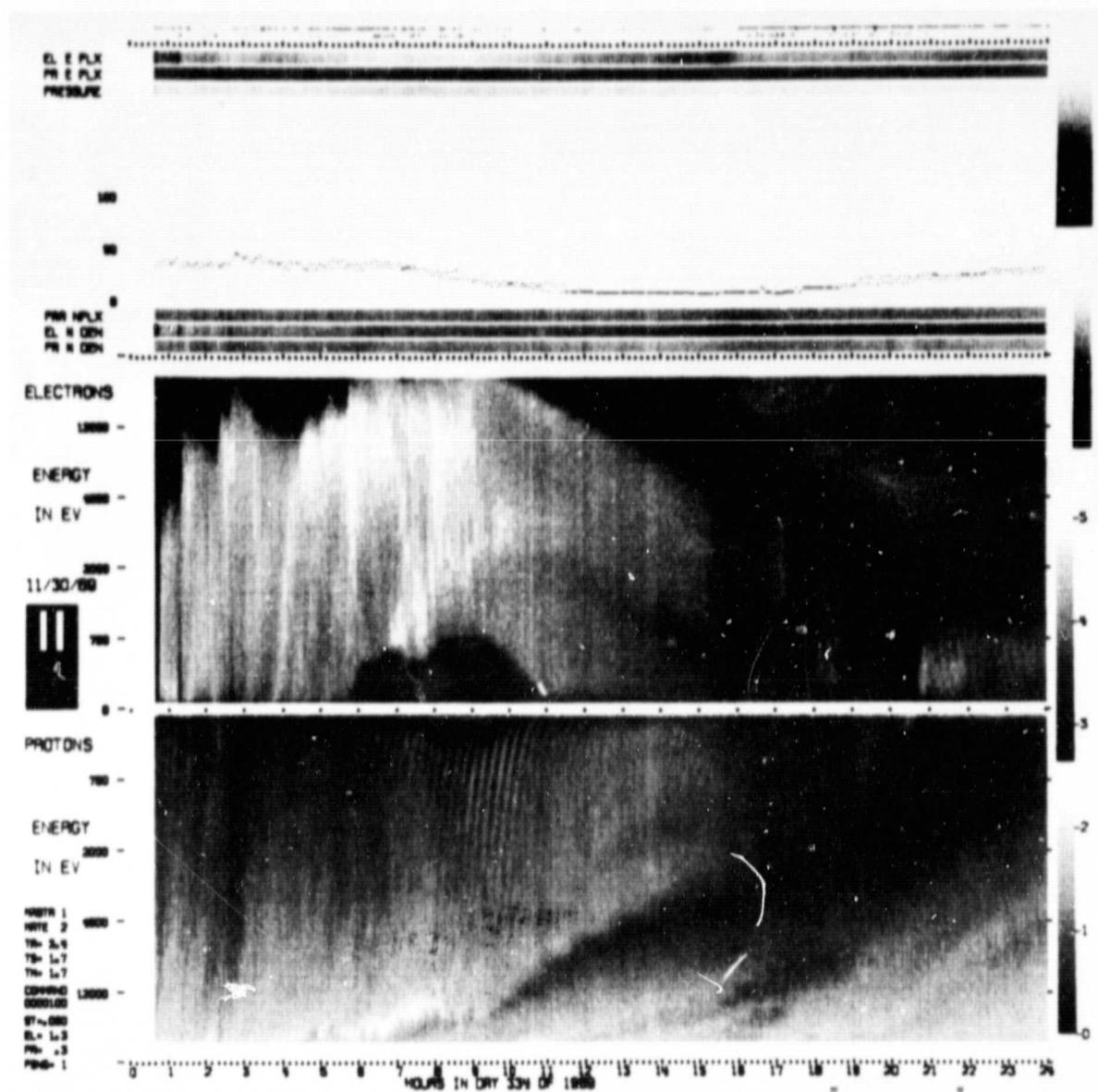
Spectrogram 10a. ATS 5: Differential Charging, Parallel Detector: 11/30/69
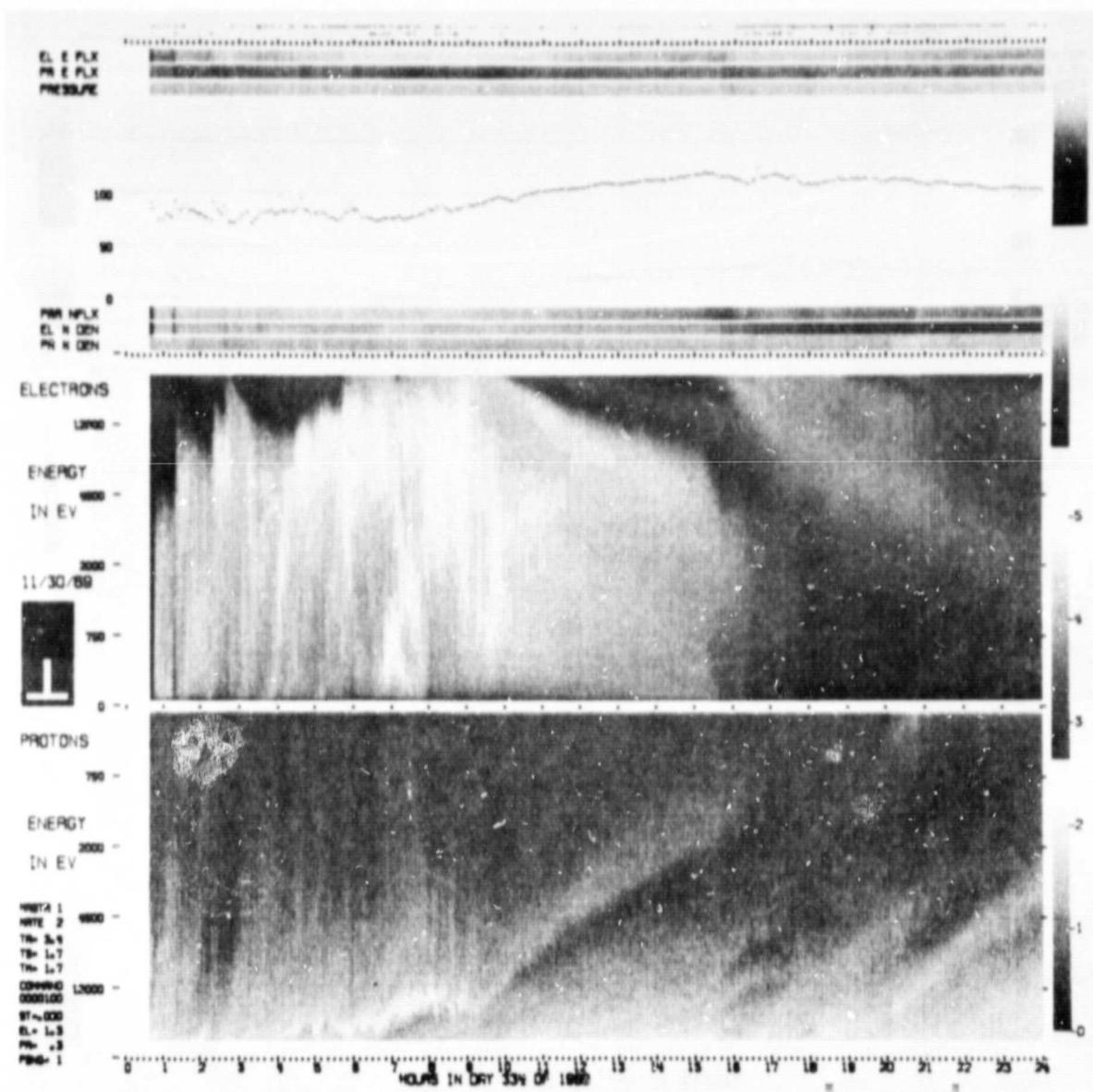
Spectrogram 10b. ATS·5: Differential Charging,
Perpendicular Detector: 11/30/69
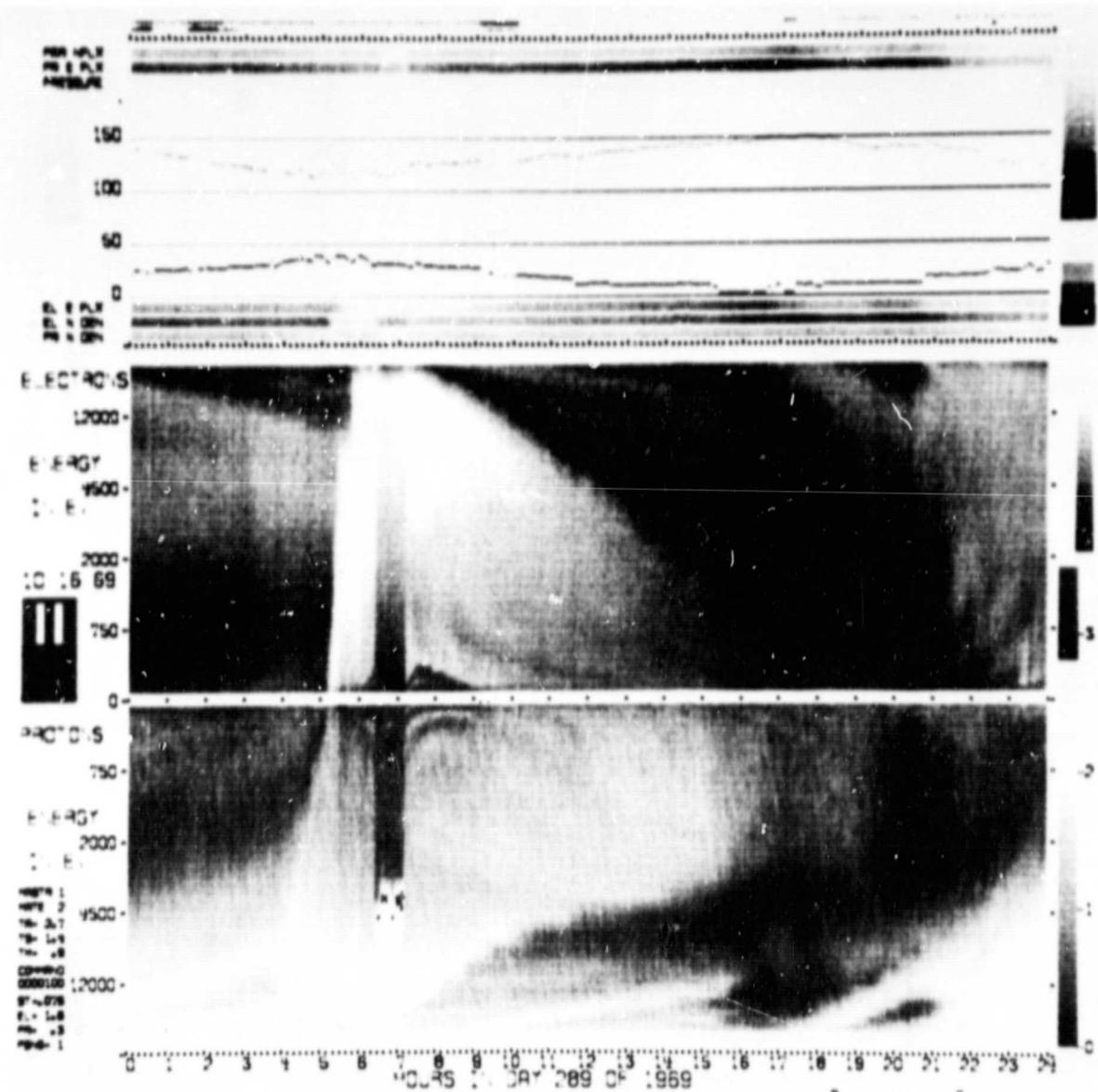
Spectrogram II. ATS-5: Differential Charging in Eclipse: 10/16/69

Spectrogram 12. ATS 6: Differential Charging: 9/5/74

Spectrogram 13. ATS·6: Differential Charging: 2/2/75

C-2

BIBLIOGRAPHY

_____, Applications technology satellite ATS-6. Experiment checkout and continuing spacecraft evaluation report, NASA-X-460-74-340, December, 1974, Goddard Spaceflight Center, 17-1 - 17-15.

Arnoldy, R. L., R. A. Hendrickson and J. R. Winckler, Echo 2: Observations at Fort Churchill of a 4-keV peak in low level electron precipitation, J. Geophys. Res., 80, 2316, 1975.

Bartlett, R. O., S. E. DeForest and R. Goldstein, Spacecraft charging control demonstration at geosynchronous altitude, AIAA Paper 75-359, AIAA 11th Electron Propulsion Conference, New Orleans, La., March 19-21, 1975.

Bartlett, R. O., and C. K. Purvis, Summary of the Two Year NASA Program for Active Control of ATS-5/6 Environmental Charging, USAF/NASA Spacecraft Charging Technology Conference, Colorado Springs, Colorado, Oct. 31-Nov. 2, 1978.

Bechtel, Robert T., Discharge chamber optimization of the SERT II thruster, J. Spacecraft and Rockets, 5, 795-800, 1968.

Bien, Fritz and Howard R. Baum, Detailed investigation of transient electron beam deposition into the atmosphere, Final Report, Contract #F19628-73-C-0048, subcontract #PO43081, May 1974, Utah State University, AFGRL/DNA.

Bien, Fritz, Howard Baum and K. Tait, An analysis of transient vehicle charging in the EXCEDE experiment, AGU Fall Conference, San Francisco, Dec. 1975; EOS, 56, 1035, 1975; SA54.

Byers, David C. and John F. Staggs, SERT II: Thruster system ground testing. J. Spacecraft and Rockets, 7, 7, 1970.

Cambou, F., V. S. Dokoukine, V. N. Ivchenko, G. G. Managadze, V. V. Migulin, O. K. Nazarenko, A. T. Nesmyanovich, A. Kh. Pyatsi, R. Z. Sagdeev and I. A. Zhulin, The Zarnitza rocket experiment on electron injection, Space Research XV, 491, 1975.

Cambou, F., R. Z. Sagdeev, I. A. Zhulin, G. Charles and V. S. Dokoukine, General description of the ARAKS experiments, Symposium on Active Experiments in Space Plasmas, Boulder, Colorado, June, 1976.

Cambou, F., J. Lauvergnat, V. V. Migulin, A. I. Morozov, B. E. Paton, R. Pellat, A. Kh. Pyatsi, H. Rème, R. Z. Sagdeev, W. R. Sheldon, and I. A. Zhulin, ARAKS-Controlled or Puzzling Experiment? Nature, 271, 723-726, Feb. 23, 1978.

Cambou, F., R. Z. Sagdeev, I. A. Zhulin, The ARAKS Project. --- Reviewing Artificial Radiation and Aurorae between Kerguelen and Soviet Union, Space Science Instrumentation, 4, 117-121, 1978.

Cartwright, D. G. and P. J. Kellogg, Controlled experiments on wave-particle interactions in the ionosphere, Nature Physical Science, 231, 11, 1971

Cartwright, D. G. and P. J. Kellogg, Observations of radiation from an electron beam artificially injected into the ionosphere. J. Geophys. Res., 79, 1439, 1974.

Charles, G. and V. S. Doukine, Payloads for Project ARAKS, Space Science Instrumentation, 4, 123-129, 1978.

Davis, T. N., T. J. Hallinan, G. D. Mead, J. M. Mead, M. C. Trichel, and W. N. Hess, Artificial aurora experiment: ground-based optical observations, J. Geophys. Res., 76, 6082, 1971.

Davis, T. N., W. N. Hess, M. C. Trichel and E. M. Wescott, Initial results of a recent electron accelerator experiment, AGU Spring Meeting, Washington, D.C., 1973, EOS, 54, 436, 1973.

DeForest, S. E., Electrostatic Potentials Developed by ATS-5, Photon and Particle Interactions with Surfaces in Space, Grard, Ed., pp. 263-276, 1973.

DeForest, S. E. and R. Goldstein, A study of electrostatic charging of ATS-5 satellite during ion thruster operation, Final Technical Report, NAS JPL 953675, 1973, Jet Propulsion Lab., Pasadena, Calif.

DeForest, S. E., Effects of charged particle emitters in space, EOS, p. 1159, 1978.

Gendrin, R., The French-Soviet 'ARAKS' experiment, Space Science Reviews, 15, 905, 1974.

Goldstein, R. and S. E. DeForest, Active control of spacecraft potentials at geosynchronour orbit, SPACECRAFT CHARGING BY MAGNETO-SPHERIC PLASMAS, Progress in Astronautics and Aeronautics, 47, Rosen, ed.; AIAA, MIT Press, 1976.

Gringauz, K. I. and N. M. Shutte, Altitude changes of the electrical potential of the 'Eridan' rocket during ARAKS experiment, ARAKS Symposium, France, May 1976.

Hallinan, T. J., H. C. Stenbaek-Nielsen and J. R. Winckler, The Echo 4 Electron Beam Experiment: Television Observation of Artificial Auroral Streaks Indicating Strong Beam Interactions in the High-Latitude Magnetosphere, Journal of Geophysical Research, 83, 3263, 1978.

Hanser, Frederick A. and Bach Sellers, Comment on 'Measurements of 3914 Å light production and electron scattering from electron beams artificially injected into the ionosphere,' by Gordon Israelson and John R. Winckler, J. Geophys. Res., 81, 6243, 1976.

Hendrickson, R. A., R. W. McEntire and J. R. Winckler, Electron echo experiment: A new magnetospheric probe, Nature, 230, 564, 1971.

Hendrickson, Richard Arthur, The electron echo experiment, observations of the charge neutralization of the rocket and analysis of the echo from electrons artificially injected into the magnetosphere, Tech. Report CR-160, School of Physics and Astronomy, Univ. of Minn., Minneapolis, Dec. 1972 (Ph. D. thesis, Univ. of Minn.).

Hendrickson, R. A., R. W. McEntire and J. R. Winckler, Echo I: An experimental analysis of local effects and conjugate return echoes from an electron beam injected into the magnetosphere by a sounding rocket, Planet. Space Sci., 23, 1431, 1975a.

Hendrickson, R. A. and J. R. Winckler, Electron Echo III: Comparison of observed echo results and various magnetic field models, AGU Spring Meeting, June 16-20, 1975, Washington, D. C., EOS, 56, 436, 1975; SM117, 1975b.

Hendrickson, R. A. and J. R. Winckler, Echo III: The study of electric
    and magnetic fields with conjugate echoes from artificial electron beams
    injected into the auroral zone ionosphere. Geophys. Res. Letters, 3,
    409, 1976.

Hess, W. N., Generation of an artificial aurora, Science, 164, 1512, 1969.

Hess, W. N., M. C. Trichel, T. N. Davis, W. C. Beggs, G. E. Kraft,
    E. Stassinopolous, and E. J. Maier, Artificial aurora experiment:
    Experiment and principal results, J. Geophys. Res., 76, 6067, 1971.

Hunter, Robert E., Robert O. Bartlett, Robert M. Worlock, and Edmund L.
    James, Cesium contact ion microthruster experiment aboard applica-
    tions technology satellite (ATS)-IV, J. Spacecraft and Rockets, 6, 968,
    1969.

Israelson, Gordon, The electron echo III experiment, Analysis of electron
    beam interactions with the upper atmosphere for mass density and N_2
    number density measurements, Tech. Report CR-166, School of Physics
    and Astronomy, Univ. of Minnesota, Minneapolis, Minn., 1974.

Israelson, G. and J. R. Winckler, Measurements of 3914 Å light production
    and electron scattering from electron beams artificially injected into the
    ionosphere, J. Geophys. Res., 80, 3709, 1975.

Israelson, G. and J. R. Winckler, Reply, J. Geophys. Res., 81, 6248, 1976.

Israelson, G. A., J. R. Winckler, Effect of a neutral N_2 cloud on the
    electrical charging of an electron beam emitting rocket in the iono-
    sphere: Echo IV, submitted to JGR, June 1978, University of Minnesota
    Technical Report No. 176.

James, E., R. Worlock, T. Dillon, G. Grant, L. Jan and G. Trump, A one
    millipound cesium ion thruster system, AIAA Paper 70-1149, AIAA 8th
    Electric Propulsion Conference, Stanford, Ca., Aug. 31-Sept. 2, 1970.

James, E. L., W. Ramsey, G. Gant, L. Jan and R. Bartlett, A north-
    south station keeping ion thruster system for ATS-F, AIAA Paper
    73-1133, AIAA 10th Electric Propulsion Conference, Lake Tahoe,
    Nevada, Oct. 31-Nov. 2, 1973.

James, E. L. and W. D. Ramsey, A prototype 12 centimeter cesium ion thruster for north-south station keeping, AIAA Paper 75-387, AIAA 11th Electric Propulsion Conference, New Orleans, La., Mar. 19-21, 1975.

Johnson, Bruce and E. C. Whipple, Characteristics of Differential Charging of the ATS-6 Satellite, USAF/NASA Spacecraft Charging Technology Conference, Colorado Springs, Colorado, Oct. 31-Nov. 2, 1978.

Jones, Sanford, G., John V. Staskus and David C. Byers, Preliminary results of SERT II spacecraft potential measurements using hot wire emissive probes, AIAA Paper 70-1127, AIAA 8th Electric Propulsion Conference, Stanford, Ca., 1970, or NASA Technical Memorandum X-2083, 1970.

Kawashima, N., S. Sasaki, O. Kaneko, Y. Nakamura, H. Kubo, T. Obayashi and S. Miyatake, Experiments of electron beam emission from rocket, unpublished manuscript, Institute of Space and Aeronautical Science, Univ. of Tokyo, Tokyo, Japan, May, 1976.

Kellogg, P. J., D. G. Cartwright, R. A. Hendrickson, S. J. Monson and J. R. Winckler, The University of Minnesota electron echo experiments, Space Research XVI, 589, 1976.

Kerslake, W. R., D. C. Byers and J. F. Staggs, SERT II: Mission and experiments, J. Spacecraft and Rockets, 7, 4, 1970.

Kerslake, W. R., R. G. Goldman and W. C. Nieberding, SERT II: Mission, thruster performance and inflight thrust measurements, J. Spacecraft and Rockets, 8, 213, 1971.

Kerslake, W. R. and R. C. Finke, SERT II hollow cathode multiple restarts in space, AIAA Paper 73-1136, AIAA 10th Electric Propulsion Conference, Lake Tahoe, Nevada, 1973.

Kerslake, W. R. and R. C. Finke, SERT II thruster space restart-1974, AIAA Paper 75-365, AIAA 11th Electric Propulsion Conference, New Orleans, La., 1975.

Kerslake, W. R., Status of SERT II ion thrusters and spacecraft-1976, AIAA Paper 76-1061, AIAA International Electric Propulsion Conference, Florida, 1976.

Knott, K., Equilibrium potential of a magnetospheric satellite in an eclipse situation, Planetary and Space Science, 20, 1137, 1972.

Lovell, R. R., N. J. Stevens, W. Schober, C. P. Pike, and W. Lehn, Spacecraft charging investigation: A joint research and technology program, SPACECRAFT CHARGING BY MAGNETOSPHERIC PLASMAS, Progress in Astronautics and Aeronautics, 47, Rosen, ed.; AIAA, MIT Press, 1976.

Matsumoto, Hiroshi, Sadao Miyatake, Iwane Kimura, Rocket experiment on spontaneously and artificially stimulated VLF plasma waves in the ionosphere, J. Geophys. Res., 80, 2829, 1975.

McEntire, R. W., R. A. Hendrickson and J. R. Winckler, Electron echo experiment I: Comparison of observed and theoretical motion of artificially injected electrons in the magnetosphere, J. Geophys. Res., 79, 2343, 1974.

McPherson, D. A., D. P. Cauffman and W. Schober, Spacecraft charging at high altitudes - The SCATHA satellite program, SPACECRAFT CHARGING BY MAGNETOSPHERIC PLASMA, Progress in Astronautics and Aeronautics, 47, Rosen, ed.; AIAA, MIT Press, 1976.

Miyatake, S., H. Matsumoto and I. Kimura, Rocket experiment on non linear wave-wave interaction in the ionospheric plasma, Space Research, 14, 385, 1974.

Morgan, B. G. and R. L. Arnoldy, Electron echo III: In situ measurement of vector ion flow in the ionospheric F-region, AGU Spring Meeting, June 16-20, 1975, Washington, D.C.; EOS, 56, 436, 1975, SM116.

Olsen, R. C., Potential modification on ATS-5 by electron emission, EOS, p. 1215, 1977.

Olsen, R. C., E. C. Whipple, and C. K. Purvis, Active modification of ATS-5 and ATS-6 spacecraft potentials, EFFECT OF THE IONOSPHERE ON SPACE AND TERRESTRIAL SYSTEMS, John Goodman, ed., NRL and ONR, 1978.

Olsen, R. C., Operation of the ATS-6 ion engine and plasma bridge neutralizer at geosynchronous altitude, AIAA/DLGR 13th International Electric Propulsion Conference, paper 78-663, San Diego, Calif., April, 1978a.

Olsen, R. C. and E. C. Whipple, Operations of the ATS-6 ion engine, USAF/NASA Spacecraft Charging Technology Conference, Colorado Springs, Colorado, Oct. 31-Nov. 2, 1978.

Olsen, R. C., Effects of operating a cesium ion engine on low energy particle data, EOS, p. 1159, 1978b.

O'Neil, R. R., F. Bien, D. Burt, J. A. Sandock and A. T. Stair, Summarized Results of the Artificial Auroral Experiment, Precede; Journal of Geophysical Research, 83, 3273, 1978a.

O'Neil, R. R., W. P. Reidy, J. W. Carpenter, T. N. David, D. Newell, J. C. Ulwick and A. T. Stair, Excede 2 Test, an Artificial Auroral Experiment: Ground-Based Optical Measurements, Journal of Geophysical Research, 83, 3281, 1978b.

Purvis, C. K., R. O. Bartlett and S. E. DeForest, Active control of spacecraft charging on ATS-5 and ATS-6, Spacecraft Charging Technology Conference, Colorado Springs, Colorado, October 27-29, 1976.

Rawlin, V. K. and E. V. Pawlik, A mercury plasma-bridge neutralizer, J. Spacecraft and Rockets, 5, 814, 1968.

Rawlin, V. K. and W. R. Kerslake, SERT II: Durability of the hollow cathode and future applications of hollow cathodes, J. Spacecraft and Rockets, 7, 14, 1970.

Reasoner, D. L., W. Lennartsson and C. R. Chappel, Relationship between ATS-6 spacecraft charging occurrences and warm plasma encounters, SPACECRAFT CHARGING BY MAGNETOSPHERIC PLASMAS, Progress in Astronautics and Aeronautics, 47, Rosen, ed.; AIAA, MIT Press, 1976.

Reme, H., A. Saint-Marc, J. M. Vigo, K. I. Gringauz, G. G. Managadze, S. B. Lyakhov, L. P. Smirnova, N. M. Schutte and W. R. Sheldon, Results of the ARAKS particle experiments, Symposium on Active Experiments in Space Plasmas, Boulder, Colo., June, 1976.

Rosen, A., Spacecraft charging: Environmental induced anomalies, J. Spacecraft and Rockets, 13, 129, 1976.

Trichel, M. C., E. J. R. Maier and W. C. Beggs, Artificial aurora experiment: Electron spectrum and return current measurements, unpublished manuscript, 1971.

Ward, J. W., H. J. King, Mercury hollow cathode plasma bridge neutralizers, J. Spacecraft and Rockets, 5, 1161, 1968.

Weill, G., M. Fehrenbach, J.-P. Berger, C. Barat, and C. Magene, Optical Observation Systems for the ARAKS Experiment, Space Science Instrumentation, 4, 239-250, 1978.

Whipple, E. C., Jr., The equilibrium potential of a body in the upper atmosphere and in interplanetary space, NASA Technical Note X-615-65-296, 1965.

Whipple, E. C., Jr., Theory of the spherically symmetric photoelectron sheath: A thick sheath approximation and comparison with the ATS-6 observation of a potential barrier, J. Geophys. Res., 81, 601, 1976a.

Whipple, E. C., Jr., Observation of photoelectrons and secondary electrons reflected from a potential barrier in the vicinity of ATS-6, J. Geophys. Res., 81, 715, 1976b.

Winckler, J. R., An investigation of wave-particle interactions and particle dynamics using electron beams injected from sounding rockets, Space Science Reviews, 15, 751, 1974a.

Winckler, J. R., Investigation of electron dynamics in the magnetosphere with electron beams injected from sounding rockets, J. Geophysics, 40, 729, 1974b.

Winckler, J. R., R. L. Arnoldy and R. A. Hendrickson, Echo 2: A study of electron beams injected into the high-latitude ionosphere from a large sounding rocket, J. Geophys. Res., 80, 2083, 1975a.

Winckler, J. R., R. L. Arnoldy and R. A. Hendriskson, Electron Echo III: Description of geophysical conditions and comparison of radar and inflight ion drift measurements, AGU Spring Meeting, June 16-20, 1975, Washington, D.C.; EOS, 56, 436, 1975, SM115, 1975b.

Winckler, J. R., A summary of recent results under the 'Echo' program for the study of the magnetosphere by artificial electron beams, Cosmic Physics Technical Report 168, School of Physics and Astronomy, Univ. of Minnesota, Minneapolis, September, 1976.

Worlock, R., G. Trump, J. M. Sellen and R. F. Kemp, Measurement of ion thruster exhaust characteristics and interaction with simulated ATS-F spacecraft, AIAA Paper 73-1101, AIAA 10th Electric Propulsion Conference, Lake Tahoe, Nevada, Oct. 31-Nov. 2, 1973.

Worlock, R., J. J. Davis, E. James, P. Ramirez, and O. Wood, An advanced contact ion microthruster system, J. Spacecraft and Rockets, 6, 424, 1969.

Worlock, R. M., E. L. James, R. E. Hunter and R. O. Bartlett, ATS-6 cesium bombardment engine north-south stationkeeping experiment, IEEE Transactions Aerospace and Electronic Systems, AES-11, #6, 1176, November 1975.

Zhulin, I. A., I. M. Kopsev, T. E. Rocheletts and A. M. Moskaleuko, On rocket charge neutralization in 'Zarnitza experiments,' ARAKS Symposium, France, May 1976.

APPENDICES

Appendix 1.   Bibliographical Notes

Aerobee

The most useful published material is in the paper by Hess (1971). This paper also contains an extensive bibliography on the ionosphere, magnetosphere, aurora, and early experiments (mainly particle detectors and barium releases).

Additional information is in papers by Davis (1971, 1973), Hess (1964), and Trichel (1971).

Echo

The Echo Series has an extensive bibliography, which breaks down into the following categories:

Echo I:

Cartwright (1971, 1974)

Hendrickson (1971, 1972, 1975)

McEntire (1974)

Winckler (1974a)

Echo II:

Kellogg (1976)

Winckler (1974a, b, 1975a)

Echo III:

Hanser (1976)

Hendrickson (1975, 1976)

Israelson (1974, 1975, 1976)

Kellogg (1976)

Morgan (1975)

Winckler (1974b, 1975b)

Echo IV:

Winckler (1976)

Echo I:

The most useful information on the neutralization of the rocket is contained in two technical reports (Hendrickson (1972); Winckler (1976)). The instruments are discussed and data is presented.

Hendrickson (1971) and Cartwright (1971), give quick summaries of Echo I, with Hendrickson describing the neutralizer apparatus. Hendrickson's thesis (1972) provides the best set of information on neutralization, and is essential in any study of Echo I data.

The other Echo I papers concentrate on the magnetosphere and traveling beam physics.

Echo II:

The papers on this experiment are concerned with things other than neutralization, as was the experiment.

Echo III:

The Israelson-Winckler dialogue with Hanser and Sellers has some of the most pertinent information on the satellite (Israelson (1975, 1976); Hanser (1976)). The most useful information, however, is in the technical report by Winckler (1976). The remaining papers serve mainly as background, from the neutralization viewpoint.

Echo IV:

The Winckler technical report (1976) includes a great deal of information. Published data by Israelson and Winckler (1978) and Hallinan (1978) is good.

PRECEDE and EXCEDE

O'Neil et al. (1978a) and (1978b) have covered both rocket shots.

ARAKS

The ARAKS data was first presented at a symposium in 1976 in Toulouse, France. Data has been unavailable except for a graph in Winckler (1076). The ARAKS talks are referenced by him. The Boulder Symposium provided abstracts from which the basic data presented in this paper was obtained.

An overview is given in Nature by Cambou (1978).

The authors involves are Cambou (1975, 1976), Gendrin (1974), Gringauz (1976), Rème (1976), and Zhulin (1976). There is a host of co-authors whose names could be checked for publication in the future.

The Space Science Instrumentation articles, Cambou (1978), Charles (1978), and Weill (1978) have not been reviewed.

Japan

Japanese experiments are not yet well published in the U. S. The most useful information is in a paper by Kawashima (1976).

One plasma operation was reported by Kawashima (1978).

The University of Tokyo publication is complete in items, but thin in coverage.

SERT II

Most of the information on the spacecraft potential is in Jones (1970) and Kerslake (1975). A good set of data is in Kerslake (1971). For descriptions of the neutralizer, see Rawlin (1968) and Ward (1968). Ward is a good general reference on neutralizers which would also be useful for ATS-6. In turn, Worlock (1973) is useful as a reference for SERT as well as ATS.

The remaining papers give background information, diagrams and test results from ground and space. These are by: Bechtel (1968), Byers (1970), Kerslake (1970, 1973, 1976), and Rawlin (1970).

ATS-4, 5, 6

ATS-4 is represented solely by the paper by Hunter (1969).

ATS-5 papers consist mainly of environmental results from the UCSD detectors.

The published data on the ATS-5 thruster is represented by a paper by Worlock (1969).

DeForest (1973) details the unneutralized operation of the ATS-5 thruster.

Goldstein (1976) describes all other significant results, but for completeness, the paper by Bartlett (1975) is useful.

The operations of the ATS-6 ion thrusters received an early write-up by Worlock (1975), including the engine failures and clean-up attempts.

Good background material on the engines is contained in the papers by James (1970, 1973, 1975). The most useful ground tests were by Worlock (1973), including biasing of the neutralizer. This paper als contains a good comparison between ATS-6 and SERT II.

Papers and Talks

A number of presentations have been made of the data obtained under this contract.

At the beginning of the contract, Bartlett et al. (1975) presented a paper at the AIAA. Goldstein and DeForest (1976) published this work in an AIAA book, accompanied by Whipple's (1976a) JGR paper.

The USAF/NASA charging conference in 1976 was marked by the paper by Purvis et al. (1976). (The Conference Proceedings were published by Pike & Lovell in Feb. 1977, as AFGL-TB-77-0051 or NASA-TMX-73537.)

The only 1977 publication was the first major contract report on this work, by Olsen & Whipple in 1977. It is superseded by this report. Olsen (1977) presented ATS-5 results at the Dec. 1977 AGU Conference in San F ancisco.

Things picked up in 1978. Olsen et al. (1978) spoke at the Ionospheric Effects Symposium in January 1978 at Arlington, Va.

Olsen (1978a) presented the same information at the AIAA Conference in San Diego, Calif. , April 1978.

At the USAF/NASA Charging Conference in Colorado Springs, Bartlett and Purvis (1978), Olsen and Whipple (1978), and Johnson and Whipple (1978) all presented results from this work.

The year was rounded out by AGU presentations by DeForest (1978) and Olsen (1978b).

Appendix 2. ATS-5 Command Log

Engine Commands

Ionizer Heater ON

This command activates the ionizer converter which supplies power
to the ionizer heater, the neutralizer heater, and supplies power to internal
logic circuitry. All the remaining telemetry and command discriminators
are active at this point. The High Voltage ON command should be given
within 15 minutes of this command in order to preclude the possibility of
emitting neutral cesium.

High Voltage ON

This command activates the high voltage converter supplying plus
3000 volts to the ionizer button and minus 2000 volts to the accelerator
electrodes. In addition this converter supplies power to the vaporizer
heater and the beam deflection supplies, which are not active at this time
since each is controlled by separate commands. The automatic neutralizer
select circuitry also becomes active at this time.

The currents in both the plus and minus high voltage leads are con-
tinuously monitored. If they exceed their predetermined trip level, the
high voltage converter will shut down and automatically come on again after
approximately 10 milliseconds. If the overload is again present the cycle
will repeat. An arc counter circuit accumulates the net duration of the
converter "off-time" and after about one and a half minutes of continuous
arcing, the experiment is automatically turned off. The thrust on com-
mand may now be given if it has been preceded by the ionizer on and high
voltage on commands.

High Voltage OFF

This command removes the high voltage accelerating potentials from
the ion engine by turning off the high voltage converter. It may be pre-
empted by the Ionizer Heater OFF command if desired, since a High Voltage
OFF command would then automatically be issued internally.

2-1

Ionizer Heater OFF

The Ionizer Heater OFF command turns off the ionizer converter. This removes power from the ionizer heater, the neutralizer heater, and most of the telemetry as previously described. In addition, this command internally generates a High Voltage OFF and a Thrust OFF command. This is done to preclude the possibility of shutdown commands being given in an improper sequence. The ion engine experiment is now shutdown. The system may be immediately restarted by repeating the turn-on procedure.

ATS-5 Neutralizer Legend

CMD	Description
150	Ion Engine #2 High Voltage ON
171	Ion Engine #2 Heater OFF
254	Ion Engine #2 heater ON
246	Ion Engine #2 Regulator ON
310	Ion Engine #2 Regulator OFF
EN	Enter Eclipse (umbra)
EX	Exit Eclipse (umbra)

Eclipse times are predicted, and have not been measured.

Command times come from the command logs supplied by Goddard Space Flight Center.

ATS-5   Ion Engine Test

July 20, 1972
202/72

Time	CMD	Function
20:36:00	254	Ion heater OFF
20:36:30	150	HV ON
20:41:00	171	Ion heater OFF
21:26:00	254	Ion heater ON
21:26:30	150	HV ON
21:31:00	171	Ion heater OFF
21:31:04	150	HV ON

September 26, 1973
Day 269

Time	CMD	Function
03:19:40	246	Ion eng 2 P/L reg on
03:20:45	254	Ion hts on
03:20:55	150	HV on
03:25:55	171	Ion htr off
03:26:03	150	HV on
03:35:55	254	Ion htr on
03:36:02	150	HV on
03:40:55	171	Ion htr off
03:41:02	150	HV on
03:50:55	254	Ion htr on
03:51:01	150	HV on
03:57:55	171	Ion htr off
05:04:05	254	Ion htr on
05:04:16	150	HV on
05:06:25	254	Ion htr on
05:06:30	150	HV on
05:08:10	254	Ion htr on
05:12:00	150	HV on
05:13:00	171	Ion htr off
05:13:08	150	HV on
05:14:50	275	HV off
05:48:10	254	Ion htr on
05:51:10	150	HV on
05:54:00	171	Ion htr off
05:54:06	150	HV on
05:55:00	310	Ion eng 2 reg off

No data taken with operations before September 2, 1974

September 3, 1974

Day 246 - Note: No data was received for this day.

CMD	Time
246	06:04:35
254	06:05:05
171	06:07:20
EN	06:37:52
254	06:43:45
171	06:48:45
254	07:14:00
171	07:19:00
EX	07:26:46
150	07:45:00
254	07:45:50
171	07:53:00
150	07:53:25
310	07:56:00

No log available for September 4, no data recorded.

No neutralizer operations for September 5 and 6.

No data received, September 6.

ATS-5 Eclipse Season Neutralizer Operations
1974

CMD	Sept. 7 250	CMD	Sept. 12 255	CMD	Sept. 16 259
EN	6:31:55	EN	6:26:53	EN	6:24:14
254	6:41:35	254	6:20:40	254	6:33:40
171	6:46:35	171	6:25:40	171	6:37:40
254		254	7:01:55	254	7:14:15
171		171	7:06:55	171	7:18:15
EX	7:29:53	EX	7:31:25	EX	7:31:16

	Sept. 8 251		Sept. 13 256		Sept. 17 260
EN	6:30:47	EN	6:26:04	EN	6:23:43
254	6:40:15	254	6:35:15	254	6:33:25
171	6:45:15	171	6:40:15	171	6:37:25
254	7:36:00	254	7:15:20	254	7:13:20
171	7:41:00	171	7:20:20	171	7:17:20
EX	7:30:24	EX	7:31:32	EX	7:31:04

	Sept. 9 252		Sept. 14 257		Sept. 18 261
EN	6:29:39	EN	6:25:24	EN	6:23:17
254	6:39:05	254	6:34:40	254	6:32:45
171	6:44:05	171	6:38:40	171	6:36:45
254	7:30:40	254	7:13:15	254	7:12:05
171	7:35:45	171	7:17:15	171	7:16:05
EX	7:30:45	EX	7:31:30	EX	7:30:47

	Sept. 10 253		Sept. 15 258		Sept. 19 262
EN	6:28:36	EN	6:24:44	EN	6:22:56
254	6:38:15	254	6:34:10	254	6:32:30
171	6:43:15	171	6:38:10	171	6:36:30
254	7:24:05	254	7:11:05	254	7:11:45
171	7:29:20	171	7:15:05	171	7:15:45
EX	7:31:06	EX	7:31:27	EX	7:30:26

Sept. 11
254
3DLE off
No operations

CMD	Sept. 20 263	CMD	Sept. 24 267	CMD	Sept. 28 271
EN	6:22:40	EN	6:22:16	EN	6:23:13
254	6:31:25	254	6:32:20	254	6:33:55
171	6:35:25	171	6:36:20	171	6:37:55
254	7:09:10	254	7:15:30	254	7:12:45
171	7:13:10	171	7:25:20	171	7:16:45
EX	7:30:01	EX	7:27:35	EX	7:24:04

	Sept. 21 264		Sept. 25 268		Sept. 29 272
EN	6:22:28	EN	6:22:23	EN	6:23:43
254	6:32:00	254	6:32:35	254	6:33:50
171	6:36:00	171	6:36:35	171	6:37:50
254	7:11:35	254	7:16:45	254	7:13:10
171	7:15:35	171	7:20:45	171	7:17:10
EX	7:29:30	EX	7:26:51	EX	7:23:01

	Sept. 22 265		Sept. 26 269		Sept. 30 273
EN	6:22:21	EN	6:22:35	EN	6:24:14
254	6:32:05	254	6:36:55	254	6:34:20
171	6:36:05	171	6:40:55	171	6:38:20
254	7:14:15	254	7:14:55	254	7:13:25
171	7:18:15	171	7:18:55	171	7:17:25
EX	7:28:55	EX	7:26:01	EX	7:21:48

	Sept. 23 266		Sept. 27 270		Oct. 1 274
EN	6:22:19	EN	6:22:52	EN	6:24:53
254	6:32:30	254	6:33:05	254	6:35:05
171	6:36:30	171	6:37:05	171	6:39:05
254	7:11:45	254	7:12:25	254	7:13:10
171	7:19:00	171	7:16:25	171	7:18:15
EX	7:28:20	EX	7:25:03	EX	7:20:31

CMD	Oct. 2 275	CMD	Oct. 6 279	CMD	Oct. 10 283
EN	6:25:43	EN	6:30:33	EN	6:41:30
254	6:35:55	254	6:40:45	254	6:49:25
171	6:39:55	171	6:45:00	171	--
254	7:13:50	254	7:00:40	254	--
171	7:17:50	171	7:04:50	171	6:54:25
EX	7:19:04	EX	7:11:58	EX	6:59:04
	Oct. 3 276		Oct. 7 280	End of eclipse season.	
EN	6:26:41	EN	6:32:23		
254	6:36:45	254	6:43:20		
171	6:40:45	171	6:47:25		
254	7:13:55	254	6:54:35		
171	7:17:55	171	6:58:40		
EX	7:17:33	EX	7:09:39		
	Oct. 4 277		Oct. 8 281		
EN	6:27:45	EN	6:34:37		
254	6:38:00	254	6:45:40		
171	6:42:00	171	6:50:00		
254	7:15:45	254	6:54:50		
171	7:20:15	171	6:59:00		
EX	7:15:52	EX	7:06:58		
	Oct. 5 278		Oct. 9 282		
EN	6:29:07	EN	6:37:28		
254	6:40:15	254	6:50:20		
171	6:45:00	171	--		
254	6:58:35	254	--		
171	7:03:20	171	6:55:30		
EX	7:14:02	EX	7:03:38		

No operations Feb. 20-24

CMD	Feb. 25 56	CMD	March 2 61	CMD	March 6 65
EN	6:54:15	EN	6:45:23	EN	6:40:47
254	7,05:55	254	7:05:00	254	6:54:20
171	7:14:00	171	7:10:00	171	6:59:40
EX	7:32:37				
		254	7:28:25	254	7:25:35
	Feb. 26 57	171	7:33:00	171	7:30:35
		EX	7:39:27	EX	7:42:11
EN	6:52:02		March 3 62		March 7 66
254	7:06:00				
171	7:12:00	EN	6:44:01	EN	6:39:53
EX	7:34:27	254	6:50:00	254	6:52:40
		171	6:55:00	171	6:57:40
	Feb. 27 58	254	7:20:00	254	7:26:05
		171	7:25:00	171	7:31:05
EN	6:50:07	EX	7:40:16	EX	7:42:32
254	7:05:00				
171	7:10:00		March 4 63		March 8 67
EX	7:35:59				
		EN	6:42:53	EN	6:39:04
	Feb. 28 59	254	6:47:00	254	6:51:25
		171	6:52:00	171	6:56:25
EN	6:48:22				
254	7:05:00	254	7:23:00	254	7:22:15
171	7:10:00	171	7:28:00	171	7:27:25
EX	7:37:16	EX	7:41:01	EX	7:42:53
	March 1 60		March 5 64		March 9 68
EN	6:46:45				
254	7:05:00	EN	6:41:45	EN	6:38:19
171	7:10:00	254	6:46:00	254	6:51:20
EX	7:38:29	171	6:51:00	171	6:56:20
		254	7:24:00	254	7:23:40
		171	7:29:00	171	7:28:55
		EX	7:41:41	EX	7:43:10

CMD	March 10 69	CMD	March 14 73	CMD	March 18 77
EN	6:37:39	EN	6:35:42	EN	6:34:55
254	6:49:50	254	6:43:45	254	6:47:35
171	6:54:55	171	6:47:45	171	6:51:35
254	7:20:10	254	7:33:40	254	7:32:30
171	7:25:25	171	7:37:40	171	7:36:30
EX	7:43:17	EX	7:43:07	EX	7:41:48
	March 11 70		March 15 74		March 19 78
EN	6:37:04	EN	6:35:26	EN	6:34:53
254	6:49:20	254	6:42:40	254	6:47:50
171	6:54:20	171	6:46:40	171	6:52:50
254	7:19:55	254	7:34:00	254	7:29:15
171	7:24:55	171	7:38:00	171	7:34:15(7:36:10)
EX	7:43:19	EX	7:42:51	EX	7:41:13
	March 12 71		March 16 75		March 20 79
EN	6:36:34	EN	6:35:09	EN	6:34:55
254	6:49:25	254	6:48:00	254	6:47:30
171	6:54:25	171	6:52:05	171	6:52:30
254	--	254	7:34:05	254	7:25:00
171	--	171	7:38:20	171	7:30:00
EX	7:43:22	EX	7:42:35	EX	7:40:37
	March 13 72		March 17 76		March 21 80
EN	6:36:02	EN	6:35:02	EN	6:35:02
254	--	254	6:47:50	254	6:47:35
171	--	171	6:51:50	171	6:52:35
	no ops				
254	--	254	--	254	7:25:00
171	--	171	--	171	7:30:00
EX	7:43:15	EX	7:42:14	EX	7:39:58

Spring 1975   (Continued)

CMD	March 22 81	CMD	March 26 85	CMD	March 30 89
EN	6:35:14	EN	6:36:48	EN	6:40:09
254	6:47:30	254	6:50:30	254	7:00:30
171	6:52:30	171	6:55:30	171	7:05:45
254	7:25:00	254	--	254	--
171	7:30:00	171	--	171	--
EX	7:39:13	EX	7:35:23	EX	7:29:51

	March 23 82		March 27 86		March 31 90
EN	6:35:30	EN	6:37:28	EN	6:41:22
254	6:40:10	254	6:50:00	254	7:00:25
171	6:45:10	171	6:55:00	171	7:05:30
				EX	7:28:10
254	7:10:15	254	7:20:00		
171	7:15:15	171	7:25:00		April 1
EX	7:38:24	EX	7:34:11		91

	March 24 83		March 28 87	EN	6:42:44
				254	7:01:00
				171	7:06:00
EN	6:35:52	EN	6:38:12	EX	7:26:15
254	--	254	6:50:00		
171	--	171	6:55:00		April 2
	no ops				92
254	--	254	7:22:00		
171	--	171	7:27:00	EN	6:44:20
EX	7:37:30	EX	7:32:53	254	7:05:00
				171	7:10:00
	March 25 84		March 29 88	EX	7:24:06
					April 3
					93
EN	6:36:17	EN	6:39:06		
254	6:50:30	254	6:50:00	EN	6:46:20
171	6:55:30	171	6:55:00	254	7:00:30
254	7:20:35	254	7:20:00	171	7:05:30
171	7:25:45	171	7:25:00	EX	7:21:38
EX	7:36:27	EX	7:31:27		

CMD	April 4
	94
EN	6:48:43
254	7:00:35
171	7:05:35
EX	7:18:43

	April 5
	95
EN	6:51:48
254	7:00:35
171	7:05:35
EX	7:15:05

	April 6
	96
EN	6:56:45
254	7:01:10
171	7:06:10
EX	7:09:39

	April 7
	97
EN	--
254	--
171	--
EX	--

End of
eclipse
season.

Fall 1975

CMD	Sept. 20 263	CMD	Sept. 24 267	CMD	Sept. 28 271
EN	6:20:47	EN	6:20:57	EN	6:22:31
254	6:29:55	254	6:30:10	254	6:31:35
171	6:34:55	171	6:35:10	171	6:36:35
254	7:03:00	254	6:59:25	254	7:01:25
171	7:08:00	171	7:04:25	171	7:06:25
EX	7:27:26	EX	7:24:32	EX	7:20:29
	Sept. 21 264		Sept. 25 268		Sept. 29 272
EN	6:20:40	EN	6:21:13	EN	6:23:10
254	6:28:35	254	6:30:35	254	6:32:20
171	6:33:35	171	6:35:35	171	6:37:20
254	7:00:00	254	7:00:30	254	7:02:00
171	7:05:00	171	7:05:30	171	7:07:00
EX	7:26:51	EX	7:23:39	EX	7:19:16
	Sept. 22 265		Sept. 26 269		Sept. 30 273
EN	6:20:43	EN	6:21:34	EN	6:23:55
254	6:30:00	254	6:30:55	254	6:33:05
171	6:35:00	171	6:35:55	171	6:38:05
254	7:00:20	254	7:01:05	254	7:02:35
171	7:05:20	171	7:06:05	171	7:07:35
EX	7:26:06	EX	7:22:40	EX	7:17:54
	Sept. 23 266		Sept. 27 270		Oct. 1 274
EN	6:20:50	EN	6:22:00	EN	6:24:49
254	6:30:00	254	6:32:00	254	6:34:20
171	6:35:00	171	6:37:00	171	6:39:20
254	6:59:50	254	7:01:40	254	7:10:05
171	7:04:50	171	7:06:40	171	7:15:05
EX	7:25:22	EX	7:21:37	EX	7:16:27

CMD	Oct. 2 275		CMD	Oct. 5 278
EN	6:25:52		EN	6:30:12
254	6:35:25		254	6:39:40
171	6:40:25		171	6:44:40
			EX	7:08:53
254	--			
171	--			Oct. 6
EX	7:14:51			279
	Oct. 3		EN	6:32:17
	276		254	6:41:50
			171	6:46:50
EN	6:27:05		EX	7:06:25
254	6:36:35			
171	6:41:35			Oct. 7
				280
254	--			
171	--		EN	6:34:44
EX	7:13:06		254	6:44:50
			171	6:49:50
	Oct. 4		EX	7:03:20
	277			
				Oct. 8
EN	6:28:32			281
254	6:38:00			
171	6:43:00		EN	6:38:13
			254	6:48:45
254	--		171	6:53:45
171	--		EX	6:59:28
EX	7:11:06			
				Oct. 9
				282
				3DLE off
				End of eclipse season

CMD	Feb. 20 51	CMD	Feb. 24 55	CMD	Feb. 28 59
EN	7:04:28	EN	6:52:49	EN	6:46:16
254	7:16:30	254	7:04:00	254	6:58:00
171	7:21:30	171	7:09:00	171	7:03:00
254	--	254	--	254	7:27:30
171	--	171	--	171	7:32:30
EX	7:24:46	EX	7:35:10	EX	7:40:10
	Feb. 21 52		Feb. 25 56		Feb. 29 60
EN	7:00:31	EN	6:50:54	EN	6:44:58
254	7:11:50	254	7:03:20	254	6:55:00
171	7:16:50	171	7:08:20	171	7:00:00
254	--	254	--	254	7:25:00
171	--	171	--	171	7:30:00
EX	7:28:24	EX	7:36:41	EX	7:41:04
	Feb. 22 53		Feb. 26 57		March 1 61
EN	6:57:26	EN	6:49:09	EN	6:43:46
254	7:08:35	254	7:00:25	254	6:56:30
171	7:13:35	171	7:06:25	171	7:01:30
254	7:14:25	254	--	254	7:27:00
171	7:17:05	171	--	171	7:32:00
EX	7:31:11	EX	7:37:59	EX	7:41:48
	Feb. 23 54		Feb. 27 58		March 2 62
EN	6:54:58	EN	6:47:38	EN	6:42:42
254	7:05:45	254	6:55:00	254	6:55:00
171	7:10:45	171	7:00:05	171	7:00:00
254	--	254	7:20:00	254	7:28:00
171	--	171	7:25:00	171	7:32:00
EX	7:33:20	EX	7:39:11	EX	7:42:24

CMD	March 3 63	CMD	March 7 67	CMD	March 11 71
EN	6:41:44	EN	6:38:41	EN	6:36:44
254	6:55:00	254	6:48:55	254	6:46:50
171	7:00:00	171	6:53:55	171	6:51:50
254	7:25:00	254	7:20:05	254	7:18:25
171	7:30:00	171	7:25:05	171	7:23:30
EX	7:42:54	EX	7:44:09	EX	7:44:04

	March 4 64		March 8 68		March 12 72
EN	6:40:50	EN	6:38:06	EN	6:36:23
254	6:51:30	254	6:48:15	254	6:46:35
171	6:56:30	171	6:53:15	171	6:51:35
254	7:22:10	254	7:19:00	254	7:17:00
171	7:27:10	171	7:24:00	171	7:22:10
EX	7:43:20	EX	7:44:16	EX	7:43:53

	March 5 65		March 9 69		March 13 73
EN	6:40:05	EN	6:37:35	EN	6:36:11
254	6:50:25	254	6:47:40	254	6:46:20
171	6:55:25	171	6:52:40	171	6:51:20
254	7:19:40	254	7:18:00	254	7:17:20
171	7:24:40	171	7:23:00	171	7:22:20
EX	7:43:41	EX	7:44:14	EX	7:43:36

	March 6 66		March 10 70		March 14 74
EN	6:39:21	EN	6:37:05	EN	6:35:59
254	6:49:45	254	6:47:15	254	6:50:50
171	6:54:45	171	6:52:15	171	6:55:50
254	7:18:45	254	7:16:50	254	7:20:25
171	7:23:45	171	7:21:50	171	7:25:25
EX	7:43:57	EX	7:44:11	EX	7:43:15

CMD	March 15 75	CMD	March 19 79	CMD	March 23 83
EN	6:35:52	EN	6:36:06	EN	6:37:35
254	6:46:25	254	6:54:35	254	6:49:10
171	6:51:25	171	6:59:35	171	6:54:10
254	7:17:20	254	7:10:00	254	7:04:10
171	7:22:20	171	7:15:00	171	7:09:10
EX	7:42:49	EX	7:40:29	EX	7:36:48

	March 16 76		March 20 80		March 24 84
EN	6:35:50	EN	6:36:23	EN	6:38:15
254	6:46:20	254	no	254	6:49:05
171	6:51:20	171	operation	171	6:54:05
254	7:01:20	254	--	254	7:04:05
171	7:06:20	171	--	171	7:09:10
EX	7:42:19	EX	7:39:39	EX	7:35:40

	March 17 77		March 21 81		March 25 85
Data unprocessable					
EN	6:35:52		3DLE on	EN	6:38:55
254	6:46:25		no	254	6:50:05
171	6:51:25		operation	171	6:55:05
254	7:01:30		March 22 82	254	7:05:05
171	7:06:30			171	7:10:05
EX	7:41:48			EX	7:34:28

	March 18 78		3DLE off no operation		March 26 86
Data unprocessable					
EN	6:35:54			EN	6:39:44
254	6:59:40			254	6:51:40
171	7:05:20			171	7:01:15
254	7:15:15			254	7:11:50
171	7:20:00			171	7:17:05
EX	7:41:09			EX	7:33:06

CMD	March 27 87	CMD	March 31 91	CMD	April 3 94
EN	6:40:43	EN	6:46:20	EN	6:54:49
254	6:51:25	254	6:58:00	254	7:05:20
171	6:56:25	171	7:03:00	171	7:10:20
254	7:06:25	254	7:14:00	254	7:20:25
171	7:11:25	171	7:19:00	171	7:25:30
EX	7:31:39	EX	7:24:04	EX	7:14:11
	March 28 88		April 1 92		End of eclipse season
EN	6:41:51	EN	6:48:29		
254	6:53:00	254	6:59:35		
171	6:58:10	171	7:05:05		
254	7:08:00	254	7:15:10		
171	7:13:00	171	7:20:10		
EX	7:30:03	EX	7:21:27		
	March 29 89		April 2 93		
EN	6:43:08	EN	6:51:06		
254	6:55:20	254	7:00:10		
171	7:00:20	171	7:05:10		
254	7:10:20	254	7:15:15		
171	7:15:20	171	7:20:20		
EX	7:28:17	EX	7:18:17		
	March 30 90				
EN	6:44:35				
254	6:56:15				
171	7:01:15				
254	7:11:15				
171	7:16:15				
EX	7:26:18				

CMD	Aug. 20 233	CMD	Aug. 20 233	CMD	Sept. 1 245
254	6:01:15	254	18:03:25	254	6:25:15
171	6:11:15	171	18:14:50	EN	6:31:43
				171	6:35:15
254	7:00:50	254	19:00:25	EX	7:28:07
254	7:02:55	171	19:10:25		
171	7:15:20				Sept. 2 246
		254	20:00:46		
254	8:00:50	171	20:10:50	254	6:26:05
254	8:02:40			EN	6:30:26
171	8:10:50	254	21:00:25	171	6:38:50
171	8:11:50	171	21:10:55	EX	7:28:43
171	8:12:55				
		254	22:00:25		Sept. 3 247
254	9:00:45	171	22:10:05		
171	9:10:45				
		254	23:00:25	EN	6:29:18
254	10:00:45	171	23:10:00	254	6:35:10
171	10:10:45			171	6:45:10
			Aug. 21 234	EX	7:29:08
254	11:00:40				
171	11:10:40	254	00:00:30		Sept. 9 253
		171	00:12:40		
254	12:00:50				
171	12:10:00	254	01:04:00	EN	6:24:08
		171	01:12:05	254	6:25:30
254	13:01:10			171	6:35:30
171	13:10:25	254	02:00:30	EX	7:30:14
		171	02:10:00		
254	14:04:40				Sept. 15 259
171	14:14:20	254	03:00:40		
		171	03:09:30		
254	15:00:30			EN	6:21:24
171	15:10:45	254	04:00:25	254	6:25:00
		171	04:10:40	171	6:35:45
254	16:02:25			EX	7:28:50
171	16:11:30				
254	17:00:30				
171	17:10:30				

Neutralizer Operation, 1976 (Continued)

CMD	Sept. 22 266	CMD	Nov. 14 319	CMD	Nov. 14 319
EN	6:21:27	254	5:33:40	254	19:31:50
254	6:25:15	171	5:38:55	171	19:37:05
171	6:35:20				
EX	7:24:15	254	6:31:50	254	20:32:35
		171	6:36:50	171	20:37:35
	Sept. 29 273				
		254	7:30:15	254	21:30:40
		171	7:35:15	171	21:38:15
EN	6:25:38				
254	6:25:00	254	8:30:50	254	22:32:15
171	6:35:00	171	8:36:15	171	22:37:15
EX	7:15:56				
		254	9:29:40	254	23:31:15
		171	9:34:55	171	23:36:15
	Oct. 4 278				
		254	10:30:30		Nov. 15 320
		171	10:35:35		
EN	6:33:33				
254	6:35:00	254	11:30:35	254	00:30:40
171	6:45:00	171	11:35:50	171	00:35:40
EX	7:05:30				
		254	12:31:35	254	01:30:25
	Oct. 5 279	171	12:36:35	171	01:35:30
		254	13:30:55	254	02:30:00
EN	6:36:15	171	13:35:55	171	02:35:00
254	6:40:00				
171	6:50:00	254	15:30:40	254	03:31:55
EX	7:02:16	171	15:35:40	171	03:36:55
	Oct. 6 280	254	16:30:55	254	04:30:30
		171	16:35:55	171	04:35:40
EN	6:40:12				
254	6:45:00	254	17:34:45		
171	6:55:00	171	17:40:05		
EX	6:57:56				
		254	18:31:40		
		171	18:36:40		

ATS-5 Operations - 1977

Eclipse and Neutralizer Times

Neutralizer 2	March 31, 1977	April 1, 1977
Enter Eclipse	05:20:40	05:22:11
Neutralizer On (254)	05:31:10	05:32:45
Neutralizer Off(171)	05:49:30	05:43:XX **
Exit Eclipse	05:52:14	05:47:44

Neutralizer 1	August 30	August 31	September 1	September 2
Enter Eclipse	04:12:39	04:11:27	04:10:19	04:09:11
Neutralizer 1 on (044)	04:22:35	04:21:15	04:20:35	04:18:45
Neutralizer 1 off(112)	04:28:00	04:26:15	04:26:15	04:23:45
Exit Eclipse	05:08:31	05:09:06	05:09:32	05:09:58

Neutralizers 1 and 2	October 2	October 3	October 4
Enter Eclipse	04:12:04	04:14:13	04:12 *
Neutralizer 1 on (044)	04:12:30	04:12:50 **	04:15:55
Neutralizer 2 on (254)	04:16:20	04:16:00	04:20:55
Neutralizer 1 off(112)	04:19:45	04:20:20	04:25:55
Neutralizer 2 off(171)	04:24:10	04:25:45	04:30:55
Exit Eclipse	04:48:33	04:45:56	04:42:46

Neutralizers 1 and 2	October 5, 1977
Enter Eclipse	04:20:47
Neutralizer 2 on (254)	04:20:05 **
Neutralizer 2 off(171)	04:24:00
Neutralizer 1 on (044)	04:25:55
Neutralizer 2 on (254)	04:28:55
Neutralizer 1 off(112)	04:34:55
Neutralizer 2 off(171)	04:36:50
Exit Eclipse	04:38:31

** Within accuracy of eclipse prediction and log times, there is overlap
   between eclipse transition and neutralizer command.

Note: Eclipse times are based on prediction generated at GSFC unless time
       is starred (*). In this case time is taken from change in particle
       data.

ATS-5 Operations - 1978

Eclipse and Neutralizer Times

Command	February 18	February 19	February 20	February 21
enter eclipse	04:36	04:32 ★	04:32	04:30
Neut. 1 on	04:36:25	04:34:05	04:32:30	04:29:20
Neut. 2 on	04:39:20	04:37:35	04:36:00	04:32:45
Neut. 1 off	04:41:55	04:40:35	04:39:00	04:35:50
Neut. 2 off	04:44:55	04:42:55	04:42:00	04:38:55
exit eclipse	05:12	05:14	05:16	05:17

Command	February 22	February 23	February 24	February 25
enter eclipse	04:29	04:27	04:26	04:25
Neut. 1 on	04:27:30	04:26:05	04:24:35	04:23:30
Neut. 2 on	04:30:50	04:29:30	04:28:00	04,26:35
Neut. 1 off	04:33:50	04:32:30	04:31:00	04:29:35
Neut. 2 off	04:37:00	04:35:35	04:34:00	04:32:35
exit eclipse	05:19	05:20	05:20	05:21

No Operations February 26, 27, March 2, 3, 6

Command	February 28	March 1	March 4	March 5
enter eclipse	04:18 ★	04:21	04:19	04:18
Neut. 1 on	04:19:50	04:19:25	-	-
Neut. 2 on	04:23:10	04:22:45	04:21:50	04:20:10
Neut. 1 off	04:26:10	04:25:45	-	-
Neut. 2 off	04:29:10	04:28:45	04:37:15	04:43:30
exit eclipse	05:23	05:24	05:24	05:24

Command	March 7	March 8	March 9	March 10
enter eclipse	04:13 ★	04:17	04:17	04:17
Neut. 2 on	04:19:00	04:18:50	04:18:20	04:19:00
Neut. 2 off	04:34:25	04:34:00	04:33:35	04:34:15
exit eclipse	05:24	05:24	05:24	05:24

Command	March 11	March 12	March 13	March 14
enter eclipse	04:16	04:16	04:12 ★	04:11 ★
Neut. 2 on	04:17:30	04:17:15	04:17:10	04:16:50
Neut. 2 off	04:32:30	04:32:25	04:32:35	04:32:00
exit eclipse	05:23	05:23	05:23	05:22

Command	March 15	March 16	March 17	March 18
enter eclipse	04:16	04:12 ★	04:11 ★	04:17
Neut. 2 on	04:17:15	04:17:15	04:18:00	04:18:10
Neut. 2 off	04:32:35	04:32:20	04:33:00	04:33:20
exit eclipse	05:22	05:21	05:21	05:20

ATS-5 Operations - 1978
Eclipse and Neutralizer Times
page 2

Command	March 19	March 20	March 21	March 22
enter eclipse	04:10 ★	04:18	04:18	04:14 ★
Neut. 2 on	04:18:20	04:18:45	04:18:50	04:19:45
Neut. 2 off	04:33:20	04:33:45	04:33:50	04:34:50
exit eclipse	05:19	05:18	05:17	05:16

No Operations March 25

Command	March 23	March 24	March 26	March 27
enter eclipse	04:14 ★	04:21	04:17 ★	04:19 ★
Neut. 2 on	04:21:00	04:21:30	04:25:00	04:24:45
Neut. 2 off	04:36:20	04:36:30	04:40:00	04:39:45
exit eclipse	05:15	05:13	05:10	05:09

Command	March 28	March 29	March 30	March 31
enter eclipse	04:20 ★	04:21 ★	04:29	04:28 ★
Neut. 2 on	04:26:25	04:28:10	04:30:15	04:33:30
Neut. 2 off	04:41:30	04:43:10	04:47:50	04:48:35
exist eclipse	05:07	05:04	05:02	04:59

Command	April 1
enter eclipse	04:30 ★
Neut. 2 on	04:38:00
Neut. 2 off	04:51:05
exit eclipse	04:55

Appendix 3. ATS-6 Command Log

Appendix 3. GSFC ION ENGINE EXPERIMENT

The Ion engine experiment is important because of the effect its operation has on particle data. The spacecraft potential is shifted, and the diffusion of particles around the spacecraft reduces or eliminates differential charging.

Experiment Description

The objective of the ATS-6 Ion Engine Experiment was to demonstrate north-south stationkeeping for a geostationary spacecraft. It was the second ion engine experiment to successfully fly on a satellite.(SERT II was the first. ATS-4 & 5 both carried good engines, but the spacecraft failed.)

There are two ion engine systems on the spacecraft with their thruster subsystems mounted on the north and south faces of the Earth Viewing Module (EVM). The Z-axis(yaw axis) is Earth pointing and the velocity vector of the spacecraft lies in the X-axis(roll axis). The thrust vector makes a 36° angle with the yaw axis in the roll rotation plane and passes through the spacecraft center of mass.

The cesium bombardment ion thruster utilizes the magnetoelectrostatic plasma containment concept. A two grid extraction system is employed with 1.1 kv across the grids. At full power the thruster supplies about .1 Amp. Neutralizing electrons are produced by a plasma bridge neutralizer. The thruster floats with respect to the spacecraft. The outer grid is nominally at -550 volts. The beam and thruster are tied to the spacecraft through the neutralizer, which works within a volt of the spacecraft ground. There is a potential drop associated with the beam tie-in of a few volts.

The exhaust from the ion thruster consists of a semi-collimated cesium ion beam, with a half angle of 15°, and an efflux of uncollimated cesium ions, neutral cesium(which can charge exchange with the beam) and aluminum atoms. The ion beam, which constitutes 90% of the exhaust, impinges on no spacecraft component or structure. The remaining ions and neutral atoms leave the thruster with an approximate cosine distribution into a solid angle of 1.8 pi sr.(There were tests on the spacecraft to see how much cesium did hit the spacecraft surface. Results were mostly negative, i.e. no more than a monolayer during all experiments.)

Operations

There were two major operational periods of the Ion Engines. The first lasted for about one hour, and came on July 17, 1974 (day 199). Note that this was the only operation that ocurred while all of the UCSD detectors were operating at full capacity. A spectrogram for this operation is in section VII. The second operation was for 92 hours, beginning October 19, 1974 (day 292). Although only the north/south head was functioning properly, this data is excellent for the study of low energy(1-1000 ev) particles, particularly during substorms. This is because this operation of the thruster clamped the spacecraft at about -5 volts, and almost totally eliminated differential charging. A spectrogram of the on transition is in the charging appendix.

The main thrusters of both the north and south ion engines became flooded with cesium at the end of their initial operations. This was caused by the faulty design of the feed valve.(This was one of those unique cases where zero gravity did make a difference.) The plasma bridge neutralizers were still usable as plasma sources.

During the initial attempts to restart the engine(July) the south engine became so flooded with cesium that the power supplies were loaded down by the resulting short circuit. After day 202/74, even the neutralizers failed to operate, because not enough power was supplied to the heaters. This slowed the on transitions of the neutralizers in the early part of day 202, providing another useful data set.

Additional operations of the plasma bridge neutralizer on the north engine were run in 1976 and 1977 as part of the spacecraft charging project. These were short operations (10-20 minutes), primarily during eclipses.

Following this section is a list of the times when the engines or neutralizers were operated successfully. Logs of all the times the engines were commanded on are not necessary for studying particle data, but are available in a contract report by Olsen & Whipple(1977). The information on the status of the engine/neutralizer was obtained from a telemetry print out for the ion engine.

Engine Vocabulary

The important terms used in commanding the engine and interpreting its status are given below.

LIC   Load Interface Circuit-the connection between the s/c and engine

MC   Master Converter- the power converting circuitry of the ion engine.

Neutralizer on   Supplies power to the heaters in the neutralizer, which causes cesium flow. Voltage is applied to bridge where discharge will occur.

plume mode   When cesium flow is high enough, an arc strikes across the plasma bridge. This is a low density plasma. It is capable of supplying enough electrons to discharge a negative spacecraft.

spot mode   As flow increases(hotter cathode etc.), a transition occurs in the type of discharge. A nice dense plasma, all at the plasma probe potential. It is capable of supplying ions in the spacecraft current balance. In this mode, a positive spacecraft will swing negative.

AV,KV   Anode Vaporizer and Cathode Vaporizer. Turning these on turn on heaters in the main thruster cesium supply loop. Low voltages are applied to begin discharge. (After chamber was flooded, AV or KV on caused arcing, which causes MC off internally)

HV   High Voltage- this command sets up the voltage on the extraction grids.

Ion Engine Operations

The following times were obtained from the ion engine
telemetry printouts provided by GSFC. Times are accurate to
within one minute. Further accuracy requires more careful
consideration of the nature of the ion engine, and a more
careful definitions of terms. The identification of plume
mode is usually not possible in the telemetry, and it must
either be inferred from normal (laboratory and flight) en-
gine behaviour or from the particle data.

DAY	TIME	DESCRIPTION
199/74	00:30	LIC on, MC on, engine #2(south)
	02:55	Neutralizer on, begin startup
	03:00	Neutralizer ignition, plume mode
	03:10	Neutralizer into spot mode
	03:14	HV,AV,KV ON, caused
	03:15	Neutralizer off because of arcing
	03:20	Restart
	03:31	Neutralizer spot mode
	03:32	AV,KV,HV on, thruster ignited ran smoothly for 30 min. Insufficient neutralizer cesium flow caused
	04:03	Neutralizer to plume mode, thruster off
	04:12	Neutralizer in spot mode, thruster on
	04:33	heaters off, begin shutdown
	04:35	Neutralizer, thruster extinguished
201/74		Engine #2 restart attempts Neutralizer tended to go into spot mode briefly, then fall back into plume mode.
	05:50	Neutralizer on
	06:05	Neutralizer ignition, plume mode
	06:14	briefly in spot mode, then plume
	06:20	Neutralizer off
	06:31	Neutralizer on
	?	plume mode
	06:50	spot mode
	06:54	Neutralizer off

201/74	07:06	Neutralizer on
	?	plume mode
	07:18	spot mode, for 20 sec.
		then return to plume
	07:28	spot mode
	07:33	Neutralizer off
	19:31	Neutralizer on
	?	plume mode
	19:56	spot mode for 20 sec.
	20:00	Neut. off
	20:26	Neut. on
	?	plume mode
	20:42	spot mode for 20 sec.
	20:49	spot mode
	20:52	neut off
202/74	02:08	Neut. on
	?	plume mode
	02:27	spot mode for 20 sec.
	02:29	neut. off
	03:04	Neut. on
	?	plume mode
	03:32	spot mode
	03:38	Neut. off
	03:43	Neut. on
	?	reignited very quickly
		plume mode
	03:49	spot mode for 20 sec.
	03:57	spot mode
	04:15	Neut. off
	04:20	Neut. on
	?	plume mode
	04:34	spot mode
	04:37	Neut. off
292/74		Ion Engine #1 (north)
	07:27	Neutralizer on
	07:38	plume mode(change in s/c pot.)
	07:43	spot mode
	08:01	thruster struck
		on continuously until
		day 296

296/74	03:45	thruster off
	03:47	Neutralizer off
	03:48	Magnetospheric substorm
	05:46	Neutralizer on
	06:03	spot mode
	06:04	Neut. off
57/76	20:56	I.E. #1 neutralizer operation
	21:06	Neutralizer on
	21:26	ignition(change in s/c pot.)
	21:28	spot mode
	21:32	Neutralizer off
	21:33	(injection)
233/76		I.E. # 1 Neutralizer op.s
	05:43	Neut. on
	?	plume mode
	06:05	spot mode
	06:19	Neut. off
	07:41	Neut. on
	?	plume mode
	08:02	spot mode
	08:14	Neut. off
	09:41	Neut. on
	?	plume mode
	10:03	spot mode
	10:14	Neut. off
	11:42	Neut. on
	?	plume mode
	12:03	spot mode
	12:14	Neut. off
	13:41	Neut. on
	?	plume mode
	14:02	spot mode
	14:13	Neut. off
	15:41	Neut. on
	?	plume mode
	16:02	spot mode
	16:12	Neut. off
	17:41	Neut. on
	?	plume mode
	18:01	spot mode
	18:12	Neut. off

233/74	19:42	Neut. on
	?	plume mode
	20:01	spot mode
	20:11	Neut. off
	23:42	Neut. on
	?	plume mode
	?	spot mode(between 23:50 & 00:07)
234/76	00:15	Neut. off
234/76	03:42	Neut. on
	?	plume mode
	04:03	spot mode
	04:15	Neut. off
244/76	23:51	Neut. on
245/76	00:05	plume mode(photo-elec. disappear)
	00:11	spot mode
	00:14	enter eclipse
	00:27	LIC off(causes neut off)
	00:37	exit eclipse
	23:39	Neut. on
	?	plume mode
246/76	23:59(est.)	spot mode
	00:15	enter eclipse
	00:29	LIC off
	00:55	exit eclipse
	23:43	Neut. on
247/76	?	plume mode
	00:03	spot mode
	00:19	enter eclipse
	00:31	LIC off
	00:55	exit eclipse
285/76	03:09	Neut. on
	?	plume mode
	?	spot mode
	?	enter eclipse
	03:59	LIC off
	?	exit eclipse
286/76	03:?7	Neut. on
	?	plume mode
	?	spot mode
	?	enter eclipse
	04:06	LIC off
	?	exit eclipse

288/76	03:33	Neut. on
	03:50	plume mode
	03:57	spot mode
	04:13	enter eclipse
	04:21	LIC off
	04:29	exit eclipse

319/76	05:11	Neut. on
	05:34	spot mode
	05:46	Neut. off

	07:12	Neut. on
	07:33	spot mode
	07:44	Neut. off

	09:11	Neut. on
	09:33	spot mode
	09:43	Neut. off

	11:11	Neut. on
	11:25	plume mode(change in s/c pot)
	11:33	spot mode
	11:43	Neut. off

	13:11	Neut. on
	13:25	plume mode(" " " ")
	13:33	spot mode
	13:43	Neut. off

	15:12	Neut. on
	15:33	spot mode
	15:43	Neut. off

	17:11	Neut. on
	17:33	spot mode
	17:43	Neut. off

	19:12	Neut. on
	19:33	spot mode
	19:46	Neut. off

	21:11	Neut. on
	21:32	spot mode
	21:44	Neut. off

	23:11	Neut. on
	23:32	spot mode
	23:45	Neut. off

320/76	01:11	Neut. on
	01:32	spot mode
	01:44	Neut. off
	03:11	Neut. on
	03:32	spot mode
	03:44	Neut. off
58/77	08:55	Neut. on
	09:17	enter eclipse
	09:17	spot mode
	09:30	LIC off(=neut. off)
	09:48	exit eclipse
59/77	08:51	Neut. on
	09:14	spot mode
	09:15	enter eclipse
	09:26	LIC off
	09:51	exit eclipse
60/77	08:49	Neut. on
	09:12	enter eclipse
	09:12	spot mode
	09:24	LIC off
	09:53	exit eclipse
96/77	09:01	Neut. on
	09:02	enter eclipse
	09:25	spot mode
	09:36	LIC off
	09:43	exit eclipse
97/77	09:03	Neut. on
	09:04	enter eclipse
	09:15	plume mode(change in s/c pot.)
	09:25	spot mode
	09:33	LIC off
	09:41	exit eclipse
98/77	09:00	Neut. on
	09:06	enter eclipse
	09:13	plume mode
	09:21	spot mode
	09:30	LIC off
	09:38	exit eclipse
99/77	08:57	Neut. on
	09:09	enter eclipse
	09:18	spot mode
	09:27	LIC off
	09:35	exit eclipse

Appendix 4

ATS-6 Eclipse Times

Fall 1974 Eclipse Times

		Umbra	
Day	**Enter**	**Exit**
249	6:04	6:25
250	6:00	6:28
251	5:57	6:31
252	5:54	6:33
253	5:52	6:34
254	5:50	6:36
255	5:48	6:37
256	5:46	6:38
257	5:45	6:39
258	5:43	6:40
259	5:42	6:40
260	5:41	6:41
261	5:40	6:41
262	5:39	6:41
263	5:38	6:42
264	5:37	6:42
265	5:36	6:42
266	5:35	6:42
267	5:35	6:42
268	5:34	6:42
269	5:34	6:41
270	5:33	6:41
271	5:33	6:41
272	5:33	6:40
273	5:33	6:40
274	5:33	6:39
275	5:33	6:38
276	5:33	6:38
277	5:33	6:37
278	5:33	6:36
279	5:34	6:35
280	5:34	6:34
281	5:35	6:32
282	5:35	6:31
283	5:36	6:30
284	5:37	6:28
285	5:38	6:27
286	5:40	6:25
287	5:41	6:22
288	5:43	6:20
289	5:45	6:17
290	5:48	6:14
291	5:52	6:09

Spring 1975 Eclipse Times

Day	Umbra Enter	Exit
62	6:19	6:37
63	6:15	6:41
64	6:12	6:44
65	6:09	6:46
66	6:06	6:48
67	6:04	6:50
68	6:03	6:51
69	6:01	6:52
70	5:59	6:53
71	5:58	6:54
72	5:57	6:55
73	5:56	6:56
74	5:54	6:56
75	5:54	6:56
76	5:53	6:57
77	5:52	6:57
78	5:51	6:57
79	5:51	6:57
80	5:50	6:57
81	5:50	6:57
82	5:49	6:57
83	5:49	6:56
84	5:49	6:56
85	5:48	6:56
86	5:48	6:55
87	5:48	6:54
88	5:48	6:54
89	5:48	6:53
90	5:49	6:52
91	5:49	6:51
92	5:49	6:50
93	5:50	6:49
94	5:50	6:48
95	5:51	6:46
96	5:52	6:45
97	5:53	6:43
98	5:54	6:42
99	5:55	6:40
100	5:57	6:37
101	5:59	6:35
102	6:01	6:32
103	6:04	6:28
104	6:09	6:23

Fall 1975 Eclipse Times

Umbra

Day	Enter	Exit
246	21:32	21:47
247	21:27	21:51
248	21:23	21:54
249	21:20	21:56
250	21:18	21:58
251	21:16	22:00
252	21:14	22:01
253	21:12	22:02
254	21:10	22:03
255	21:09	22:04
256	21:07	22:05
257	21:06	22:05
258	21:05	22:06
259	21:04	22:06
260	21:03	22:06
261	21:02	22:06
262	21:01	22:06
263	21:01	22:07
264	21:00	22:06
265	20:59	22:06
266	20:59	22:06
267	20:58	22:06
268	20:58	22:05
269	20:58	22:05
270	20:58	22:05
271	20:57	22:04
272	20:57	22:03
273	20:57	22:03
274	20:58	22:02
275	20:58	22:01
276	20:58	22:00
277	20:58	21:59
278	20:59	21:58
279	21:00	21:57
280	21:00	21:55
281	21:01	21:54
282	21:02	21:52
283	21:03	21:51
284	21:05	21:49
285	21:06	21:46
286	21:08	21:44
287	21:11	21:41
288	21:14	21:37
289	21:19	21:31

Spring 1976 Eclipse Times

	Umbra	
Day	Enter	Exit
59	21:46	21:59
60	21:41	22:04
61	21:37	22:08
62	21:34	22:10
63	21:32	22:12
64	21:30	22:14
65	21:28	22:15
66	21:26	22:16
67	21:24	22:18
68	21:23	22:18
69	21:22	22:19
70	21:21	22:20
71	21:20	22:20
72	21:19	22:21
73	21:18	22:21
74	21:17	22:21
75	21:16	22:22
76	21:15	22:22
77	21:15	22:22
78	21:14	22:21
79	21:14	22:21
80	21:14	22:21
81	21:13	22:21
82	21:13	22:20
83	21:13	22:20
84	21:13	22:19
85	21:13	22:19
86	21:13	22:18
87	21:13	22:17
88	21:13	22:16
89	21:14	22:15
90	21:14	22:14
91	21:15	22:13
92	21:15	22:12
93	21:16	22:11
94	21:17	22:09
95	21:18	22:07
96	21:19	22:06
97	21:21	22:04
98	21:23	22:01
99	21:25	21:59
100	21:27	21:55
101	21:31	21:51
102	21:38	21:43

Fall 1976 Eclipse Times

Umbra

Day	Enter	Exit
245	0:18	0:32
246	0:18	0:42
247	0:20	0:52
248	0:23	1:00
249	0:27	1:07
250	0:30	1:15
251	0:34	1:22
252	0:36	1:29
253	0:42	1:35
254	0:47	1:42
255	0:51	1:49
256	0:56	1:55
257	1:00	2:01
258	1:05	2:07
259	1:10	2:13
260	1:15	2:19
261	1:20	2:25
262	1:25	2:31
263	1:30	2:37
264	1:36	2:43
265	1:41	2:48
266	1:46	2:54
267	1:52	2:59
268	1:57	3:05
269	2:03	3:10
270	2:09	3:15
271	2:14	3:20
272	2:20	3:26
273	2:28	3:31
274	2:32	2:36
275	2:38	2:40
276	2:45	3:45
277	2:51	3:50
278	2:57	3:55
279	3:04	3:59
280	3:11	4:03
281	3:18	4:08
282	3:25	4:12
283	3:32	4:15
284	3:39	4:19
285	3:47	4:22
286	3:56	4:25
287	4:05	4:27
288	4:16	4:27

>

Spring 1977 Eclipse Times

		Umbra	
Day	**Enter**	**Exit**
57	9:25	9:41
58	9:20	9:46
59	9:17	9:49
60	9:14	9:51
61	9:12	9:53
62	9:10	9:55
63	9:08	9:56
64	9:06	9:57
65	9:05	9:58
66	9:03	9:59
67	9:02	10:00
68	9:01	10:01
69	9:00	10:01
70	8:59	10:01
71	8:58	10:02
72	8:57	10:02
73	8:56	10:02
74	8:56	10:02
75	8:55	10:02
76	8:55	10:02
77	8:54	10:02
78	8:54	10:02
79	8:54	10:01
80	8:54	10:01
81	8:53	10:00
82	8:53	10:00
83	8:54	9:59
84	8:54	9:58
85	8:54	9:58
86	8:54	9:57
87	8:55	9:56
88	8:55	9:55
89	8:56	9:53
90	8:56	9:52
91	8:57	9:51
92	8:58	9:49
93	8:59	9:48
94	9:00	9:46
95	9:02	9:44
96	9:04	9:41
97	9:06	9:38
98	9:09	9:35
99	9:13	9:30

Appendix 5

Guide to Detector Commands on Spectrograms

In order to interpret the commands printed on spectrograms and line plots, a guide is supplied which gives the most useful subset of commands. Commands printed on the spectrograms have syllable 1 at the beginning and syllable 10 at the end, with leading zeroes deleted.

Syllable 1 controls the flow of data from the five UCSD detectors into the five accumulators provided in the Westinghouse EME encoder. In the normal mode each detector is gated to a single accumulator which is sampled four times a second. The superfast modes direct data from a single detector into all five accumulators. This mode only functions during the dwell portion of the dwell-scan cycle (see syllable 4). During the scan portion of the dwell-scan cycle data is gated as in the normal mode.

Syllable 2 controls the position of the rotating heads. Theta is the angle of rotation for the NS detector, with theta = 0 corresponding to north. Phi is the angle of rotation for the EW detector, with Phi = 0 corresponding to west. The normal south triad mode (180, 90) is specified by two redundant commands. During the normal sweep mode (sync 1), the detectors are synched 90° out of step, with the NS detector leading. The other sweep mode (sync 2) sweeps the two detectors independently.

Most of the normal combinations of syllables 1-3 are shown in the table. Note that since syllable 3 consists of only one bit, syllables 1 and 2 are shifted two bits when outputted.

Syllable 4 determines the mode of operation of the energy analyzers, choosing between scan only and scan/dwell modes. A8 determines this portion, while bits A9 and A10 are concerned with motor voltages and pulse widths as follows.

A9	Voltage	A10	Pulse Width
0	40 volts	0	80 ms
1	30 volts	1	40 ms

Syllables 5 and 6 determine the first energy step in a dwell cycle. Syllable 7 determines the length of time of each dwell step. Syllable 8 selects the size of the energy step between dwells in one cycle. Syllable 9 chooses the number of dwells in one cycle.

Syllable 10 determines the spiraltron biasing for the individual detectors. High bias corresponds to increased sensitivity.

ATS-6 Commands

Syllables 1-3

Accumulator Gating	Detector Position		Inter-calibrate	Syllables 1-3
	θ	φ		Octal
Normal	0°	90°	Normal	000
	90°	90°		010
	180°	90°		004
	180°	90°		014
	mtr	off		002
	sweep	0°		012
	sync 1			006
	sync 2			016
Super fast protons north/south	0°	90°	Normal	060
	90°	90°		070
	180°	90°		064
	180°	90°		074
	mtr	off		062
	sweep	0°		072
	sync 1			066
	sync 2			076
Super fast electrons north/south	0°	90°	Normal	100
	90°	90°		110
	180°	90°		104
	180°	90°		114
	mtr	off		102
	sweep	0°		112
	sync 1			106
	sync 2			116

Syllable 4

Scan/motor power

Mode	Octal
Scan/dwell	0, 1, 2, or 3
Scan only	4, 5, 6, or 7

Syllables 5 & 6

First dwell step

Step	Octal	Step	Octal	Step	Octal	Step	Octal
63	00	47	02	31	01	15	03
62	40	46	42	30	41	14	43
61	20	45	22	29	21	13	23
60	60	44	62	28	61	12	63
59	10	43	12	27	11	11	13
58	50	42	52	26	51	10	53
57	30	41	32	25	31	9	33
56	70	40	72	24	71	8	73
55	04	39	06	23	05	7	07
54	44	38	46	22	45	6	47
53	24	37	26	21	25	5	27
52	64	36	66	20	65	4	67
51	14	35	16	19	15	3	17
50	54	34	56	18	55	2	57
49	34	33	36	17	35	1	37
48	74	32	76	16	75	0	77

Syllable 7

Dwell time (seconds)	1	2	4	8	16	32	64	128
Octal	0	1	2	3	4	5	6	7

Syllable 8

Dwell Step Size	0	1	2	4	8	16	32	0
Octal	0	1	2	3	4	5	6	7

ATS-6 Commands

Syllable 9

Number of dwell steps

#	2	4	8	16	32	64	64	64
Octal	0	1	2	3	4	5	6	7

Syllable 10

Spiraltron bias

Octal	0	1	2	3	4	5	6	7
NS	lo	lo	lo	lo	hi	hi	hi	hi
EW	lo	lo	hi	hi	lo	lo	hi	hi
FD	lo	hi	lo	hi	lo	hi	lo	hi